NOTICE

The quality of this microform is heavily dependent upon the quality of the original thesis submitted for microfilming. Every effort has been made to ensure the highest quality of reproduction possible.

If pages are missing, contact the university which granted the degree.

Some pages may have indistinct print especially if the original pages were typed with a poor typewriter ribbon or if the university sent us an inferior photocopy.

Reproduction in full or in part of this microform is governed by the Canadian Copyright Act, R.S.C. 1970, c. C-30, and subsequent amendments.

AVIS

La qualité de cette microforme dépend grandement de la qualité de la thèse soumise au microfilmage. Nous avons tout fait pour assurer une qualité supérieure de reproduction.

S'il manque des pages, veuillez communiquer avec l'université qui a conféré le grade.

La qualité d'impression de certaines pages peut laisser à désirer, surtout si les pages originales ont été dactylographiées à l'aide d'un ruban usé ou si l'université nous a fait parvenir une photocopie de qualité inférieure.

La reproduction, même partielle, de cette microforme est soumise à la Loi canadienne sur le droit d'auteur, SRC 1970, c. C-30, et ses amendements subséquents.

ISBN 0-315-53813-9

STUDIES ON THE FORMATION OF POLYETHERSULFONE MEMBRANES

by

Lucie Lafreniere

Thesis presented to the School of Graduate Studies of the University of Ottawa as partial Fulfilment of the requirements for the degree of Master of Applied Science in Chemical Engineering

University of Ottawa

A mon époux, Dennis, et mes chers parents.

ABSTRACT

A viscoelastic approach has been applied to study the formation of polyethersulfone (PES) membranes which resulted in a method for controlling the membrane surface pore structure and, hence, performance. The structure of the casting solution in presence of the polymeric nonsolvent swelling agent, polyvinyl pyrrolidone (PVP), and the solvent, N-methyl-pyrrolidone (NMP), was determined on the basis of viscometric data for a range of compositions. The pore size distribution at the surface of the resulting membrane was determined on the basis of the Surface Force Pore Flow model by use of the membrane separation data on reference solutes.

It was observed that PVP-PES interactions existed in the casting solution which were strongest when their weight ratio was unity. Coincidentally, inflexions in the pore size distribution and product rate curves at the PVP/PES weight ratio of 1.0 for the casting solution were observed for the polyethersulfone membrane. It was concluded that the PVP-PES interactions had an effect on the polymer structure in the casting solution which, in turn, controlled the membrane pore structure, particularly at the surface.

RÉSUMÉ

L' approche viscoélastique dans l' étude de la formation des membranes de polyéthersulfone a donné suite a une méthode pour le contrôle de la structure des pores à la surface et, donc, de la performance de ces membranes. La structure de la solution de polymère en présence du nonsolvent polymérique, polyvinyl pyrrolidone (PVP), et du solvent, N-méthyl-pyrrolidone, (NMP), a été déterminée sur la base de données viscométriques pour un ensemble de compositions. La distribution de grosseur des pores à la surface des membranes a été déterminée par analyse des données de séparation par membrane pour des solutés de référence. Le modèle de transport basé sur les forces de surface et l' écoulement par pore a été utilisé.

Il a été observé que des intéractions de type PVP-PES existent dans la solution de polymère qui sont plus fortes lorsque le rapport de poids est un. Coincidemment, au rapport de poids PVP/PES de 1.0 dans la solution de polymère, des maxima dans la distribution de grosseur des pores et dans la courbe de productivité ont été observées avec ces membranes de polyethersulfone. Il a été conclu que les intéractions PVP-PES ont eu un effet sur la structure de la solution de polymère qui, en retour, controlla la structure des pores de la membrane, particulièrement a la surface.

TABLE OF CONTENTS

TABLE OF CONTENTS (CONT'D)

TABLE OF CONTENTS (CONT'D)

LIST OF ILLUSTRATIONS

Page

TABLES

LIST OF ILLUSTRATIONS (CONT'D)

FIGURES

INTRODUCTION

This thesis is concerned with the development of asymmetric membranes of polyethersulfone for reverse osmosis and ultrafiltration (RO/UF) applications. More specifically, it is concerned with the study of the membrane formation process whereby a thin film of polymer casting solution is formed into a solid polymer network - the membrane - with a definite porous structure. The purpose of the study is to enable the control of the membrane porous structure in its preparation; concurrently, to improve membrane performance and reproducibility.

It follows then that the prime objective of this research project was to study the effect of the casting solution composition and of the resulting solution structure on the pore structure at the surface of the polyethersulfone membrane ultimately produced. The secondary objective was to establish a standard fabrication technique for the polyethersulfone membrane in the study using performance and reproducibility as criteria.

The approach to the study was to first investigate the effect of the casting solution composition on membrane performance. Subsequently, the average pore size and pore size distribution at the membrane surface was determined on the basis of the Surface Force - Pore Flow model by analysis of the membrane performance data on reference solutes. The outcome was the determination of the effect of the casting solution composition on the pore size distribution. This was further related to the solution structure predicted on the basis of the intrinsic viscosity data for the range of casting solution composition.

BACKGROUND

This study is presented as part of a series of works at the National Research Council of Canada (NRCC) in which the effect of the structure of the casting solution on the performance of the resulting membrane is investigated.

In previous works (Matsuura and Sourirajan (1); Nguyen et al. (2); Nguyen et al. (3)), the study was focused on the aromatic polyamide polymer. The effects of the polymer molecular weight and of the casting solution composition on the structure of the casting solution was investigated by using viscoelastic experiments and results related to the average pore size and the pore size distribution on the surface of resulting membranes. Recently, the above approach was extended to the study of the effect of the nonsolvent swelling agent on the casting solution structure of aromatic polyamide polymer (Nguyen et al. (4); Nguyen and Matsuura (5)). The objective of the present work is to conduct a similar investigation on the structure of the casting solution prepared for the formation of ultrafiltration (UF) membranes from polyethersulfone - Victrex material. The choice of the latter polymeric material is due to its excellent characteristics for UF membrane applications, which include chemical and thermal stability and mechanical strength.

The nonsolvent swelling agent added to the casting solution of polyethersulfone membranes is a polymeric compound such as polyvinyl pyrrolidone. Unlike it, the nonsolvent swelling agents added to the casting solution of aromatic polyamide membranes consist of mostly inorganic electrolytes; these form ion-polymer complexes, bringing several polymer molecules into one supermolecular polymer aggregate. The function of the polymeric type nonsolvent swelling agent such as polyvinyl pyrrolidone, by comparison, could be expected to be very different. To elucidate the structure of the casting solution in the presence of the polymeric additive and its effect on the surface pore structure and, hence, the performance of polyethersulfone UF membranes is, therefore, the goal of this work.

Though there have been several investigations on the preparation of flat polyethersulfone UF membranes in the literature (Tweddle et al. (6); Kai et al (7)), this work is unique in this respect.

1. LITERATURE REVIEW

Research papers in the area of membrane development are usually classified on the basis of (a) the polymer membrane material and casting system (solvent - nonsolvent swelling agent) under investigation and (b) the fundamental concepts applied to the data or brought into discussion. These fundamental concepts primarily include the membrane formation mechanism, the transport model and the membrane characterization technique.

Accordingly, this literature review will discuss the fundamental concepts of membrane development, as it relates to this work. Subsequently, the earlier work on the development of polysulfone membranes and, more specifically, polyethersulfone membranes will be discussed.

1.1 FUNDAMENTAL CONCEPTS

The first synthetic membranes to offer the possibility of an economic separation process were prepared by Loeb and Sourirajan (8) in 1960. The membranes which were made of cellulose acetate had a distinct asymmetric porous structure and a water permeability about one hundred times larger than the earlier membranes of Reid and Breton (9) which, by comparison, had a homogeneous structure. The asymmetric porous structure was the result of a unique membrane preparation technique - called the immersion precipitation technique - which essentially began with the proper formulation of the casting solution (polymer-solvent- nonsolvent swelling agent). Merten et al. (10) observed the asymmetric membrane by Scanning Electron Microscope (SEM) and described it as a very thin, dense layer resting on a more porous supporting matrix present for mechanical support only and offering negligible hydrodynamic resistance.

Following the discovery by Loeb and Sourirajan, there were important advances made in the science and engineering of reverse osmosis and ultrafiltration. Concurrently, a large number of patents and publications were generated on topics encompassing the development of asymmetric membranes from new polymeric materials, methods for improving membrane performance, new membrane process applications and new configurations of membranes.

Potential applications of membranes were being identified which required membranes with improved chemical, thermal and mechanical properties, and with the suitable pore size to achieve specific separations by allowing only desired molecules to permeate. The challenge to design membranes for use in specific applications prompted researchers to understand the membrane formation mechanism and also the transport mechanism for material through membranes resulting in the separation.

MEMBRANE FORMATION MECHANISM

The Scanning Electron Microscope (SEM) technique was used by several workers (9, 10, 11, 12) to elucidate the mechanism by which the polymer casting solution is coagulated to yield the asymmetric membrane. The SEM has since become a popular tool to conduct phenomenological studies on the effects of varying casting parameters on the structure of membranes.

The general procedure for making membranes by precipitating a polymer solution - of which the immersion precipitation technique is a special case - was called the phase inversion process by Kesting (13). According to this process a one-phase polymer solution is converted into a two phase system consisting of a solid (polymer-rich) phase which forms the membrane structure and a liquid (polymer-poor) phase which forms the pores in the final membrane.

Strathman and coworkers (14) introduced the original concept that the graded structure in asymmetric membranes arised from a decreasing rate of precipitation from the upper to the lower surface. In their work the phase diagram of the system polymer/ solvent/precipitant was used extensively in discussions of this precipitation process. Since its introduction, the phase diagram has become a valuable tool in several membrane formation studies.

An approach for understanding the formation of asymmetric membranes was to also understand the mechanism of formation for homogeneous membranes. Based on this approach, Koenhen (15) was the first to suggest that the two distinct layers of the membrane, the skin and the porous sublayer, were formed by two distinct mechanisms: gelation and liquid-liquid phase separation by nucleation and growth. Wijmans et al (16) gathered experimental evidence which supported the two different types of phase separation phenomena responsible for the asymmetric structure. They also discovered (17) that with the immersion precipitation technique it is also possible to obtain homogeneous (microporous) membranes; this was achieved by adding solvent to the precipitation bath. This observation was a step forward in the rationalization of the formation mechanism since knowledge about ways to avoid the formation of a skin may lead to a better understanding of skin formation.

PORE FORMATION MECHANISM

A proper understanding of the pore formation mechanism, more specifically in the thin surface layer, would allow the control of pore size at the membrane surface. This would represent a significant step towards the objective of tailoring membranes for specific applications since the pore size at the membrane surface is a principal factor governing the performance.

The mechanism of pore formation at the surface of the membrane has not received as much attention as the mechanism of formation for the asymmetric membrane as a whole. The study of pore formation is complicated by the fact that there exists no simple methods to measure the pore size at the surface of the membrane.

Kesting (18) attempted to describe the origin of pores at the membrane surface from the formation of patches of gels and almost clear solvent during the phase inversion process. Pores result from cracks within the gels as their density increases and from the solvent patches as the solvent is leached out in the gelation (or precipitation) bath. In Kesting's mechanism the growth of gel patches occurs under a driving force which is the gradient of chemical potential.

Neogi's (19) approach was to model the pore formation mechanism using thermodynamic parameters. The model shows that the evaporation of solvent combined with the decrease in volume gives rise to the pores in the skin. The results emphasize the importance of the solvating and swelling properties of the solvent. Skin formation is dependent on the solution satisfying a swelling criterion which also governs the formation of the porous sublayer.

In the context of the phase inversion process depicted by Kesting, Sourirajan (20) proposed that the structure of the casting solution and the rate of desolvation during film formation (in the evaporation and gelation step) together governed the orientation of the polymer network and hence the pore size. The solution structure, or the precise disposition of the polymer material within the casting solution, gives rise to the existence of supermolecular polymer aggregates within the casting solution, each aggregate having its own network of polymer segments. Based on the above concept of solution structure Sourirajan (21) identified two distinct pore systems at the surface of membranes: the network pores and the aggregate pores. While the first originate from the void spaces between polymer segments within the network of each individual polymer aggregate, the second originate from the void spaces among neighbouring polymer aggregates themselves.

Subsequently, a new approach was proposed to study the pore structure at the membrane surface on the basis of the polymer structure in the casting solution, using viscoelastic measurements of the polymer solution. The method was applied to study pore formation in aromatic polyamide membranes (1, 2, 3, 4, 5) and more recently in polyethersulfone membranes (this work).

MEMBRANE CHARACTERIZATION

The capability to characterize membranes would greatly facilitate the selection of membranes for use in specific applications. In the context of membrane development, however, the purpose for the characterization of membranes is to quantify the effects of varying the casting conditions on the pore structure, to provide a method of quality control, and also to understand the transport mechanisms in membrane separation.

Several characterization methods for pore size and pore size distribution as well as separation properties have been reported. They are indirect methods only since the dimensions of interest are not resolved under the electron microscope. Two types of methods have been considered:

a) Determination of pore size and pore size distribution by a physical method, as summarized in Table 1 (12).

b) Determination of retention coefficients for some reference molecules obtained by permeation experiments under defined conditions. A particular method concerns the determination of the "molecular weight cut-off" designated as an upper molecular weight limit above which over 90% of the solute molecules are retained (or less than 10% transport occurs).

Moreover, the pore size distribution may be calculated from the experimental retention coefficients data and vice versa. However, this requires the use of transport models for mass transfer in the membrane, and these are based on some assumptions. Some of the work on membrane characterization which has been reported in the literature will now be discussed.

Three methods to characterize the top layer of asymmetric membranes have been developed or refined by Smolders and Vugteveen (22) during the past few years: a) the gas adsorption/desorption method, b) thermoporometry and c) selective permeation (fractional rejection). These have been valuable methods in many studies which followed.

Bodzek (23) studied the effects of casting conditions on the membrane pore structure by comparing the macromolecular transport results for the different membranes, and comparing these with the pore size data and skin thickness obtained with the aid of gas adsorption/desorption (BET) and water permeability studies. He also demonstrated a dependence between the molecular weight "cut-off" of ultrafiltration membranes and the molecular configuration of macromolecules (eg. proteins, polyethylene glycols, and dextrans) used as probes. It is based on this dependence that other workers (24, 25) have preferred Crown ethers for use in membrane characterization because of their spherical shape and solubility in water.

TABLE 1

METHODS FOR THE CHARACTERIZATION OF THE STRUCTURE OF SYNTHETIC MEMBRANES (12)

Microstructure (pore diameter <50 Å)	Macrostructure (pore diameter >50 Å)
Diffraction of slow neutrons	Electron microscopy
Gas permeation with the help of the free-volume theory	Gas and liquid permeation using the Hagen-Poiseuille law and the Knudsen relationship
Gas adsorption using the BET isotherm, the dual-sorption model, and the free-volume theory	Porosimetry (e.g. Hg-intrusion method)
Thermodynamic characterization of the water structure	Bubble pressure method
Thermomechanical analysis (TMA)	
Determination of the limits of molecular separation	
IR absorption spectroscopy	
X-ray scattering and diffraction	X-ray small-angle scattering
Differential thermoanalysis and scanning calorimetry (DTA and DSC)	

Zeman and Tkacik (26) reported on the characterization of asymmetric membranes of polysulfone by a) high-resolution scanning electron microscopy (SEM), b) nitrogen sorption/desorption isotherms as well as by c) water permeability and d) polydisperse solute rejection. The prediction of solute rejections using the log-normal distribution of pore radii, determined by SEM of the membrane surface, resulted in satisfactory agreement with the experimental data. Pore radii calculated from sorption/desorption isotherms were significantly larger than those suggested by SEM and thus it was concluded that the isotherms reflect primarily pore volume distributions in the subsurface (matrix) region of the asymmetric structures and the method is inadequate for evaluating the pore structure at the membrane surface.

In addition to the pore structure at the membrane surface, it is well known that the physico-chemical interactions between membrane polymer material, solute and solvent in the feed solution also govern membrane performance. This further emphasizes the need to specify the chemical nature of the membrane together with the pore structure in order to more completely characterize the membrane. The solubility parameter of the polymer was a property used in several studies to quantify the chemical nature of the membrane material. This has also become a common criteria for the selection of polymer membrane materials.

A method to quantify the membrane-solute -solvent interactions which uses the High Performance Liquid Chromatography technique was developed by Matsuura et al (27). The resulting interaction parameters together with the rejection data for reference solutes were used for the calculation of the pore size distribution at the membrane surface by applying the Surface Force-Pore Flow model (28). It was shown (29) that two distinct Gaussian normal distributions of pore sizes were required to more adequately predict the experimental rejection data. According to Sourirajan information on the pore size distribution parameters (determined on the basis of the transport model) and the interaction parameters for reference solute-solvent systems (determined by HPLC) are required to adequately characterize the membrane.

TRANSPORT MODELS

Although much effort has been devoted to the subject no transport mechanism has yet gained general acceptance. Two major theories have been proposed which basically involve pore flow and/or diffusive flow. In pore flow the membrane is pictured as a bundle of capillaries where the flow is determined by the application of Poiseuille's equation; the physical structure determines the transport behaviour. In diffusive flow material transport is determined by the dissolution of the components in the membrane followed by diffusion through the membrane. The solute-polymer and the solvent-polymer forces together with the chemical properties of the membrane material are the dominant factors in this case.

The preferential sorption - capillary flow mechanism proposed by Sourirajan (30) extended the pore flow theory by incorporating the physico-chemical forces at the membrane-solution interface to reflect the existance of a steep concentration gradient. According to this mechanism, reverse osmosis separation is the result of the preferential sorption of one of the constituents of the feed solution at the membrane-solution interface, and mass transport by permeation under pressure through the capillaries of the microporous membrane. It follows that the twin-requirement for the practical success of the membrane separation process is (i) an appropriate chemical nature of the membrane material, and (ii) pores of appropriate size and number at the membrane surface.

The surface force-pore flow model was developed by Matsuura and Sourirajan (28, 31) as a quantitative expression of the preferential sorption - capillary flow mechanism. Integrated into the transport equations were the following forces: interfacial surface forces, pressure, friction and viscous shear forces. The interfacial surface forces, expressed by parameters, were obtained by analysis of liquid chromatography data. The transport equations initially derived (27, 28, 31) for an individual pore radius R were extended to the multipore system of the actual membrane involving one (or more) equivalent average pore radius $\bar{R}$ and corresponding standard deviation σ' . The resulting model consists of general expressions for solute separation and fluid flux which are valid whether the solute is negatively or positively adsorbed at the membrane - solution interface.

Several transport mechanisms for reverse osmosis separations have also been proposed in terms of diffusive flow. Among the latter was the solution - diffusion mechanism developed by Lonsdale and co-workers (32) which is described by the dissolution of the solute and the solvent in the membrane material and subsequent diffusion through the homogeneous nonporous surface layer. Transport equations have been derived (33) in which fluid flux is a function of the diffusivity in the membrane and the effective transmembrane pressure ($\Delta P - \Delta \pi$); solute separation is a function of the relative fluxes of solvent and solute, or hence, their relative diffusivities in the membrane material.

Either one of the mechanisms discussed or variations of these mechanisms have been applied by different workers to interpret their results. According to a review by M.A. Mazid (34) further developments in transport mechanisms have somehow depended on the recognition of membrane - solution interfacial or surface forces.

1.2 PERSPECTIVE ON POLYSULFONE MEMBRANES

Owing to their excellent thermal and chemical resistivity and mechanical strength, the polysulfones are attractive polymer membrane materials and ,thus, they are extensively studied for membrane applications. The improved properties of the polysulfone membranes over the more traditional cellulose acetate membranes would extend the potential applications of membrane separation to processes involving severe chemical and/or thermal conditions; for example, medical devices and food processing applications requiring sterilization and sanitization.

Membrane Development

Asymmetric polysulfone membranes are made by the usual immersion- precipitation technique from casting solutions prepared using polar, aprotic solvents such as dimethylformamide (DMF), dimethyl acetamide (DMA), N-methyl-pyrolidone (NMP) or cyclohexanone. As it is generally known for asymmetric membranes the formation of the active layer as well as of the pore structure again depends on the viscosity of the polymer solution and on the interaction with the precipitation bath.

A disadvantage of polysulfone (PS) membranes has been identified (35, 36) as their low permeability when prepared from a solution containing a high enough polymer concentration to provide an adequate viscosity for casting. As a remedy, polymer additives such as polyethylene glycol (PEG) and polyvinyl pyrrolidone (PVP) have been added to the casting solution to yield a membrane structure with improved permeability. While it artificially increases the viscosity of the casting solution, the additive also contributes to pore formation; because it is a water-soluble polymer it is extracted in the precipitation bath. Of particular interest, PVP was found (36) most effective in increasing the permeability of the PS membrane without changing the separation characteristics. The high compatibility of the two polymers (PVP and PS) was suggested as a possible cause.

Membrane Characterization

There have been several attempts to characterize quantitatively the pore structures of polysulfone asymmetric ultrafiltration membranes. Zeman et al (26) used the high-resolution scanning electron microscopy technique to measure the pore radius range of three membranes with different ultrafiltration properties. A log-normal distribution was found to best fit the pore radius population, as shown below.

Pore Size Analysis by SEM

Membrane	1	2	3
Mean pore radius (Å)	21.3	40.4	41.0
Standard deviation, σ	0.62	0.56	0.74
No. of pores per cm sq. ($\times 10^{-10}$)	3.94	3.44	1.49

The range of pore radius was found to be commensurate with the range of radii of rejected solutes observed from polydisperse solute rejection measurements. Moreover, predicted rejection curves determined using equations based on the steric rejection theory in straight cylindrical pores were in agreement with the experimental solute rejection data. By comparison, two different methods of sorption/desorption isotherms resulted in unreliable pore radii measurements. The pore radii which was substantially larger than suggested by SEM appeared to reflect the subsurface region of the membrane rather than the surface.

M. Bodzek (23) investigated the structure of the polysulfone membranes by means of pure water permeability measurements and BET-surface area determination. Mean pore radius of 47.5, 30.0 and 25.0 Å respectively were obtained for membranes from casting solutions with 15, 17.5 and 20 wt% polymer respectively. A broad pore size distribution was observed from gas adsorption/desorption isotherms.

Polysulfones - Types and Properties

Polysulfone is a generic name for the family of polymers characterized by the sulfone groups, which provide thermal stability and high-temperature rigidity, and ether groups, for toughness. Each commercially available polysulfone is produced by a single supplier. While polyethersulfone is supplied by Imperial Chemical Industries (ICI) under the trade name Victrex, polyphenylsulfone and polysulfone are supplied by Union Carbide Corp. under the trade names Radel and Udel respectively. The chemical structure of the three kinds of polysulfone polymers is shown below. Typical mechanical properties are listed in Table 2 (37).

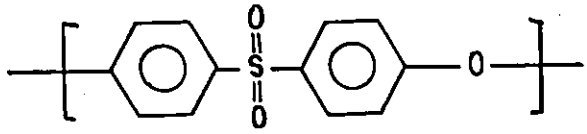

Polyethersulfone (Victrex)

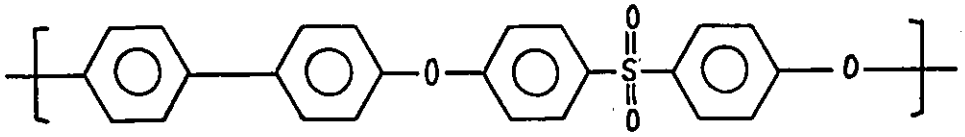

Polyphenylsulfone (Radel)

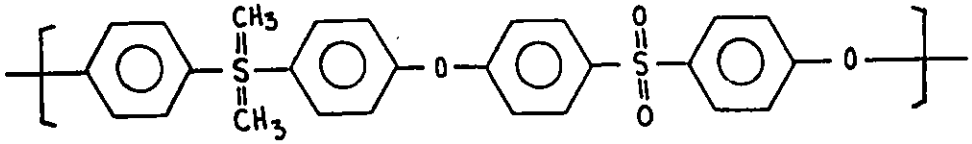

Polysulfone (Udel)

TABLE 2

TYPICAL PROPERTIES OF COMMERCIAL POLYSULFONE POLYMERS (37)

ASTM Test	Property	Polysulfone	Polyether-sulfone	Polyphenyl-sulfone
D1505	Density (gm/cm^3)	1.24	1.37	1.29
D570	Water Absorp., Equilibrium at 20°C (%)	0.85	2.1	1.3
D785	Hardness, Rockwell	M69(R120)	M88	M83
D638	Tensile Str at Yield (psi)	10,200	12,200	10,400
D638	Tensile Modulus (psi)	360,000	391,000	310,000
D638	Elongation at Break (%)	50—100	40—80	60
D790	Flexural Strength (psi)	15,400	18,650	12,400
D790	Flexural Modulus (psi)	390,000	373,000	330,000
D256	Impact Strength, Izod (ft-lb/in. of notch)	1.3	1.6	12
D648	Deflection Temperature, 264 psi (°F)	345	398	410
D696	Coef of Thermal Expansion (in./in.—°F)	3.1×10^{-5}		3.1×10^{-5}
D2863	Oxygen Index Rating	30	34—38	38
D149	Dielectric Strength, ⅛ in., Short Time (V/mil)	425	400	371
D257	Volume Resistivity, (ohm—cm)	5×10^{16}	$10^{17} - 10^{16}$	3.52×10^{15}
D150	Dielectric Constant, 60 Hz—1 MHz	3.07—3.03	3.5	3.44—3.45
D150	Dissipation Factor, 60 Hz—1 MHz	0.0008—0.0034	0.001-0.0035	0.00058—0.00764

Mechanical properties do not vary significantly among the three polysulfones, but in strength properties, polyethersulfone has the edge. Polyethersulfone as well as polyphenylsulfone with heat deflection temperatures of about 400 F have excellent high-temperature properties. Further, the water adsorption of polyethersulfone is higher than that of the other polysulfones.

The more polar nature of polyethersulfone relative to the other polysulfones which emanates from the water adsorption data suggests that polyethersulfone is a preferred membrane material, more specifically for aqueous applications. The work of Tweddle et al (6) demonstrated that for a given level of solute separation, product rate tended to increase with increase in the polar nature of the polysulfone polymer from which the membrane was made. Another advantage of Victrex-PES over Radel-PPS and Udel-PS for use in membranes was reported by Kai et al (7); Victrex-PES has a higher thermal stability.

1.3 POLYETHERSULFONE MEMBRANE DEVELOPMENT

Polyethersulfone was selected over the other commercial polysulfones as polymer membrane material for the study of membrane formation in this work. More specifically, Victrex-PES of grade 200P was used. Technical information on Victrex-PES was referred to Appendix 1 (38).

Solvents for Victrex-PES include polar reagents such as dimethylformamide (DMF), methylene chloride (MC), N-methyl-pyrrolidone (NMP) and dimethyl sulfoxide (DMSO). Films of uniform thickness can be readily cast from the resulting polymer solution, providing the concentration is appropriate. The technical literature on Victrex-PES (Appendix 1, Table IV) indicates that the PES-NMP system in the concentration range 10-30 wt% PES is stable for a period longer than a month. However, Tweddle et al (6) observed a stable period of longer than a year. By comparison, solutions of PES in DMF and in MC were reported stable only for periods shorter than a month. Furthermore, solutions of PES in NMP have a higher viscosity than those with DMF and MC as solvents. The higher viscosity is a good attribute for casting more uniform membranes.

For the study, in this work, the casting system for polyethersulfone used NMP as solvent and PVP as additive. The benefits of PVP in the casting solution have been previously discussed with respect to polysulfone membranes in general. Although this work is unique in its study of the membrane formation, there have been other investigations on the preparation of flat polyethersulfone membranes. These will now be discussed:

i) Tweddle et al (6)

Phenomenological studies were conducted on the effects of various casting parameters on the performance of resulting membranes. The following observations were made:

- As expected the increase in polymer concentration in the casting solution decreased the permeability but increased the solute separation of resulting membranes.

- Addition of PVP in the casting solution up to 6 wt% resulted in an almost linear increase in permeability while solute separation was practically unaffected; this phenomena had already been reported by P. Aptel et al (36) for polysulfone membranes.

- Addition of water up to 4.5 wt% to the casting solution resulted in a sharp decrease in permeability and corresponding moderate increase in solute separation.

- Temperature (up to 60 °C) and time (15 sec to 5 min) in the solvent evaporation process were shown to have no effects on membrane performance.

- The temperature and composition of the precipitant for the gelation process were investigated. Using water as precipitant, the temperature was shown to have no effect. Dilute aqueous solutions of NMP, ethanol, and sodium chloride respectively, as well as tap water had no effect relative to pure distilled water as precipitant. By comparison, dilute aqueous solutions of sulfuric acid as precipitant improved the permeability of the membrane with a corresponding decrease in solute separation.

- The effect of storing the membranes in room temperature distilled water was investigated; membranes stored for 2 months had a lower permeability but higher solute separation than when stored for 2 days.

ii) Kai et al (7)

These authors also conducted phenomenological studies, however, using Victrex-PES of grade 300P instead of grade 200P. Casting solutions containing solvents NMP, 2-pyrrolidone, DMF and DMA respectively were used for preparing membranes. Only 2-pyrrolidone resulted in a permeable membrane; the others produced membranes which had a thick layer on the bottom surface (observed by SEM) and had to be peeled off in order to render the membrane permeable. The effect observed with solvent NMP (that it produced a nonpermeable membrane) is contrary to other works (6, 36). The effect of acids, esters, amides and ketones respectively as additives in the casting solution was investigated; it either increased the permeability of the membranes or it induced permeability in the case of solvents (as NMP) which initially produced nonpermeable membranes. The additives role in increasing the sensitivity of the casting solution to imbided water and therefore in accelerating the polymer precipitation process was suggested.

The time (0 to 90 sec) and the air flow (20 to 1.75 x 10 cm/min) at the film surface during the solvent evaporation process were shown to have an effect on membrane performance. Further, the effect of time was dependent on the level of air flow. The gelation factor which is a measure of the water contained in a unit surface layer of the cast dope was used to measure the combined effects of time and air flow. The increase in the gelation factor resulted in an increase in permeability until a maximum was reached, followed by a decrease; solute separation was practically constant up to the point where maximum permeability occurred then it decreased. Use of additive in the casting dope was shown to shift the gelation factor and hence the position of the maximum.

The thermal stability of PES membranes from Kai et al, which are produced commercially by Daicel Chemical, and of PS membranes with similar capabilities were compared. While the PES membrane maintained its performance up to 130°C, the PS membrane was up to 100°C; when immersed into hot water in an autoclave for 30 min.

2. THEORY

Membranes technology constitutes a new and unique field of separation science and the theories used to describe the membrane process are distinct from the other separation processes. The membrane barrier is the active separation agent while the pressure and chemical potential gradients across the membrane constitute the driving force in this process . The appropriate chemical nature of the membrane as well as the pore structure at the membrane surface are essential requirements for the success of the separation process in a specific application.

A review of the theory on membrane separation and also on membrane formation, as it relates to this work, will be presented in this section. The surface force - pore flow model for transport through membranes developed by Matsuura , Sourirajan et al. (28), will be discussed along with a method to calculate the average and standard deviation of pore size at the membrane surface. A mechanism of pore formation based on the viscoelastic properties of the polymer casting solution (from which the membrane is prepared) proposed by Nguyen, Matsuura et al. (3, 4, 5) will also be discussed.

Although several types of membrane processes exist based on their design and operating principle the theory presented in this section is only applicable to reverse osmosis (RO) and ultrafiltration (UF) in liquid systems. These two conventional membrane processes are similar in operation. However, the UF membrane has larger pores on its surface which limits its application to processing feed solutions involving macromolecular solutes or colloidal or particulate matter in suspension. The UF process operates in a relatively lower pressure range (50 psig) than does the RO process (1000 psig). Despite these differences, the two processes are often simply referred to as reverse osmosis. This terminology has been adopted in this report, also the abbreviation RO/UF is often used.

2.1 PRINCIPLES OF MEMBRANE SEPARATION PROCESSES

The membrane process, illustrated in Figure 1, is a separation technique which can be described briefly as follows: It consists in letting the feed solution flow under pressure (greater than the osmotic pressure difference) past the surface of an appropriate porous membrane. The fraction of the feed which flows through the membrane is withdrawn generally at atmospheric pressure and ambient temperature. This stream, called permeate, is enriched in one or more constituents of the feed solution, leaving a solution of higher or lower concentration on the high pressure side of the membrane, called retentate.

The performance of a membrane is determined from data on the product rate (PR), also called permeation rate, and solute separation (f) for a given feed solution and operating conditions; and also from the pure solvent permeability, called pure water permeation (PWP) in aqueous systems. PR and PWP are defined as the rate of mass transfer accross the membrane, with dimensions $M / t L^2$. Solute separation, f, is defined as

$$f = \frac{C_{A1} - C_{A3}}{C_{A1}} \times 100\% \qquad (1)$$

where C_A is the concentration of solute in the carrier solvent (in this case water). C_{A1} and C_{A3} , defined in Figure 1, are the solute concentration of the feed in the bulk solution and of the permeate respectively.

By comparison, solute separation given as f' and which is defined as

$$f' = \frac{C_{A2} - C_{A3}}{C_{A2}} \times 100\% \qquad (2)$$

uses the feed solute concentration at the membrane interface, C_{A2} , instead of in the bulk solution, C_{A1} .

FIGURE 1

REVERSE OSMOSIS/ULTRAFILTRATION MEMBRANE SEPARATION PROCESS - ENLARGEMENT: PREFERENTIAL SORPTION CAPILLARY FLOW TRANSPORT MECHANISM

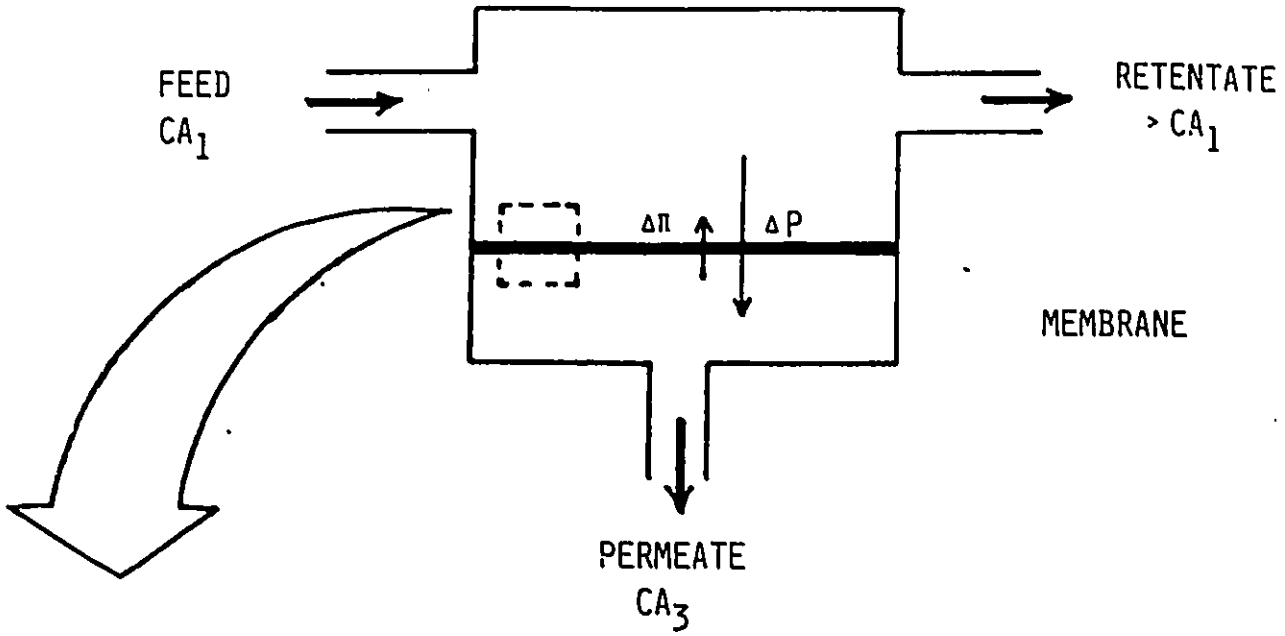
FEED
CA_1
RETENTATE
$> CA_1$
$\Delta\pi$
ΔP
MEMBRANE
PERMEATE
CA_3

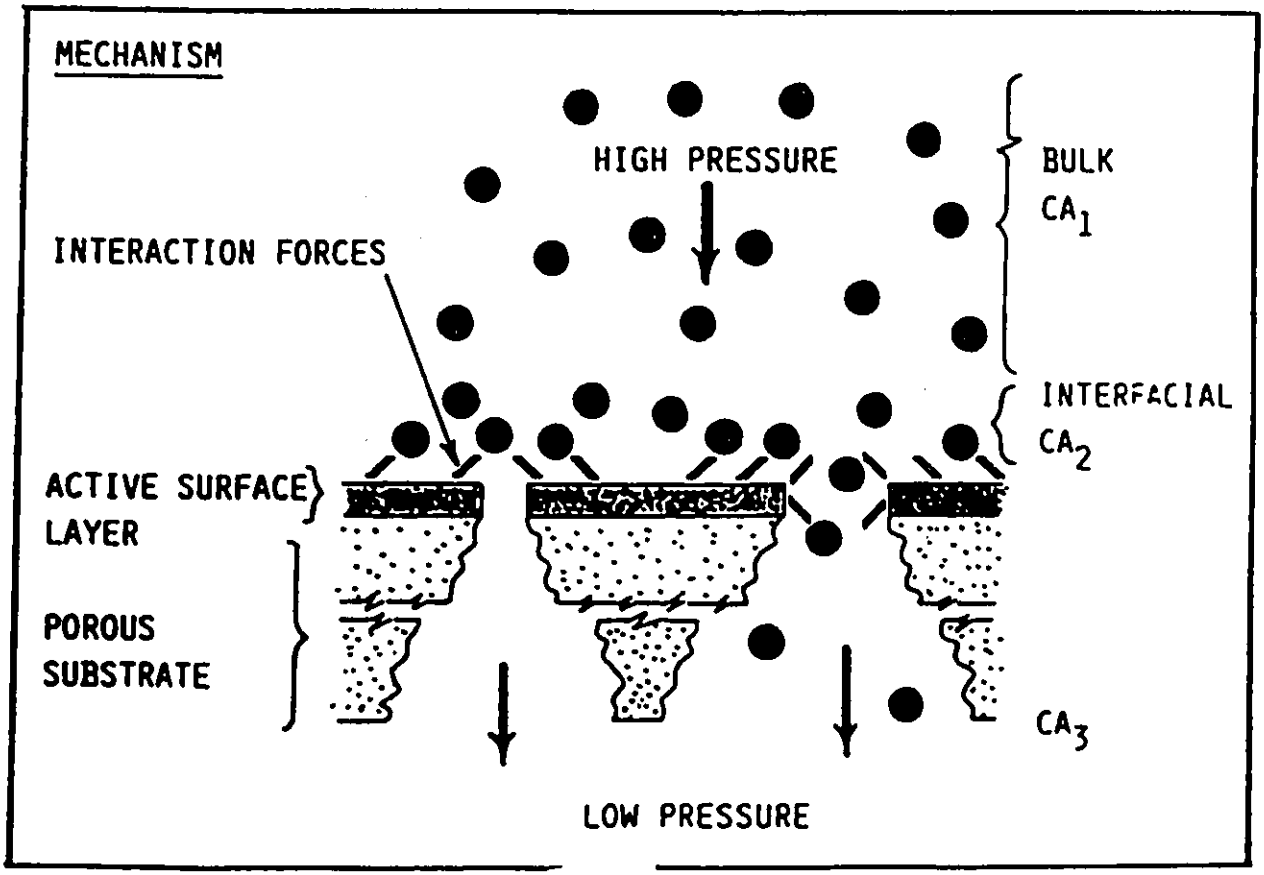
MECHANISM
HIGH PRESSURE
BULK
CA_1
INTERACTION FORCES
INTERFACIAL
CA_2
ACTIVE SURFACE LAYER
POROUS SUBSTRATE
CA_3
LOW PRESSURE

For practical considerations, in order to obtain the highest membrane productivity (i.e. permeation rate at any given level of solute separation) the porous structure of the membrane must be asymmetric. The asymmetric structure of the membrane is represented in Figure 1 as a thin active surface layer of membrane interconnected with the substratum consisting of progressively more porous membrane material. The substratum is present for mechanical support only and has negligible hydraulic resistance. Therefore, with the asymmetric type membrane the resistance to fluid flow is reduced to the minimum under reverse osmosis operating conditions.

2.2 TRANSPORT MECHANISM

Membrane processes emerged from an appreciation of the fact that surface forces can give rise to concentration gradients at interfaces. This is expressed by the Gibbs equation, relating interfacial tension of a solution, γ, and the surface excess of a solute at an interface, Γ.

Gibbs equation:

$$\Gamma = -\frac{1}{RT}\left[\frac{\delta \gamma}{\delta \ln a}\right]_{T,A} \qquad (3)$$

where R is the gas constant, T is absolute temperature and a is activity of the solute.

If the surface of a porous membrane in contact with a solution is of such chemical nature that it has preferential sorption for some components of the solution, then, a multimolecular layer of those components could exist at the solution-membrane interface. A continuous removal of this interfacial layer can then be effected by letting it flow under pressure through membrane capillaries.

Such an appreciation of surface phenomena led to the preferential sorption - capillary flow mechanism for material transport through membrane pores proposed by Sourirajan (30). Based on the mechanism the governing factors in reverse osmosis are:

i) An equilibrium effect concerned with the solute - solvent - membrane interaction forces at the solution - membrane interface.

ii) A kinetic effect concerned with the mobilities of solute and solvent through membrane pores governed both by the equilibrium effect and steric effects associated with the structure and the size of molecules relative to those of the pores at the membrane surface.

In summary, the requirements for the operational success of the membrane separation process are an appropriate chemical nature of the membrane material, and the existence of pores of appropriate size and number at the membrane surface.

2.3 TRANSPORT MODEL

The surface force - pore flow model for reverse osmosis separations was developed by Matsuura and Sourirajan (28, 31) as a quantitative expression of the preferential sorption - capillary flow mechanism. This transport model is applicable to aqueous solution - reverse osmosis membrane systems involving preferential sorption of either water or solute at the membrane - solution interface.

The transport equations which constitute the transport model were derived based on three major considerations:

1. Pore Structure: Circular cylindrical pores of radius R and effective pore length δ; equivalent to the thickness of the active skin layer.

2. Transport Mechanism: Solute-solvent transport through the membrane pores is governed by surface forces, pressure, friction and viscous shear forces.

3. Interaction Forces: The solute-membrane material interactions, relative to water, are adequately represented by electrostatic or Lennard Jones type surface potential functions expressed as interfacial parameters, $\underset{\sim}{A}$, $\underset{\sim}{B}$, $\underset{\sim}{D}$.

The interfacial parameters, defined below, depend on the chemical nature of the solute, solvent and the membrane material and their mutual interactions. The parameters $\underset{\sim}{A}$ and $\underset{\sim}{B}$ are obtained by the analysis of liquid chromatography data. $\underset{\sim}{D}$ is usually approximated by the stokes radius, although they are not identical.

Interfacial Parameters:

$\underset{\sim}{A}$ = electrostatic repulsive force constant characteristic of the ionic solute (+ L)

$\underset{\sim}{B}$ = short range van der Waals force constant characteristic of the nonionized organic solute (+/- L^3)

$\underset{\sim}{D}$ = steric hindrance of the solute at the interface (+ L)

The pore structure at the membrane surface may be represented by either of the following:

i. a single pore radius, R

ii. a normal distribution of pores with average pore radius $\bar{R}$, and standard deviation σ.

iii. a bi-normal distribution of pores with average pore radius $\bar{R}_1$ and $\bar{R}_2$, and corresponding standard deviations σ_1 , σ_2; with a factor h_2 defined as

$$h_2 = \frac{\text{no. pores in 2nd distribution}}{\text{no. pores in 1st distribution}}$$

As expressed by schemes I, II and III, given below, the surface force - pore flow model can be applied to predict membrane performance (f, PR/PWP) and, alternatively, to evaluate the surface pore structure of the membrane in each of cases i, ii and iii, above. The input variables required consist of the interfacial parameters ($\underset{\sim}{A}$ and/or $\underset{\sim}{B}$ depending on the nature of the solute, and $\underset{\sim}{D}$) and the diffusivity of solute in water (Dab).

Scheme I.:

Transport Equations I.

$\underset{\sim}{A}$, $\underset{\sim}{B}$, $\underset{\sim}{D}$, Dab, R ---------- f, PR/PWP

Scheme II.:

$\underline{A}$, $\underline{B}$, $\underline{D}$, Dab, $(\bar{R}, \sigma)$ ---(Transport Equations II.)---> f, PR/PWP

Scheme III.

$\underline{A}$, $\underline{B}$, $\underline{D}$, Dab, $(\bar{R}_1, \sigma_1)$, $(\bar{R}_2, \sigma_2)$, h_2 ---(Transport Equations III.)---> f, PR/PWP

Simplified expressions for the transport equations are given below with respect to solute separation and the ratio PR/PWP respectively. The mathematical derivations involved in the analysis and the detailed transport equations are given elsewhere (27).

Transport Equations I.

$$f = F(\alpha(\rho), b(\rho), \rho, \phi(\rho)) \quad (4a)$$

$$PR/PWP = P(\alpha(\rho), \rho, \beta_1, \beta_2) \quad (4b)$$

Transport Equations II.

$$f = \int_0^\infty Y(R) \; F \; dR \quad (5a)$$

$$PR/PWP = \int_0^\infty Y(R) \; P \; dR \quad (5b)$$

Transport Equations III.

$$f = \sum_i h_i \int_0^\infty Y(R_i) \; F \; dR_i, \; i = 1,2 \quad (6a)$$

$$PR/PWP = \sum_i h_i \int_0^\infty Y(R_i) \; P \; dR_i, \; i = 1,2 \quad (6b)$$

For the multipore systems (cases II and III), the distribution function, Y, was integrated to adequately predict membrane performance. The dimensionless quantities are defined as follows:

ρ radial distance

$\alpha(\rho)$ solution velocity in the pore

β_1 solution viscosity

β_2 operating pressure

$\phi(\rho)$ potential function

$b(\rho)$ friction function

The dimensionless radial velocity profile in the pore, $\alpha(\rho)$, is obtained by solving a differential equation.

The normal and bi-normal pore size distributions as well as the single pore are commonly used to represent the surface pore structure. However, it has been shown (29) that it is the bi-normal distribution which is often the most adequate. The later was adopted in this study to represent the surface pore structure of the polyethersulfone membrane.

2.4 DETERMINATION OF PORE SIZE DISTRIBUTION

The pore structure at the membrane surface is a physical property of the membrane which can not be accurately measured by any analytical or optical method. The average size and size distribution of pores, however, can be predicted on the basis of the transport model from the analysis of the membrane performance data for reference solutes (27). With this method the interfacial parameters $\underline{A}$ (for ionized solutes) and/or $\underline{B}$ (for nonionized organic solutes) with respect to each solute are evaluated by the High Performance Liquid Chromatography method (39) from an appreciation of the interaction forces working between the membrane material and solute. For purposes of analysis with chosen reference solutes, the value of $\underline{D}$ is equated to Stokes radius however, in principle, it is not identical with Stokes radius.

The procedure used in this work was to apply the surface force - pore flow model to the reverse osmosis data of polyethylene glycol (PEG) solutes, the molecular weight of which covered the range from 300 to 15,000. An iterative method was used by which the five parameters in the bi-normal pore size distribution were first assumed. Then by fitting the calculated separation data to the experimental ones the most probable pore size distribution for the membrane was determined. A simplified algorithm to describe the iterative procedure is given in Figure 2.

FIGURE 2

SIMPLIFIED ALGORITHM OF THE PROCEDURE IN PORE SIZE DISTRIBUTION ANALYSIS

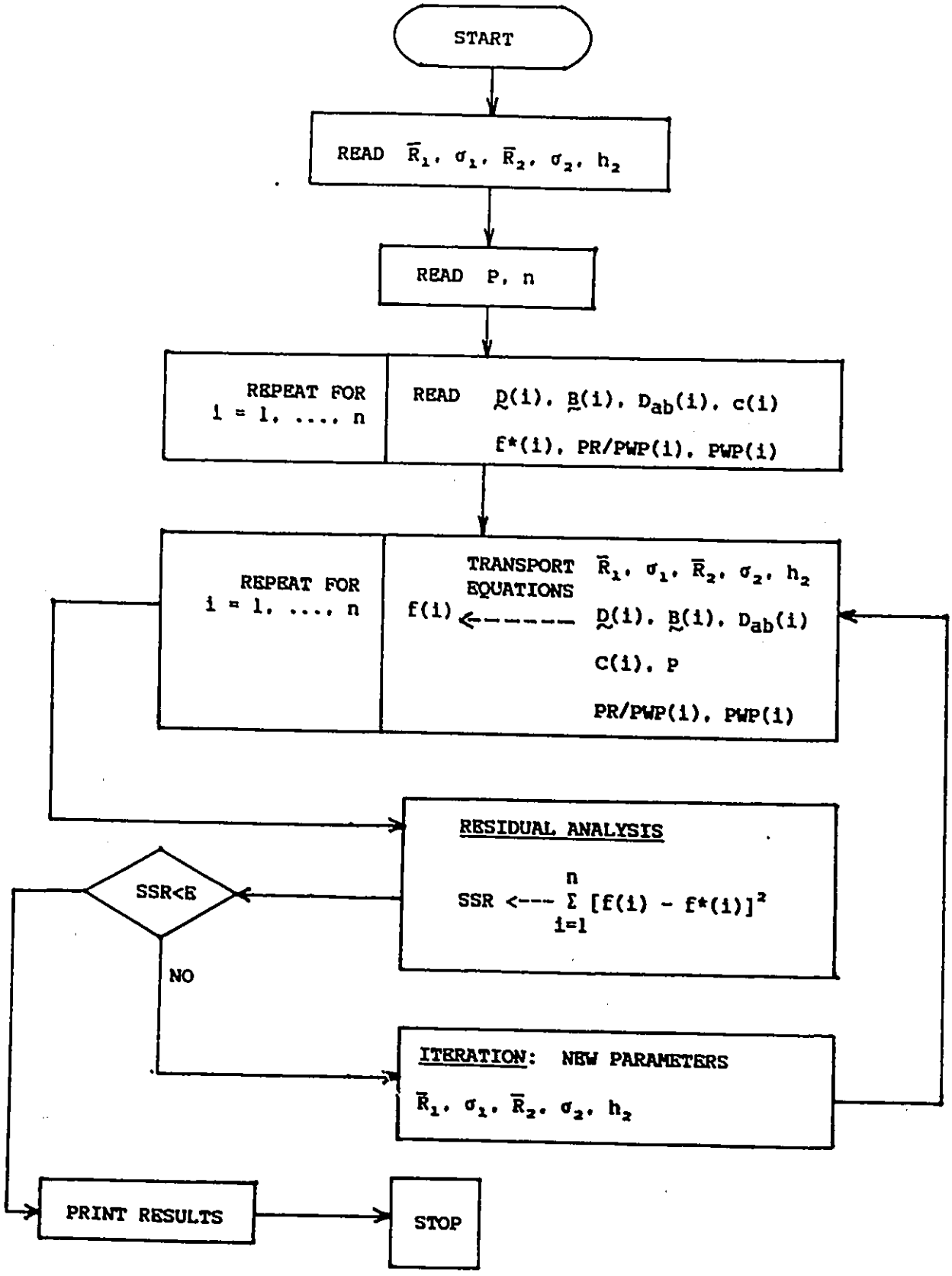
START
READ $\bar{R}_1$, σ_1, $\bar{R}_2$, σ_2, h_2
READ P, n
REPEAT FOR i = 1, ... n
READ $\underset{\sim}{D}(i)$, $\underset{\sim}{B}(i)$, $D_{ab}(i)$, c(i)
f*(i), PR/PWP(i), PWP(i)
REPEAT FOR i = 1, ... n
TRANSPORT EQUATIONS
f(i) <------
$\bar{R}_1$, σ_1, $\bar{R}_2$, σ_2, h_2
$\underset{\sim}{D}(i)$, $\underset{\sim}{B}(i)$, $D_{ab}(i)$
C(i), P
PR/PWP(i), PWP(i)
RESIDUAL ANALYSIS
SSR <--- $\sum_{i=1}^{n} [f(i) - f^*(i)]^2$
SSR<E
NO
ITERATION: NEW PARAMETERS
$\bar{R}_1$, σ_1, $\bar{R}_2$, σ_2, h_2
PRINT RESULTS
STOP

For the operation, a computer program of the transport model available from the National Research Council of Canada (NRCC) was used. A nonlinear regression routine (Nonlin from the Watfiv program library at University of Ottawa) was incorporated for improved convergence. The program algorithm is given in Appendix 2. The interfacial parameters $\underset{\sim}{B}$ and $\underset{\sim}{D}$ for the PEG solutes used as probes are given in Appendix 3.

2.5 MEMBRANE FORMATION PROCESS

The majority of synthetic membranes are made from polymer solutions by the phase inversion process. The homogeneous polymer solution is brought to phase separation by means of a penetrating nonsolvent and/or solvent outflow resulting in the formation of a solid polymer network.

The phase inversion process covers a range of different techniques, each producing a membrane with a specific structure and performance. In particular, the Loeb-Sourirajan or immersion precipitation technique produces membranes with an asymmetric porous structure as shown in Figure 1. These membranes have transport properties in RO/UF experiments governed by the transport characteristics of the thin active layer at the membrane surface. The supporting porous layer posesses negligible hydraulic resistance and is present for mechanical support only.

In the Loeb-Sourirajan technique a thin film of polymer solution is formed into a membrane following a two step process, evaporation and gelation, to precipitate the polymer. The appropriate formulation of the polymer casting solution is an essential requirement for the formation of the asymmetric structure of the membrane. The technique will be described and the membrane formation process explained:

A) Formulation of the casting solution

The casting solution consists in a binary or tertiary polymer solution . It is composed of a polymer (P), solvent (S), and optionally a nonsolvent (NS, often called swelling agent or additive) in suitable proportions for membrane making. Selection criteria are that S be relatively more volatile than the NS; and that both S and NS be highly soluble in a chosen gelation medium or precipitant (such as water) which itself is a nonsolvent for the polymer.

B) Evaporation

A film of polymer solution is first cast onto a smooth surface under controlled atmospheric conditions. Subsequently, solvent is partially removed by evaporation under controlled conditions. When a critical polymer concentration is reached, phase separation occurs leading to a network of polymer molecules in the surface layer of the film. The orientation in the polymer network depends on the polymer structure in the casting solution and on the desolvation conditions. Phase separation below the film surface, where solvent depletion was less, lead to the formation and agglomeration of droplets of the nonsolvent swelling agent.

C) Gelation

The subsequent immersion of the polymer film in the gelation medium accelerates and completes the desolvation process with respect to both the solvent and the nonsolvent swelling agent in the surface layer, and in the bulk region underneath. During the desolvation process the microporous surface structure is formed. In the interior bulk region of the film, the polymer molecules aggregate and precipitate rapidly giving rise to a spongy porous mass underneath the surface layer.

The foregoing mechanism of pore formation leading to an asymmetric porous structure for the membrane has been interpreted differently by other scientists in the field.

Parameters in Membrane Formation

Several phenomenological studies on the effects of individual parameters in membrane formation have been reported in the literature. It has been shown that the thickness of the active layer, the mean pore diameter, the shape of the pores, and the porosity of the supporting framework can be varied within certain limits by adjusting the composition of the casting solution and the conditions of membrane fabrication. Parameters at each step of the membrane formation process which have been identified as controlling the detailed porous structure of the membrane are listed below:

STEP	PARAMETER (affecting porous structure)
Casting Solution	- Composition (choice of S, NS and NS and their concentration)
	- Polymer Concentration
	- Viscosity
	- Temperature
Solvent Evaporation	- Duration
	- Nature & Conditions of Gas Phase
Gelation / Immersion Precipitation	- Nature of Gelation Medium
	- Temperature

Other parameters, more limiting, include physico-chemical properties of the polymer/solvent/nonsolvent system. In particular, the "quality" of the solvent and the "power" of the precipitation agent have solubility effects controlling the pore structure of the synthetic gel membrane. The interfacial tension is one parameter determining the relative thickness of the active layer.

2.6 VISCOELASTIC APPROACH TO PORE FORMATION

For membranes formed by the phase inversion process, the morphology is determined by the orientation of the polymer network which depends on the polymer structure in the casting solution and on the desolvation conditions. Hence forth, the thin active layer and the pore structure at the surface of asymmetric membranes which is formed upon the initial evaporation of solvent from the film of casting solution depends on the polymer structure at the surface of the casting solution and on the desolvation conditions, mostly during evaporation.

The precise disposition of the polymer material within the casting solution is determined by its solution structure (i.e. the overall thermodynamic state of the film of casting solution) which is a function of its composition and temperature. Such disposition of the polymer material gives rise to the existence of supermolecular polymer aggregates within the casting solution, each with its own network of polymer segments.

Using the concept of solution structure, the possibility of two distinct pore systems at the surface of membranes made by the phase inversion process have been identified (21). The polymer network pores, in the first distribution, originate from the void spaces between polymer segments within the network of each individual polymer aggregate. The polymer aggregate pores, in the second distribution, originate from the void spaces among neighboring polymer aggregate themselves. A schematic representation of the polymer network and aggregate pores is given in Figure 3. The network pores are relatively far smaller but more abundant compared to the polymer aggregate pores.

Prediction of Aggregate Pore Size from Viscometric Data

The average pore size and the pore size distribution at the membrane surface which are related to the polymer structure in the casting solution can be studied on the basis of the viscometric data for the polymer solution. The approach will be described.

According to the Mark-Houwink equation, the intrinsic viscosity is an exponential function of the molecular weight of the polymer aggregate, Mn.

Mark-Houwink equation:

$$[\eta] = K\, Mn^{\alpha} \qquad (7)$$

where K and α are constant for a given polymer solution and temperature.

Initially, K and α are calculated for the polymer/ solvent binary system from the intrinsic viscosity measurement at 25 °C; and given the polymer molecular weight. Subsequently, the intrinsic viscosity of the polymer solution in presence of the nonsolvent swelling agent is measured.

FIGURE 3

ORIGIN OF POLYMER AGGREGATE PORES AND POLYMER NETWORK PORES

VISCOELASTIC APPROACH TO PORE FORMATION

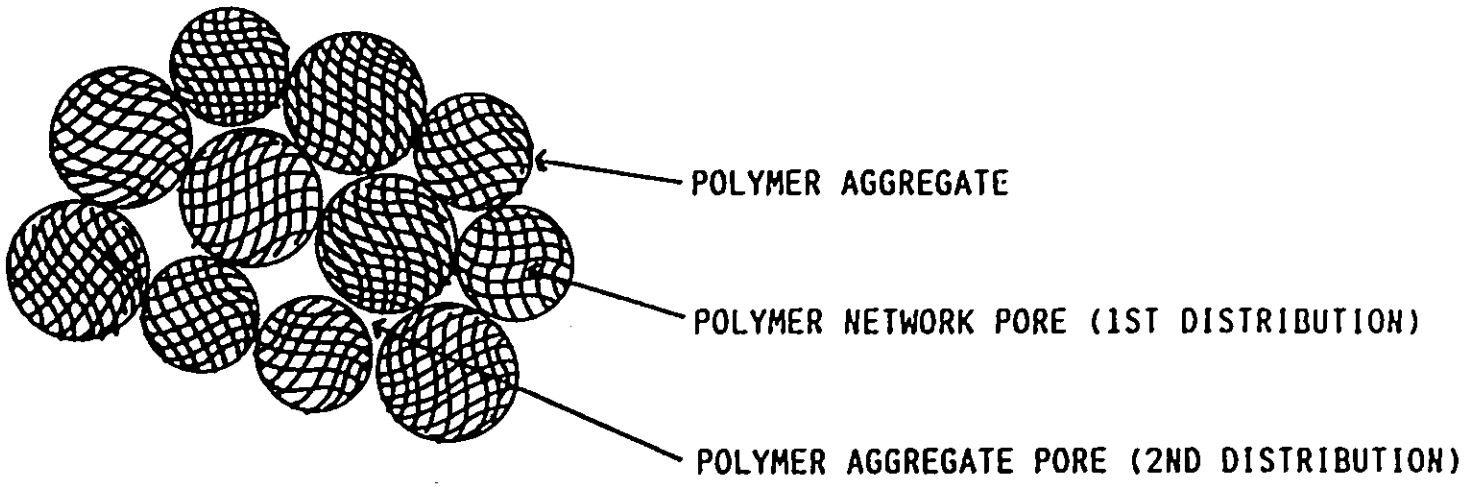

By assuming that the hydrodynamic behaviours of the polymer in the solvent in presence of nonsolvent are the same as in the absence of nonsolvent, the Mark-Houwink constants obtained above could be applied to the intrinsic viscosity in the presence of nonsolvent. Thereby, the molecular weight of the polymer aggregate in the presence of nonsolvent, designated as Mn*, could be calculated. Given the molecular weight of the polymer, Mn, the number of polymer molecules in one polymer aggregate could be calculated as follows:

$$n = Mn^* / Mn \qquad (8)$$

The quantities n and Mn* obtained above are assumed to remain constant as the polymer concentration in the solution changes; thus, representing the polymer structure as existing in the concentrated casting solution.

Based on the intrinsic viscosity results the size of polymer aggregates in the casting solution can be determined. A method was developed by Rudin and Johnston (40), whereby the radius of a spherical particle in solution (equivalent to the radius of the spherical polymer aggregate) can be calculated using

$$\langle \hat{S} \rangle = \left[\frac{3 \nu \epsilon}{4\pi} \right]^{1/3} \qquad (9)$$

where ν is the volume of an unsolvated polymer molecule and ϵ is the effective volume factor. Johnston and Sourirajan (41) modified the equation to calculate ϵ, to suit concentrated casting solutions more adequately.

This analysis led to a method for studying the pore structure of the membrane, and more specifically the average pore size and pore size distribution at the membrane surface on the basis of the viscoelastic properties of the membrane casting solution. A theoretical approach was proposed by Nguyen et al. (2); it makes use of statistical thermodynamics to predict the distribution of polymer aggregates in the film of casting solution, in particular at the solution surface. Based on the size and distribution of polymer aggregates at the solution surface the size of aggregate pores (those originating from the space devoid of aggregates) can be evaluated. The latter can be compared to the average pore size obtained by the analysis of RO/UF experimental data using the transport model.

3. EXPERIMENTAL

3.1 MATERIALS

Membranes are prepared from casting solutions consisting of homogeneous mixtures of a polymer, solvent, and nonsolvent in adequate proportions for casting The membranes prepared thereof are tested in RO/UF experiments using aqueous feed solutions of different probe solutes. The materials involved in these operations will be described in this section.

Polymer)

Polyethersulfone (PES) grade 200P supplied by Imperial Chemical Industries under the trade name Victrex was used. Its molecular weight was approximately 30,000 as determined by the method of Gel Permeation Chromatography. The chemical structure of PES is given below:

Polyethersulfone

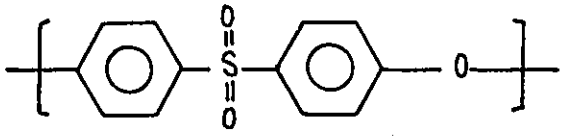

Solvent)

On the basis of the solution stability and viscosity data reported in the technical literature N-methyl-Pyrrolidone (NMP) was selected as solvent for PES in the casting solutions. The chemical structure of NMP is given below:

N-methyl-pyrrolidone

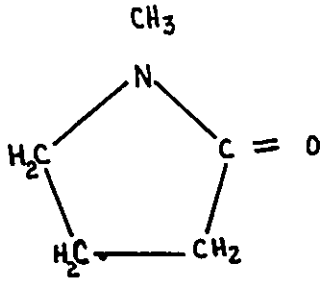

Two different grades of NMP were initially considered for use: a "purified" grade supplied by Fisher and a "practical" grade supplied by Baker. Preliminary studies used casting solutions of each solvent to prepare membranes. The performance of resulting membranes were compared to discriminate between the two solvents. The "purified" grade NMP was prefered and thus was selected for further use. It was used without further laboratory purification.

Nonsolvent)

The nonsolvent swelling agent, an optional component in the casting solution, was polyvinyl pyrrolidone (PVP). It is a water soluble, synthetic polymeric compound with 10,000 molecular weight. It has the following monomer-unit structure:

Polyvinylpyrrolidone

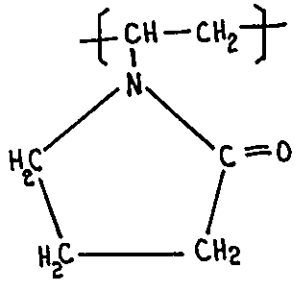

Probe Solutes)

Aqueous solutions of organic solutes were used in RO/UF experiments. These solutes included polyethylene glycol (PEG) polymers of mean molecular weights 300 to 15,000 and Dextrans of mean molecular weights 9,000 to 40M.

3.2 EQUIPMENT

The Reverse Osmosis / Ultrafiltration (RO/UF) test consisted of circulating the feed solution under pressure past the surface of the membrane which was enclosed in a laboratory test cell. The membrane permeated product was collected at atmospheric conditions.

A high pressure test cell with thin channel flow, illustrated in Figure 4, was used to hold the membrane in the RO/UF experiments. The test cell was secured between two heavy iron flanges joined by three bolts. Thin channel flow is a characteristic of the cell design meant to promote turbulence inside the chamber on the high pressure side of the membrane. The small membrane sample, with 14.5 cm sq. surface area, is supported on a porous metal plate to resist the high operating pressures. The two ports are for the permeate and retentate respectively. The material of construction was 304 SS for the cell and 316 SS for the porous plate.

The actual membrane testing unit, shown in Figure 5, consisted of twelve test cells assembled in series. The feed was circulated via a Hydracell diaphragm pump with a surge tank at the outlet to dampen fluctuations in pressure. Under normal operating mode the retentate (feed) from the last cell was recycled to the feed tank together with the permeate streams from each of the twelve cells. The feed tank was continuously stirred. The temperature of the feed was maintained at 25°C by means of a coil in the feed line immersed in a temperature controlled bath.

The pressure gauge, with 300 psig capacity, was installed on-line with connections before and after the series of test cells. The pressure drop across the twelve cells, which could easily be monitored, averaged 10 psig for a normal operating pressure of 55 psig upstream. Both the pressure gauge and rotameter had been calibrated prior to use.

3.3 MEMBRANE FABRICATION

The membranes were fabricated in the laboratory by the Loeb - Sourirajan technique which produces membranes with an asymmetric porous structure. Initially, the casting solution of appropriate composition was prepared. Then it was formed into a thin film which upon evaporation of some solvent, and subsequent extraction of the nonsolvent and remaining solvent resulted in a solid polymer network. The membrane so produced could be subjected to post-treatments to alter the pore structure and bring it up to desired specifications.

FIGURE 4

DESIGN OF A THIN CHANNEL FLOW CELL TO TEST ULTRAFILTRATION MEMBRANES

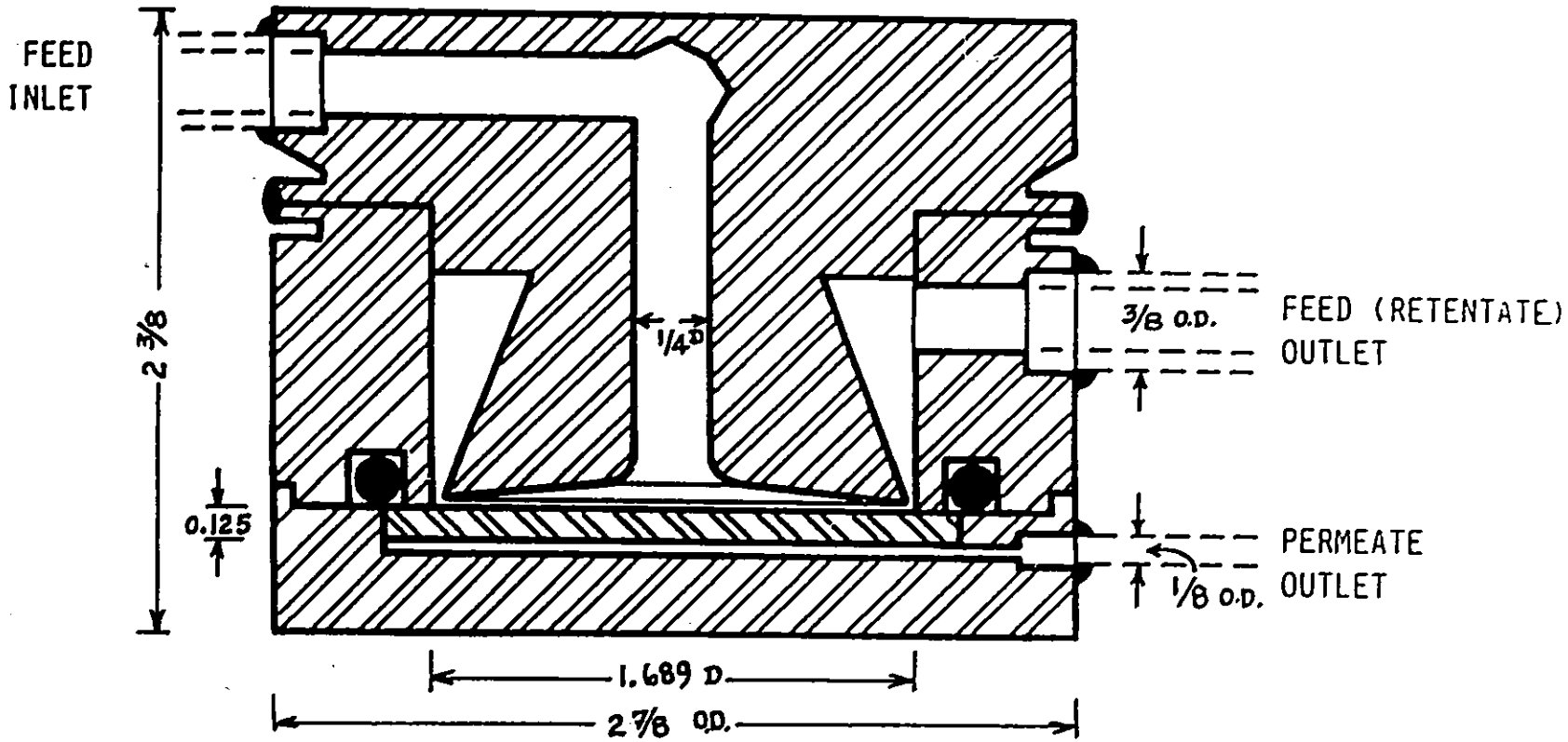

DIMENSIONS ARE IN INCHES.

FIGURE 5

ULTRAFILTRATION MEMBRANE TESTING UNIT FEATURING TWELVE TEST CELLS IN SERIES

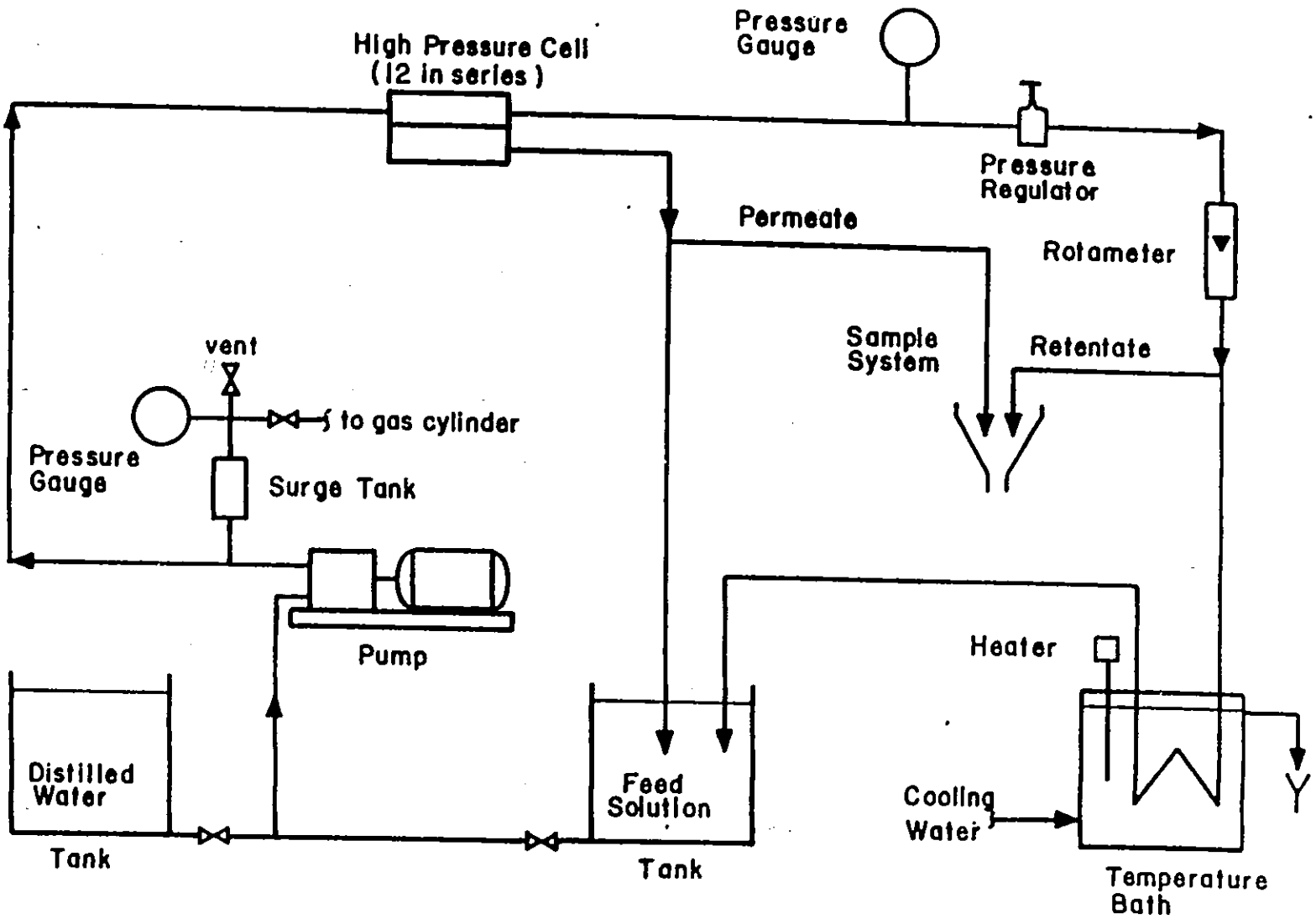
High Pressure Cell
(12 in series)
Pressure
Gauge
Pressure
Regulator
Permeate
Rotameter
Sample
System
Retentate
vent
to gas cylinder
Pressure
Gauge
Surge Tank
Pump
Heater
Distilled
Water
Tank
Feed
Solution
Tank
Cooling
Water
Temperature
Bath

3.3.1 CASTING SOLUTION PREPARATION AND HANDLING

The casting solutions used in making the membranes consisted in homogeneous mixtures of three components: polyethersulfone, N-methyl-pyrrolidone and polyvinyl- pyrrolidone, the latter being an optional component. The polymer, polyethersulfone, was dried in a convection oven at 150°C for three hours prior to preparing the solution. The other components were used without further treatment.

Casting solutions, total weight 200 g, were individually prepared in clean 500 ml stopper bottles. Weighted quantities of the componentss were incorporated in the order: solvent, polymer, nonsolvent. Dissolution was initiated by manually agitating the bottle, then gases were released by removing the stopper. The bottle was tightly closed and sealed with several layers of electric tape. The bottle was put on mechanical rollers for the solution to mix until a smooth polymer solution was obtained. Mixing could last from 3 days to 3 weeks depending on the composition of the solution. For some highly concentrated solutions, the bottles were warmed using intense lighting during the mixing process.

Prior to use in membrane making the solutions were required to stand for at least one day to allow any solid particles to settle. In most cases, the solutions were only used 1 or 2 months after they had been prepared. They had been stored at laboratory temperature and lighting. It was assumed that polymer degradation did not occur in that period of time and those conditions. As mentionned previously, the Victrex technical literature reports that such solutions should be stable for periods longer than a month; Tweddle et al. reported a period longer than a year.

For the study 36 casting solutions, different in composition, were prepared. The composition 20 wt.% PES, 80 wt.% NMP was defined as the reference casting solution.

3.3.2 SELECTION OF CASTING SOLUTION COMPOSITIONS

The tertiary diagram for the system PES/NMP/PVP was used for the systematic selection of the casting solution compositions. Initially, an apparent region of solubility was defined which incorporated the successful solutions reported in the literature, as shown in Figure 6.

The procedure for selecting the solution compositions will be explained with reference to the tertiary diagram in Figure 7. Equidistant lines of constant nonsolvent to polymer (PVP/PES) ratio were drawn originating from the pure solvent apex. Solution compositions were selected within the solubility region at each intersection of lines with PVP/PES equal to 0.0 (100% PES), 0.2, 0.5, 1.0, 2.0, and 5.0 with the following lines of constant polymer concentration: 10, 15, 20, 25, 30, 32, 35 weight percent PES. Following this procedure 27 compositions were selected. The list was increased by 4 other compositions chosen between PVP/PES lines.

On the basis of RO/UF results for membranes produced from the above solutions other solution compositions of interest were selected. Those included solutions with PVP/PES = 0.75 and polymer concentration: 15, 18, 20, 21, and 25 weight percent PES. Further, the need for a solution with 25 wt.% PES and 2 wt.% PVP was identified since the membrane from the 0.0 wt.% PVP (PVP/PES = 0) casting solution did not produce any permeate.

A code system was devised to identify the casting solutions on the basis of their composition; it was also used to identify membranes from these casting solutions. The code which had the form S(P - R) referred to the weight percent PES in the casting solution, termed P, and to the weight ratio PVP/PES, termed R. For example, S(15 - 0.5) would refer to membranes prepared from the casting solution of composition 15 wt. % PES, and PVP/PES (weight ratio) equal to 0.5.

The above casting solutions were all prepared for subsequent use in membrane making; with the exception of solution S(32 - 1.0) which did not dissolve. This brought the total number of casting solutions to 36.

FIGURE 6

CASTING SOLUTION COMPOSITIONS FOR THE SYSTEM PES-NMP-PVP REPORTED IN THE LITERATURE; AND PROPOSED SOLUBILITY LIMITS

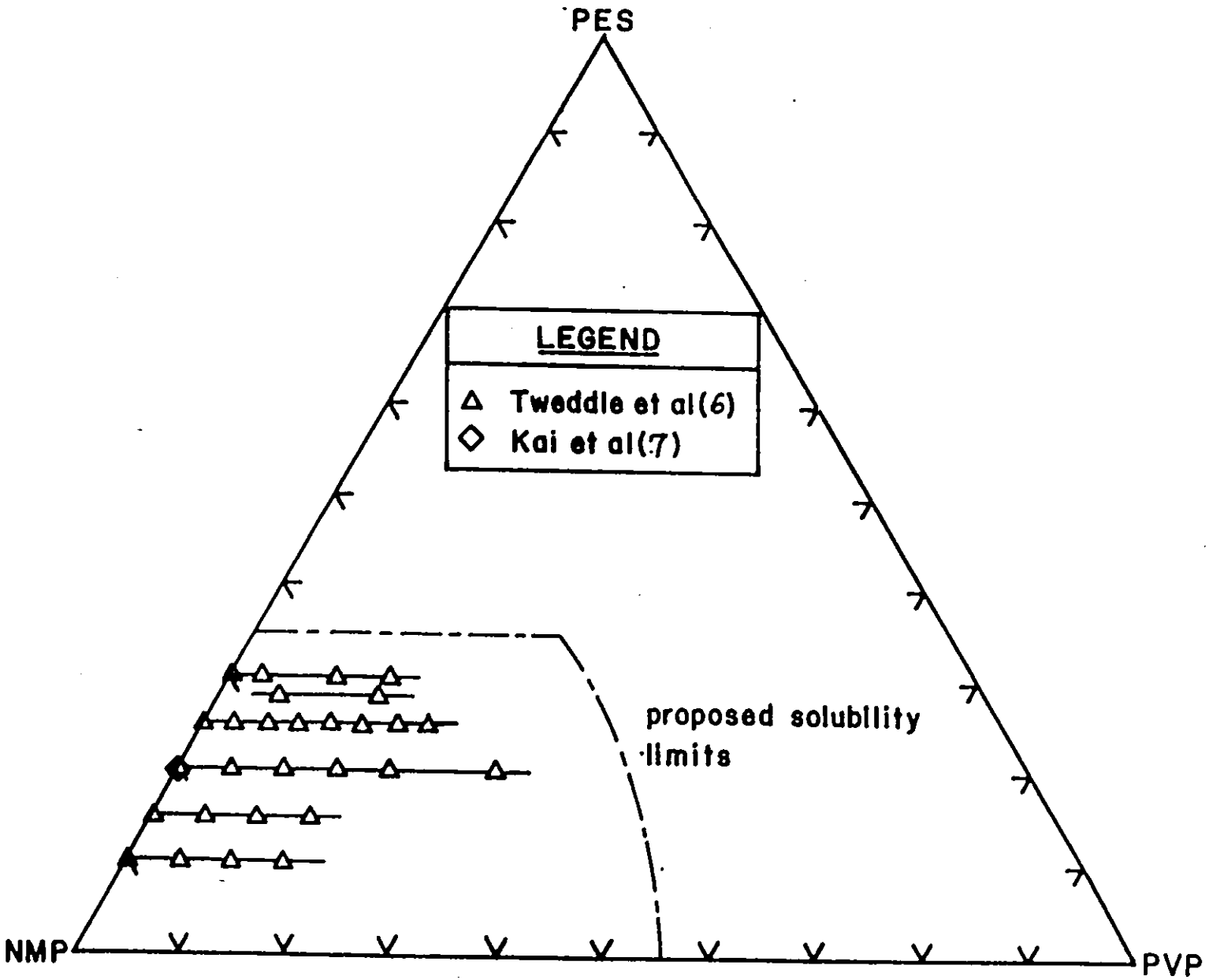
PES
LEGEND
Tweddle et al(6)
Kai et al(7)
proposed solubility limits
NMP
PVP

FIGURE 7

MAP OF CASTING SOLUTION COMPOSITIONS (PBS-NMP-PVP)
USED IN THE STUDY

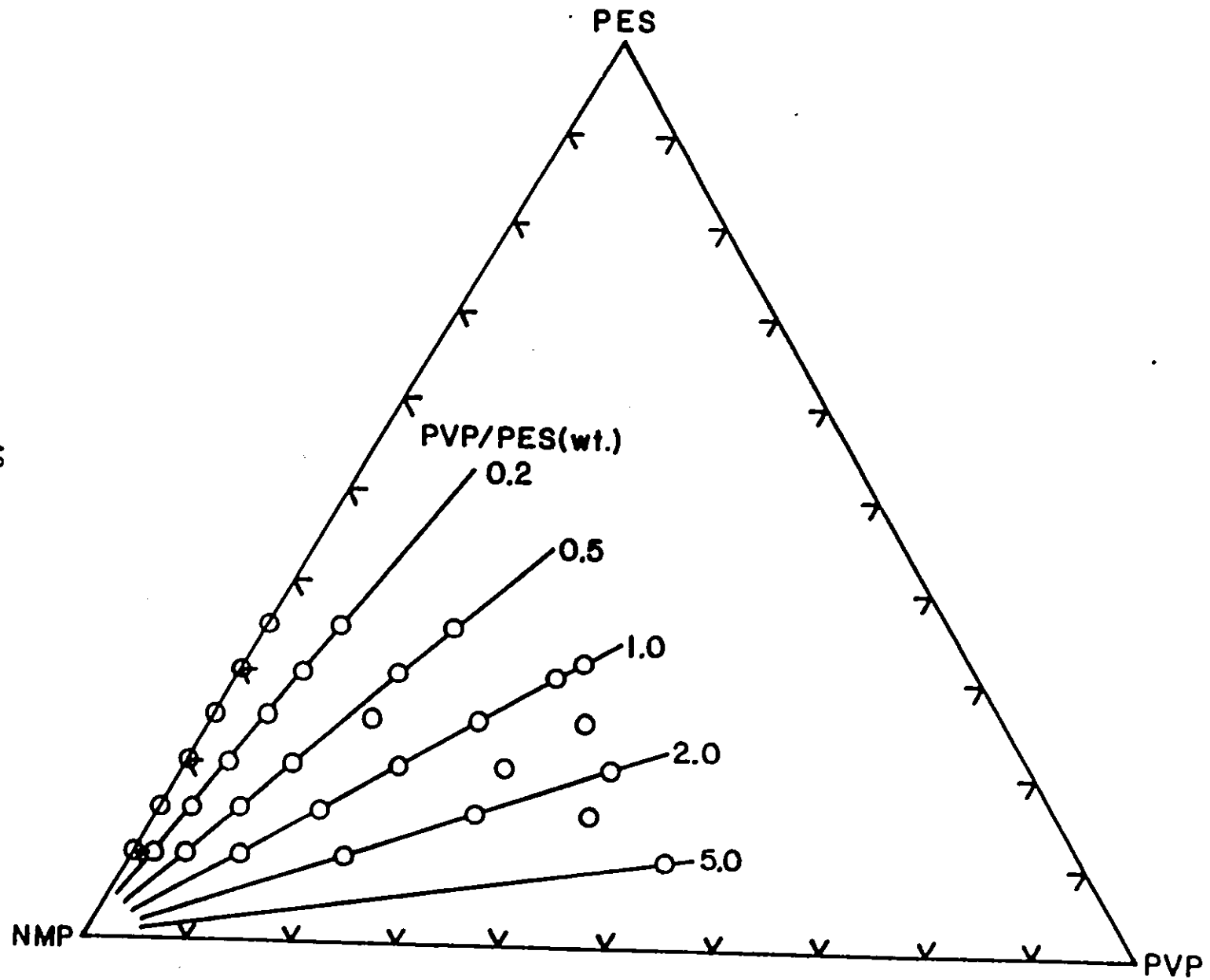
PES
PVP/PES(wt.)
0.2
0.5
1.0
2.0
5.0
NMP
PVP

3.3.3 MEMBRANE MAKING PROCEDURE

Membranes were made from each of the 36 casting solutions in several different casting sessions. As control for the reproducibility of casting conditions, a membrane of the reference casting solution S(20 - 0.0) was made at every casting session. The membrane making procedure will now be oultlined:

CASTING)

A generous amount of polymer solution was poured on one end of a smooth glass plate, previously cleaned with acetone. A thin film of the solution was applied over the plate by spreading with a doctor blade across the lenght in a smooth motion. During the process of spreading a constant pressure was applied on the blade to obtain a more uniform film thickness. The specific doctor blade used had an opening of 0.010 inch (0.025 cm).

EVAPORATION)

The thin film of polymer solution was exposed to laboratory atmosphere for a 1 minute period during which time evaporation of solvent from the cast film occured and a microscopic porous layer was formed at the surface. The prevailing atmospheric conditions were important parameters at this stage of the formation process; high relative humidities were avoided since they can be destructive. Typical conditions were 20 to 24°C room temperature and 20 to 28 % relative humidity. However, in the first part of the work which investigated the membrane fabrication technique some membranes (to be identified later) were formed under higher, 47 to 51 %, relative humidity conditions.

GELATION)

After evaporation, the thin film (on the glass plate) was immersed in a gelation bath containing ice cold water (0 - 5°C) for 15 minutes. During gelation the solvent and nonsolvent in the polymer solution film are exchanged with the gelation medium (water). Subsequently, the polymer precipitates to form the solid PES polymer matrix, called membrane. In that process the membrane naturally detached itself from the plate.

The resulting PES membrane was smaller than the cast film; during gelation shrinkage occured because of the hydrophobic character of polyethersulfone. This effect was monitored by measuring the width of the film before and of the membrane at different times through the gelation process. Typically, the reduction in width was in the 17 - 20 % range.

Following gelation, the membranes were transfered to a distilled water bath at room temperature. The membrane sheets were cut into circular coupons 6.7 cm in diameter. Approximately five coupons were obtained per membrane sheet. For each coupon the thickness was measured and a code number was written on its top surface. The membrane coupons were then stored in distilled water and refrigerated.

In the discussion (section 4) the membrane coupons will be referred to as membrane samples. This is because they are actually samples from a common set, which are the membranes prepared from a given casting solution composition; and, ideally, they should be identical.

3.3.4 MEMBRANE POST-TREATMENT

Membranes can be subjected to post-treatments to alter their porous structure and meet desired specifications. Annealing is one type of post-treatment which consists in subjecting the membrane to heat by immersion in a hot medium (liquid) for a definite time period. The variables associated with annealing are the following:

1. nature of liquid medium
2. temperature
3. duration of exposure

Several annealing post-treatments were tried which differed by one or more of the above variables. The procedure for the annealing treatment of membranes will now be described:

i) In preparation for the treatment, the membrane was set flat between two glass plates. These were separated such that the liquid could circulate and contact the membrane.

TABLE 3

DESCRIPTION OF ANNEALING POST-TREATMENTS INVESTIGATED

A - Various Annealing Conditions

Treatment	# Replicates (a)	Liquid Medium	T, °C	t, min.
I	5	Water	90	15
II	2	Aqueous H_2SO_4 (5 v%)	50	15
III	4	Ethylene glycol	100	15
Untreated	13			

B - Annealing in Ethylene Glycol - Effects of Temperature and Time

Treatment	# Replicates (a)	T, °C	t, min.
IV	4	100	15
V	4	120	15
VI	4	150	15
VII	2	170	15
Untreated	10		
VIII	2	50	5
IX	2	100	5
X	2	120	5
XI	3	150	5
Untreated	3		

(a) # replicates = no. of membrane samples subjected to the same post-treatment

ii) The liquid in the bath was preheated to the desired temperature. Good mixing was provided by a magnetic stirring bar.

iii) The membrane was immersed in the hot liquid and maintained there for a short time. The glass plates (containing the membrane) were suspended in the bath above the space for the stirring bar. A glass cover containing ice was kept above the bath to condense the vapours.

iv) At the elapsed time, the membrane was removed from the bath and promptly transfered to a distilled water bath at room temperature.

In cases where a non-aquous (organic) liquid was used, the membrane was solvent-exchanged with the liquid (to displace the water) prior to the treatment. The membrane initially in distilled water was washed with a small quantity of the organic liquid, then soaked in this for thirty minutes prior to the treatment. Following the treament, the membrane was transfered directly to distilled water to cool, and carefully washed to remove traces of the organic liquid.

3.4 EVALUATION OF MEMBRANE PERFORMANCE PARAMETERS

In the RO/UF experiments the feed solution under pressure was contacted with a small area (14.5 cm. sq.) of the membrane surface; and the membrane permeated product was recovered at ambient conditions. Membrane performance was evaluated from data on pure water permeation (PWP) using a distilled water feed; product rate (PR) and solute separation (f) for a given aqueous feed solution.

The product rate, PR, was obtained by measuring the time required to collect a small sample ($\sim$ 20 cc) of the permeate from under the membrane. The product rate at°25 C was calculated as follows:

$$PR = \frac{Ws}{ts} \times K \times 60 \qquad (g/hr.A) \qquad (10)$$

where Ws = sample weight, g
ts = sampling time, min.
K = correction factor for 25°C, based on relative viscosity and density for pure water
A = membrane surface area = 14.5 cm^2.

The pure water permeation rate, PWP, obtained using the distilled water feed as opposed to an aqueous solution (as in the case of PR) was determined by the same method as PR. Both the PR and PWP permeate samples obtained by RO/UF experiments at a given set of operating conditions were used to determine solute separation with respect to each membrane. Solute separation, f, was calculated as follows:

$$f = \frac{C^*feed - C^*pr}{C^*feed} \times 100\% \qquad (11)$$

where C*feed = Cfeed - Cdw
C*pr = Cpr - Cpwp

C = organic solute concentration, ppm
and dw = distilled water

The organic solute concentration, C, was determined using a Beckman Total Organic Carbon Analyzer Model 915 B. Prior to each session the instrument was calibrated using aqueous solutions of reference solute PEG-6000 in concentrations ranging from 10 ppm to 250 ppm. A typical calibration curve is given in appendix 4. Since 12 membranes were tested at once, each analytical session included 12 PR samples, a feed and a distilled water sample. It also included a composite PWP sample which was formed by mixing the 12 PWP samples. When the samples were not analyzed the same day they had been collected they were kept refrigerated.

3.5 REVERSE OSMOSIS / ULTRAFILTRATION EXPERIMENTS

Typically, membrane performance is determined from data on PWP, PR and f obtained by RO/UF experiments using a distilled water feed and an aqueous feed solution respectively. Membrane characterization which is determined from the performance data with respect to several solutes involves a sequence of RO/UF experiments, each using an aqueous solution with a different molecular weight solute.

There are several variables and corresponding responses involved in RO/UF experiments. These are given in Table 4, which also displays the standard test conditions used in this work. The time on stream and the membrane structural changes are the related variable and response in RO/UF experiments which can not be controlled.

The structural changes which a membrane could undergo in a given RO/UF experiment could affect its performance in subsequent RO/UF experiments. This emphasizes the need to minimize the changes in the membrane structure during a sequence of RO/UF experiments. The approach used to achieve this has been to stabilize the structure of the membrane by subjecting it to a pure water pressure prior to use in the sequence of RO/UF experiments. Another approach used in sequences of RO/UF experiments was to begin with the smaller molecular weight probe solutes. By this approach, the membrane pores blocked with the solutes from a RO/UF experiment would not affect the solute separation performance in subsequent experiments using higher molecular weight solutes. Finally, in order to detect any major changes in membrane structure during the course of the experimental program, the PWP was regularly measured.

The experimental procedure whereby 12 membranes were simultaneously tested in a sequence of RO/UF experiments will now be outlined.

EXPERIMENTAL PROCEDURE :

The membranes were carefully loaded into their individual test cells with the active surface upward to contact the feed. The membranes were assigned to the cells following the order of increasing permeability, such that the most porous was loaded in the twelfth cell.

TABLE 4

VARIABLES AND RESPONSES IN RO / UF EXPERIMENTS - DEFINITION OF STANDARD TEST CONDITIONS

VARIABLES

	Standard Condition
A. SYSTEM VARIABLES	
1. Nature of Solute	-
2. Nature of Solvent	water
3. Membrane Material	Polyethersulfone
4. Membrane Porous Structure	-
B. OPERATING VARIABLES	
1. Feed Concentration	200 ppm
2. System Pressure	50 psig
3. Feed Temperature	25 C
4. Feed Flowrate	2.2 L/min
C. Time on Stream	-

RESPONSES

A. MEMBRANE PERFORMANCE

1. Pure Water Permeation (PWP)
2. Product Rate (PR)
3. Solute Separation (f)

B. MEMBRANE PHYSICAL CHANGES (e.g. fouling, compaction)

The experimental procedure is divided into a series of steps including the actual RO/UF experiment or test run as follows:

i. Initial pure water permeation: PWPi

A pure water feed was circulated for one hour at the standard operating conditions. The initial pure water permeation rate (PWPi) was measured.

ii. Membrane stabilization:

Prior to subsequent use in RO/UF experiments the membrane was subjected to a pure water pressure of 60 psig (20% greater than the standard operating pressure) for a period of 3 hours; at standard feed flowrate and temperature. The purpose of this pre-treatment was to induce the compaction of the spongeous substructure in the membrane, thereby rendering the membrane more stable.

Following the three hours of pressurization, the membranes were relaxed by either circulating the pure water feed at reduced pressure, 50 psig, for 1 to 2 hours; or shuting down the unit overnight; or both.

iii. Pure water permeation: PWP

A pure water feed was circulated at the standard operating conditions. After 30 minutes, the pure water permeation rate (PWP) was measured by taking samples of the permeate at each cell.

iv. Test run:

A feed solution was circulated at the standard operating conditions for about 30 minutes. The product rate (PR) was measured by taking samples of the permeate at each cell. A feed sample was also taken.

v. System rinse:

The system was washed by circulating distilled water for 30 - 60 minutes at the standard operating conditions.

The procedure from step iii. to v. inclusively was repeated for each RO/UF experiment using a different test solute. In cases where an extensive amount of testing was required then step iii. was executed at every other test run only. When the set of membranes in the cells had been completely tested they were removed and stored in distilled water, and refrigerated. The PR and PWP samples were then analyzed to determine the solute separation; the procedure described in section 3.4 was followed.

3.6 INTRINSIC VISCOSITY DETERMINATION

To obtain the intrinsic viscosity of a polymer, $[\eta]$, the viscosities of the solvent and of solutions of different concentrations must be measured. The set of viscosity measurements were conducted by means of a Cannon - Ubbelohde viscometer; the capillary size was chosen so that kinetic energy corrections were not necessary. With this viscometer the solution originally introduced into the viscometer can be diluted with solvent to provide a series of concentrations. The experimental procedure for the intrinsic viscosity of a polymer is described as follows:

Prior to use the viscometer was cleaned using acetone and placed in a vented oven to dry; and subsequently allowed to cool. The viscometer was inserted into a temperature controlled bath and vertically aligned. A measured volume of solvent, 10 ml, was charged directly from a pipette into the reservoir of the viscometer. Approximately 20 minutes was allowed for the sample to come to bath temperature. The flux time was measured by allowing the liquid to flow freely down the viscometer capillary and measuring the time for the meniscus to travel from one mark to another.

A measured volume of the polymer solution (5 to 10 ml) was charged into the reservoir of the viscometer (already containing a volume of solvent) and the contents well mixed. At thermal equilibrium, the flux time for the dilute solution was measured by the above method. Henceforth, the solution composition was progressively changed with additions of solvent or polymer solution, and the flux time measured after each addition.

Possible sources of experimental error associated with this procedure are listed below in two parts:

a. Inaccuracies in

- concentration of original polymer solution
- volumes of solvent or polymer solutions
- flux time measurement
- bath temperature (controlled at 25°C)

b. Technical success in

- attainment of thermal equilibrium between the water in the bath and the contents of the viscometer
- vertical alignment of the viscometer
- cleanliness of the viscometer
- purity of solvent NMP (filtration operation)
- sensitivity of solvent to evaporation or absorption of water from the atmosphere

In making the viscosity measurements some precautions were taken in minimizing the experimental error from the sources stated above. For each flux time, check determinations were made until three exact repeats were obtained, or the average deviation was less than 0.2 seconds. The temperature was controlled at 25°C +/- 0.2°C.

The intrinsic viscosity of the polymer was determined by extrapolation of nsp/c to zero concentration. This is defined as

$$[n] = \lim_{c \to 0} (nsp/c) \qquad (12)$$

where [n] is intrinsic viscosity,

$$nsp = nrel - 1 \qquad (13)$$

is specific viscosity, and

$$nrel = (tc \times k) / (to \times k) = tc / to \qquad (14)$$

is relative viscosity , where

to = efflux time of solvent, s
tc = efflux time of solution, s
k = viscometer constant, cst/s
c = solution concentration, g/l

A linear regression program was used for the analysis. Linear plots were obtained with correlation coefficient of more than 0.99; except for the pure PES polymer solution (i.e. PVP/PES = 0.0 wt./wt.) for which it was 0.89. Values of the specific viscosity between 0.2 and 1.0 only were considered, since outside those limits the relationship becomes nonlinear.

The intrinsic viscosity of polymers consisting of PES, PVP, and mixtures thereof were evaluated by repeating the above procedure. The polymer mixtures were characterized by the weight ratio PVP/PES (as for the casting solutions), those evaluated included: 0.0 (100% PES), 0.2, 0.4, 0.5, 0.75, 1.0, 2.0, 5.0, and 1/0 (100% PVP). The initial polymer solutions were prepared using pre-filtered NMP solvent and with composite polymer (PES + PVP) concentration ranging from 0.1 to 0.25 g/l of NMP. Two different viscometers were used with constants 0.00873 and 0.01542 cst/s respectively.

4. RESULTS

This research project was conducted in two parts consisting of preliminary studies on membrane fabrication techniques, in the first part, and of a main study on the effect of casting solution composition, in the second part. Membranes used for the preliminary studies were prepared using a casting solution of reference composition while fabrication techniques were varied. Membranes for the main study, by comparison, were prepared following a standard procedure, established based on results from the preliminary studies, but from 36 casting solutions of different composition.

Experimental results mainly consisted of membrane performance data, expressed using permeation rate and solute separation, obtained by RO/UF experiments. Other results from the main study included membrane pore size distribution data, obtained by analysis of the performance data; and intrinsic viscosity data for the range of casting solution compositions, determined by analysis of viscoelastic measurements. These experimental results will now be presented in two parts to reflect the project approach:

4.1 PRELIMINARY STUDIES ON MEMBRANE FABRICATION

Preliminary studies on membrane fabrication focused on the effects of a) solvent purity in the casting solution, b) membrane annealing post-treatments, c) immersion mode in the gelation step, and d) casting on a support material.

The membranes involved were prepared from casting solutions of identical composition : 20 wt.% PES, 80 wt.% NMP , defined as the reference composition. Membranes used to study the effects of solvent purity and annealing post-treatments were cast under high, 41 to 51 %, by comparison with lower, 20 to 28 %, relative humidity conditions for all other membranes. Other distinctions in the membrane preparation procedure will be discussed when appropriate.

4.1.1 SOLVENT PURITY IN THE CASTING SOLUTION

To investigate the effect of solvent purity in the casting solution several membranes were prepared from each of two casting solutions: the reference casting solution containing purified grade NMP solvent and another, used in this investigation only, containing practical grade NMP. Several samples from each membrane were evaluated in RO/UF experiments using an aqueous solution of PEG solute.

The experimental results with respect to PEG-6000 solute are presented in Table 5 (raw data is in Appendix 5) for membranes from the casting solution containing practical grade NMP (Baker). Sample averages for each of the four membranes, and the population average for all membranes are shown with respect to each performance parameter. A significance test to determine whether the four membranes could belong to the same population was conducted; the results are shown at the bottom of Table 5. In every case the test ratio was smaller than the F value, indicating that the four membranes were not significantly different.

Similarly, the experimental results with respect to PEG-4000 solute are presented in Table 6 (raw data is in Appendix 6) for membranes from the casting solution containing purified grade NMP (Fisher). In this case also the significance test indicated that the five membranes could belong to the same population.

4.1.2 MEMBRANE ANNEALING POST-TREATMENTS

The effect of annealing on the performance of polyethersulfone membranes was investigated. Initially, three different annealing treatments were examined; they are described in Table 3A. The annealing treatment in ethylene glycol , in particular the effects of temperature and duration, were investigated further. These annealing treatments are described in Table 3B. Unlike membranes from Table 3A and previous ones, membranes from Table 3B and subsequent membranes in this work were prepared using the fast immersion mode in the gelation step (discussed in section 5.1.4). Membrane samples subjected to each treatment, as well as untreated samples for comparison, were evaluated in RO/UF experiments.

TABLE 5

PERFORMANCE OF MEMBRANES FROM THE CASTING SOLUTION WHICH USED (BAKER) PRACTICAL NMP - SAMPLE AVERAGES AND POPULATION AVERAGE SHOWN

Test Conditions: 200 ppm PEG-6000 aqueous feed
1.0 L/min feed rate
65 psig, 25°C
A = 14.5 cm^2

Membrane	# Samples	IPWP g/hr. A.	PWP g/hr. A	PR g/hr. A	f %
B1	4	36.2+/-16.6	22.6+/-11.6	22.5+/-12.4	93.4+/-3.4
B2	4	49.9 21.7	38.4 16.0	35.2 14.9	89.7 7.7
B3	3	24.0 14.7	17.1 11.1	16.2 10.8	91.4 3.2
B4	4	54.8 21.2	38.5 13.5	36.4 12.7	88.1 4.5
Population Average		42.4+/-20.0	29.9+/-14.7	28.3+/-13.8	90.6+/-4.9
Test Ratio		1.82	2.41	2.06	0.77

For Comparison, $F(3, 11, \alpha = 0.05) = 3.59$

TABLE 6

PERFORMANCE OF MEMBRANES FROM THE CASTING SOLUTION WHICH USED (FISHER) PURIFIED NMP - SAMPLE AVERAGES AND POPULATION AVERAGE SHOWN

Test Conditions: 200 ppm PEG-4000 aqueous feed
2.0 L/min feed rate
65 psig, 25°C
A = 14.5 cm^2

Membrane	# Samples	IPWP g/hr. A	PWP g/hr. A	PR g/hr. A	f %
F1	2	20.1+/- 4.5	9.0+/- 1.5	7.7+/- 1.0	79.0+/-11.0
F2	3	96.5 60.3	36.5 19.3	32.1 16.8	69.3 7.2
F3	2	85.7 85.8	50.1 50.1	48.3 49.3	80.3 3.9
F4	2	23.5 9.3	13.3 2.8	12.6 2.5	52.3 13.7
F5	3	53.6 52.9	16.3 14.9	13.9 12.7	66.6 6.1
Population Average		59.0+/-51.3	25.3+/-23.1	22.9+/-21.9	69.2+/-11.3
Test Ratio		0.97	1.26	1.30	3.57

For Comparison, $F(4, 7, \alpha = 0.05) = 4.12$

RO/UF experimental results are given in Table 7 (raw data in Appendix 7) for membranes subjected to annealing treatments in Table 3A. The effect of each post-treatment can be evaluated qualitatively by comparing the membrane performance data in Table 6 (untreated) against those in Table 7 (annealed) for membranes made from the casting solution with purified NMP. Annealing the membrane in water (treatment I) was shown to improve solute separation without affecting the product rate. Annealing in a sulfuric acid aqueous solution (treatment II) had an ambiguous effect producing a dramatic increase in solute separation with practically no product rate in one case, and no significant change in product rate in another case. Annealing in ethylene glycol (treatment III) produced the best results with improvements in both solute separation and product rate.

A test of significance to determine whether the annealed membranes were significantly different from the untreated membranes was conducted. The results, shown in Table 8, suggest that only treatment III (annealing in ethylene glycol) had a significant effect on membrane performance; more specifically on the product rate.

The effects of temperature and duration of annealing in ethylene glycol (treatments described in Table 3B) on membrane performance are shown in Figure 8 with respect to solute PEG-6000. Each point represents the average performance data for several membrane samples subjected to the same annealing treatment. The membranes performance data with respect to PEG-6000 and five other PEG probe solutes (of different molecular weight) are in appendix 8.

The results show both the temperature and duration of the annealing treatment to significantly affect the performance of resulting membranes. Compared with untreated membranes those subjected to the fifteen minutes annealing had a lower solute separation and increased product rate. This effect was accentuated with the increase in temperature. At 150°C the product rate dropped to a low level and solute separation reached only 5 %. Of the four membrane samples annealed at 150°C only one could be used in RO/UF experiments; the others were affected too severely. Membrane samples which were annealed at 170°C are not shown in Figure 8. These had shrunk and partially melted and, hence, were not suitable for use in the RO/UF experiments.

TABLE 7

EFFECT OF VARIOUS ANNEALING POST-TREATMENTS ON MEMBRANE PERFORMANCE - POLYETHERSULFONE MEMBRANES PREPARED FROM THE CASTING SOLUTION WITH (FISHER) PURIFIED NMP

Test Conditions: 200 ppm PEG-4000 aqueous feed
2.0 L/min feed rate, 65 psig, 25°C
A = 14.5 cm^2

Treatment (a)	Membrane	# Samples	IPWP g/hr. A	PWP g/hr. A	PR g/hr. A	f %
I	F2	1	76.1	27.0	24.2	82.3
	F3	2	111.2+/-50.1	53.0+/-22.3	52.3+/-22.6	84.6+/-10.0
	F4	2	31.5+/-25.2	15.8+/-11.1	15.1+/-10.5	71.3+/- 8.3
	Average (b)		72.3+/-48.8	32.9+/-22.6	31.8+/-22.8	78.9+/- 9.6
II	F2	1	1.2	0.8	0.7	96.5
	F5	1	34.2	11.0	9.6	65.4
	Average (b)		17.8+/-23.3	5.9+/- 7.2	5.1+/- 6.3	81.0+/-22.0
III	F3	2	165.2+/-79.3	79.3+/-37.1	79.9+/-38.7	84.9+/- 9.1
	F4	2	132.2+/-18.7	52.0+/- 8.8	50.9+/- 9.0	71.9+/-17.8
	Average (b)		148.9+/-50.8	65.6+/-27.1	65.4+/-28.4	78.4+/-13.8

(a) Cross-referenced with Table 3.
(b) Combined sample average.

TABLE 8

SIGNIFICANCE TESTS ON THE EFFECTS OF ANNEALING POST-TREATMENTS I, II AND III - COMPARING UNTREATED (TABLE 6) VERSUS ANNEALED (TABLE 7) MEMBRANES

Treatment	Test Ratio PR	f	F @ α = 0.05
I	0.53	2.63	F (1,15, 0.05) = 4.54
II	1.12	1.41	F (1, 12, 0.05) = 4.75
III	9.25	1.69	F (1, 14, 0.05) = 4.60

FIGURE 8

i. EFFECT OF ANNEALING IN ETHYLENE GLYCOL ON MEMBRANE PERFORMANCE - EMPHASIS ON EFFECTS OF TEMPERATURE AND DURATION OF TREATMENT

ii. EFFECT OF IMMERSION MODE (FAST VERSUS SLOW) ON MEMBRANE PERFORMANCE - USING UNTREATED MEMBRANES

Test: - Standard Conditions
- PEG-6000 solute

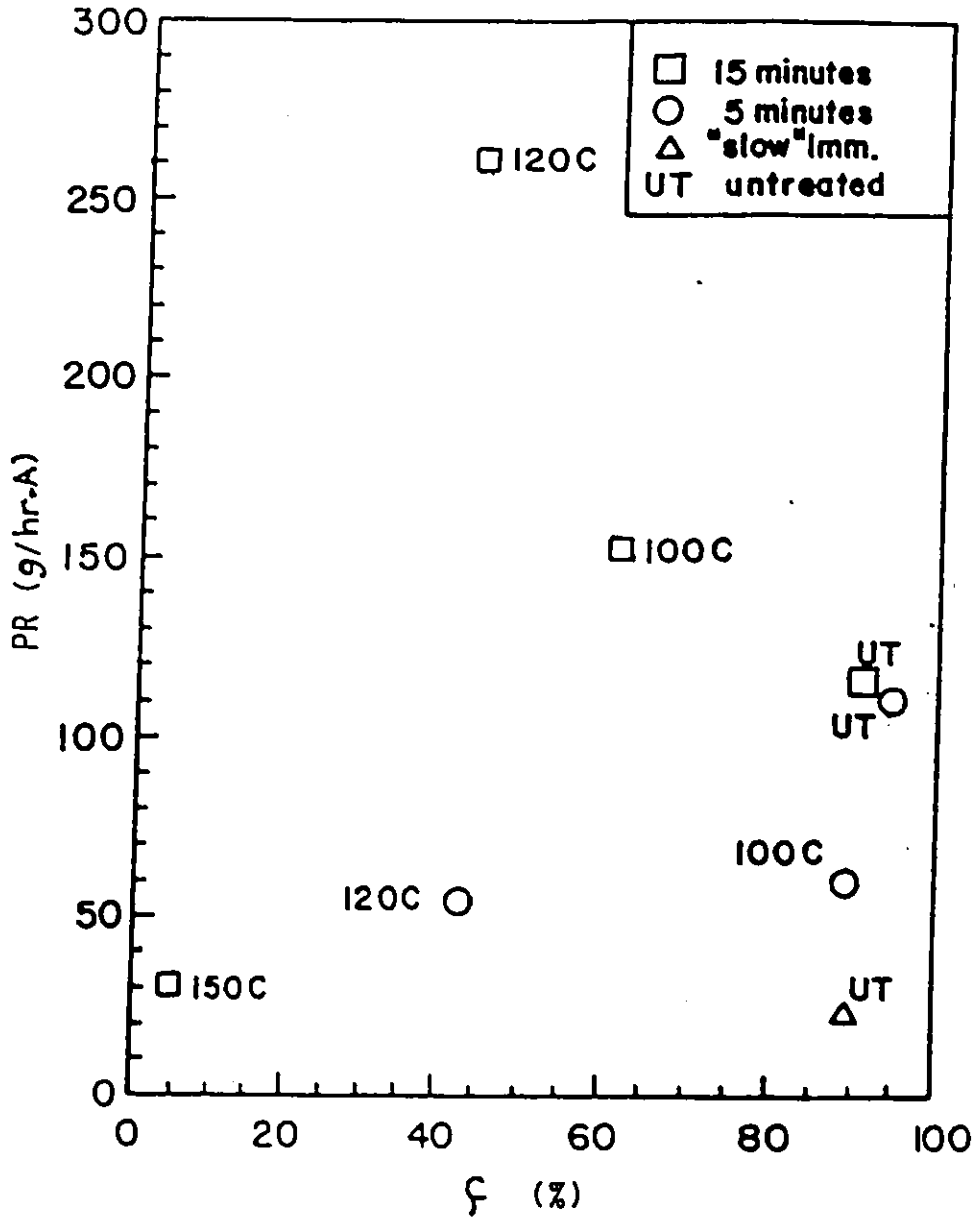
15 minutes
5 minutes
"slow" Imm.
UT untreated
120C
100C
UT
UT
100C
120C
150C
UT
PR (g/hr-A)
300
250
200
150
100
50
0
0
20
40
60
80
100
ϛ (%)

Five minutes annealing was undesirable as it produced membranes with both reduced solute separation and product rate compared to untreated membranes. In this case, the effect of increasing temperature was to reduce solute separation with very little change in product rate. Membranes annealed at 150°C were practically not permeable and, therefore, the corresponding RO/UF data was not shown in Figure 8.

4.1.3 IMMERSION MODE

Figure 8 was also used to show the effect of the immersion mode in the gelation step on the performance of resulting membranes. Membranes produced by slow immersion resulted in a significantly lower product rate but approximately equal solute separation as membranes produced by fast immersion. Consequently, membranes in Figure 8 and subsequent membranes which were made using the fast immersion mode can not be compared with previous membranes, in particular those in Table 7, made using the slow immersion mode.

4.1.4 CASTING ON A SUPPORT MATERIAL

The effect of the casting surface on membrane performance was investigated by comparing unsupported membranes, cast on a glass plate surface, with supported membranes, cast on a support material. Two types of support materials were tried.

RO/UF results in Table 9 show the supported membranes to have a lower solute separation than unsupported membranes. Moreover, the two different support materials produced membranes with different performances.

4.2 STUDY ON THE EFFECT OF CASTING SOLUTION COMPOSITION

For the study, the performance of membranes prepared from each of the 36 casting solution compositions had to be evaluated with respect to eight probe solutes of different molecular weight. The extensive number of RO/UF experiments involved made it impossible to include as many samples of each membrane as would be required for statistical analysis. As compromise, an experimental program which included two levels of membrane testing was proposed where the first was designed for the statistical analysis, and the

TABLE 9

EFFECT OF CASTING SURFACE/SUPPORT MATERIAL ON MEMBRANE PERFORMANCE

Test Conditions: 200 ppm PEG-6000
50 psig
25°C
2.2 L/min feed rate

Membrane No.	Casting Surface	PR g/hr. A	f %
1	Glass (standard)	251.±58	91.3±7.2
2	Support Material Type A	180.	74
3	Support Material Type B	458.	68

second for membrane characterization. The latter refers to the evaluation of membrane performance with respect to the eight probe solutes for use in the analysis of pore size distribution.

At the first level, four membrane samples from each casting solution composition were subjected to two RO/UF experiments with aqueous solutions of solutes PEG-6000, and one of PEG-1000 or Dextran-71,500. The objectives of the first-level tests were three- fold: (i) to perform a statistical analysis on membrane performance (e.i. evaluate the variability), (ii) to screen the best membrane samples to be included in the second-level tests, (iii) to have an appreciation of membrane performance for planning the sequence of probe solutes at the second level.

The two best membrane samples from each solution composition selected based on first-level tests results were used in the characterization experiments, at the second level. There they were subjected to eight RO/UF experiments with aqueous solutions of PEG solutes in the molecular weight range from 300 to 15,000.

By exception, membranes from the casting solution compositions S(10 - R) and S(P - 0.75) were not evaluated following the above membrane testing program. Instead, they were subjected directly to the characterization experiments such as in the second-level tests; thus omitting the first-level tests (or screening step). Because membrane performance is, to some extent, a function of the total time on stream, the performance of these membranes would better compare with that at the first rather than at the second level of the (standard) membrane testing program.

4.2.1 MEMBRANE PERFORMANCE RESULTS

The individual effect of the nonsolvent to polymer weight ratio (PVP/PES) in the casting solution was evaluated for different values of constant polymer concentration. The membrane performance data with respect to probe solute PEG-6000 was plotted as a function of the weight ratio PVP/PES. Corresponding curves for the polymer concentrations 15, 20, and 25 wt.% PES are given in Figures 9 and 10, for first and second level tests respectively.

FIGURE 9

MEMBRANE PERFORMANCE AS A FUNCTION OF THE WEIGHT RATIO PVP/PES IN THE CASTING SOLUTION - FIRST-LEVEL TESTS

Test: - Standard conditions
- PEG-6000 solute

Legend:

	wt% PES
□	15
○	20
△	25

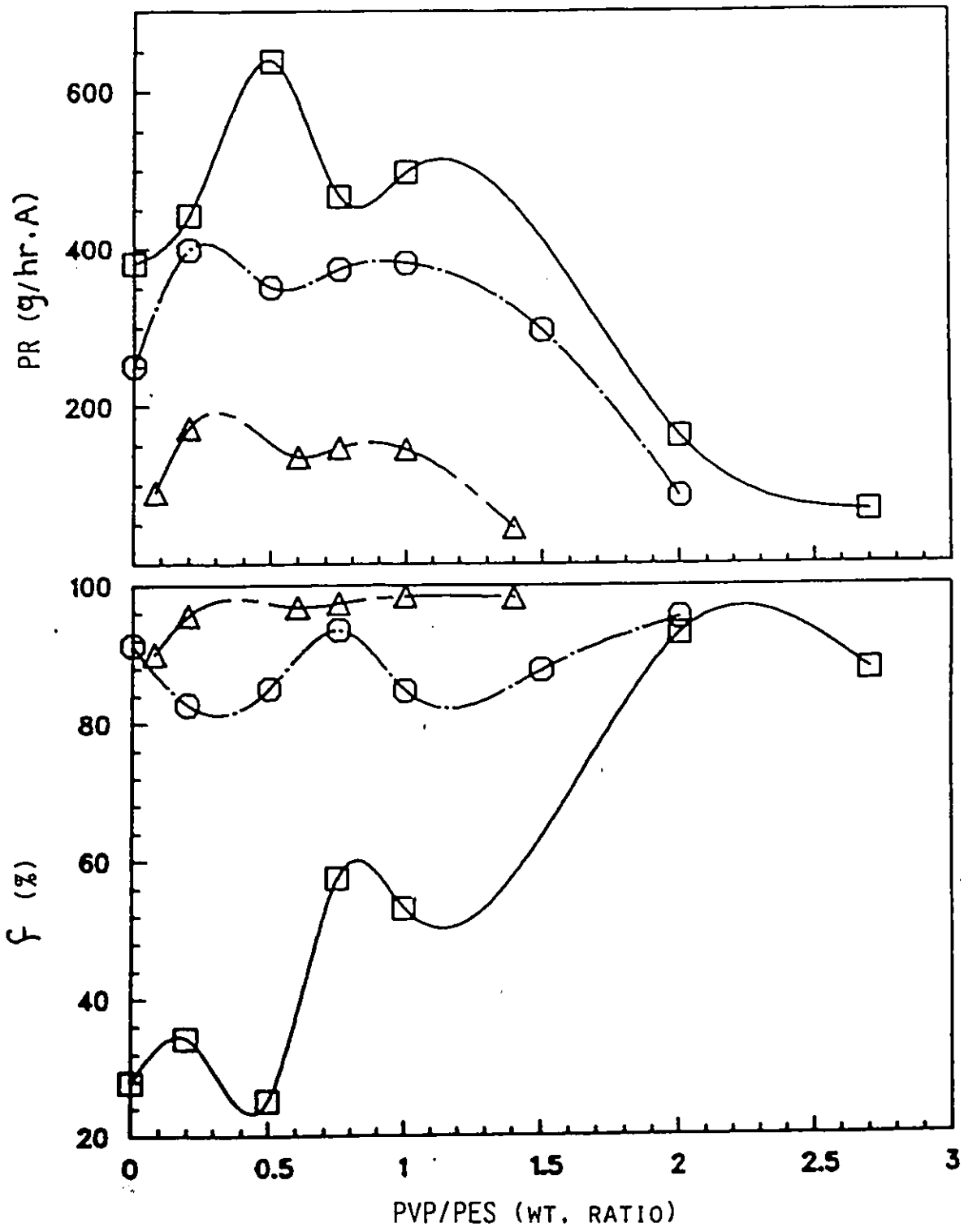
600
400
200
PR (g/hr.A)
100
80
60
40
20
F (%)
0
0.5
1
1.5
2
2.5
3
PVP/PES (WT. RATIO)

FIGURE 10

MEMBRANE PERFORMANCE AS A FUNCTION OF THE WEIGHT RATIO PVP/PES IN THE CASTING SOLUTON - SECOND-LEVEL TESTS

Test: - Standard conditions
- PEG-6000 solute

Legend:

	wt% PES
□	15
○	20
△	25

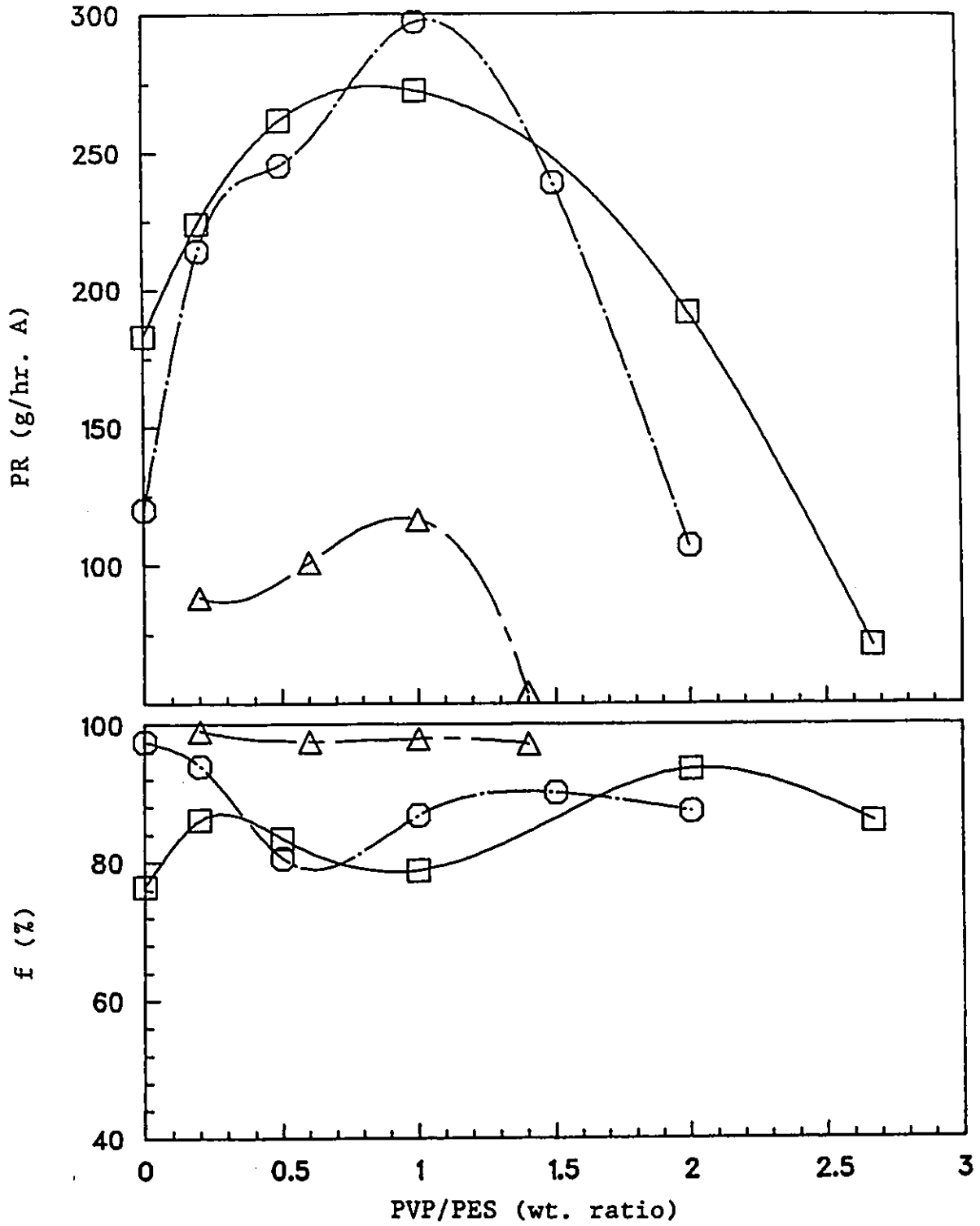
300
250
200
150
100
PR (g/hr. A)
100
80
60
40
f (%)
0
0.5
1
1.5
2
2.5
3
PVP/PES (wt. ratio)

In Figure 9 the effect of the ratio PVP/PES on membrane product rate was generally the same for the three polymer concentrations. Each product rate curve featured one local minima, and two maxima; one of which was the global maxima. Conversely, the effect of PVP/PES on solute separation could not be generalized over the polymer concentration range. The solute separation curve for 25 wt.% PES was almost constant at 96.% ; for 20 wt.% PES, it fluctuated between 80. and 95.% ; and for 15 wt.% PES, it increased from 25. to 95.%.

In Figure 10 compared to Figure 9 there was only one inflexion in the product curve. Generally, for all polymer concentrations the product rate curve had a maxima in the vicinity of PVP/PES equals 1.0. This coincides with the position of the local maxima obtained with respect to the first level tests in Figure 9.

The individual effect of the polymer concentration in the casting solution was evaluated for different constant PVP/PES ratios. The membrane performance data with respect to probe solute PEG-6000 was plotted as a function of polymer concentration in Figure 11A for PVP/PES equal to 0.2, 0.5, and 1.0, and in Figure 11B for PVP/PES equal to 1.0, 1.5, and 2.0 wt./wt.. The data from the second level tests only are represented.

For Figures 11 A and B generally, solute separation increased with increasing polymer concentration with a corresponding decrease in product rate. There is an apparent maximum in the product rate curve at the lower concentrations. Similarly, there is an apparent maximum in the solute separation curve at the higher concentrations. More experimental data would be required to verify the trend in these extremities. In addition, these results confirm that with increasing PVP/PES the product rate reaches a maximum at a PVP/PES value in the vicinity of 1.0.

The membranes from the 10 and 35 wt% PES casting solutions were not included in the plots because at the low concentration the standard deviation was too large, while at the higher concentration the product rate was too small to be measured. RO/UF results from the first-level tests are in Appendix 9 while those from the second-level tests are in Appendix 10. RO/UF results for membranes from the casting solutions S(10 - R) and S(P - 0.75), which were not involved in the two level test program, are in Appendix 11.

FIGURE 11

MEMBRANE PERFORMANCE AS A FUNCTION OF THE POLYMER CONCENTRATION IN THE CASTING SOLUTION - SECOND-LEVEL TESTS

A. for PVP/PES (wt. ratio) $\leq$ 1.0

B. for PVP/PES (wt. ratio) $\geq$ 1.0

Test: - Standard conditions
- PEG-6000

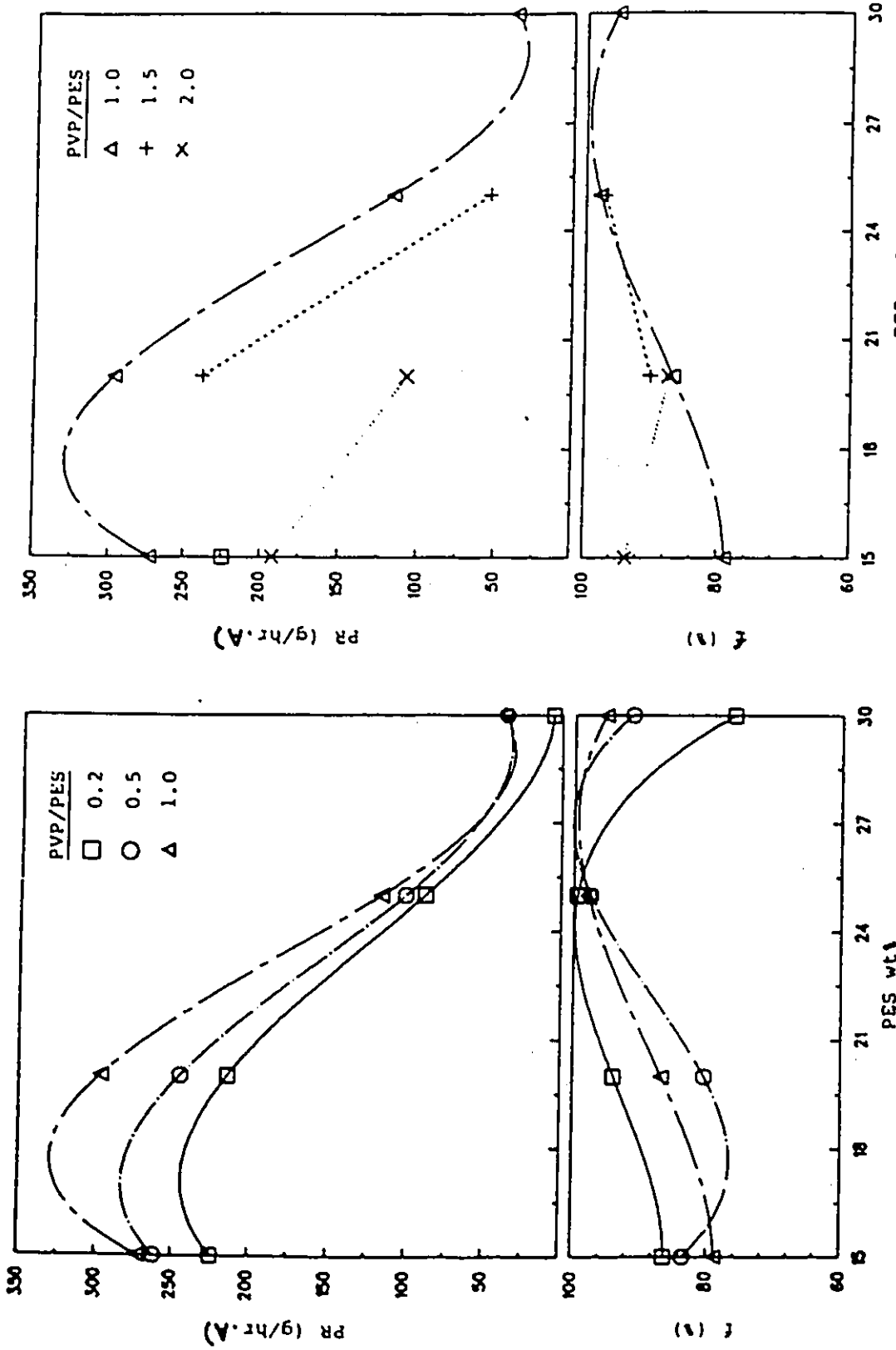

FIGURE 11A

FIGURE 11B

4.2.2 MEMBRANE PORE SIZE DISTRIBUTION DATA

To investigate the effect of the casting solution composition on the pore size distribution each polyethersulfone membrane was characterized by subjecting to a sequence of RO/UF experiments in the second level tests. The transport model was applied to the solute separation and permeation data with respect to the eight PEG solutes of different molecular weight to estimate the five parameters in the bi-normal pore size distribution: $\bar{R}_1$, σ_1, $\bar{R}_2$, σ_2 and h_2.

A computerized method involving a nonlinear regression routine was used to fit the predicted solute separation data on the basis of the transport model to the experimental data (for the eight PEG probe solutes). The optimum pore size distribution of the membrane was determined at the minimum sum of squares of residuals. Table 10 gives the pore size distribution of some PES membranes from the casting solutions of concentrations 15, 20 and 25 wt.% PES. Figure 12 is a comparison of the predicted solute separation at the optimum pore size distribution and the experimental data for two membranes; the raw data is in Appendix 13.

Generally, the network pore size $\bar{R}_1$ ranged from 5 to 17 Å and had a wide standard deviation: while the aggregate pore size $\bar{R}_2$ ranged from 30 to 47 Å and had a relatively narrower standard deviation. As expected h_2 was small since the network pores are more abundant.

4.2.3 INTRINSIC VISCOSITY OF CASTING SOLUTION

The intrinsic viscosity of polymers PVP , PES, and mixtures thereof in NMP were determined from viscosity measurements. Intrinsic viscosity was plotted as a function of the composition in the polymer mixture. In Figure 13, the composition was expressed as the weight ratio PVP/PES. Alternatively, in Figure 14 it was expressed as the weight fraction of PES in the polymer mixture. The standard deviation was calculated with respect to each intrinsic viscosity measurement and in all cases it was less than 1%; this has negligible effect on the plots in Figure 13 and 14. The viscosity data from which the intrinsic viscosity was determined by linear regression is in Appendix 15.

TABLE 10

BI-NORMAL PORE SIZE DISTRIBUTION DATA OBTAINED BY ANALYSIS OF THE RESULTS FROM THE CHARACTERIZATION EXPERIMENTS (SECOND-LEVEL TESTS)

PES wt%	PVP/PES (w/w)	$\bar{R}_1$ Å	σ_1 Å	$\bar{R}_2$ Å	σ_2 Å	h_2	Average residual, $\lvert\bar{e}_u\rvert$ (for f(%))
15	0.0	12.4	4.1	51.9	0.093	0.0084	5.6
	0.2	12.8	1.8	55.0	0.22	0.0020	3.4
	0.5	12.3	3.4	48.4	4.4	0.0006	5.0
	1.0	13.0	4.2	48.0	0.96	0.0010	7.3
	2.0	14.3	4.8	33.2	0.27	0.0047	4.6
	2.7	16.8	7.0	30.0	0.0030	0.0194	7.7
20	0.0	11.8	5.2	43.5	0.0044	0.0115	6.2
	0.2	11.1	1.6	47.0	0.12	0.0020	1.5
	0.5	12.4	3.0	44.3	0.98	0.0030	9.1
	1.0	11.5	1.4	33.3	1.1	0.0154	4.4
	1.5	13.2	2.7	45.3	0.94	0.0031	6.3
	2.0	9.4	4.2	46.3	0.0046	0.0328	11.5
25	0.2	12.4	4.8	30.0	0.078	0.0050	6.6
	1.0	12.9	5.8	32.7	0.264	0.0071	7.6
	1.4	5.05	2.0	42.8	0.0043	0.0278	10.6

$$\left|\bar{e}_u\right| = \left[\frac{\Sigma e_u^2}{n}\right]^{1/2}, \quad n = 8 \text{ probe solutes}$$

$$e_u = (f - f^*)$$

FIGURE 12

RESULTS OF CHARACTERIZATION EXPERIMENTS FOR TWO MEMBRANES FROM CASTING SOLUTIONS WITH PVP/PES (WT. RATIO) = 0.2 BUT DIFFERENT POLYMER CONCENTRATIONS. COMPARISON WITH PREDICTED SOLUTE SEPARATION ON THE BASIS OF THE TRANSPORT MODEL

Test: - Standard conditions
- PEG solute of various molecular weights

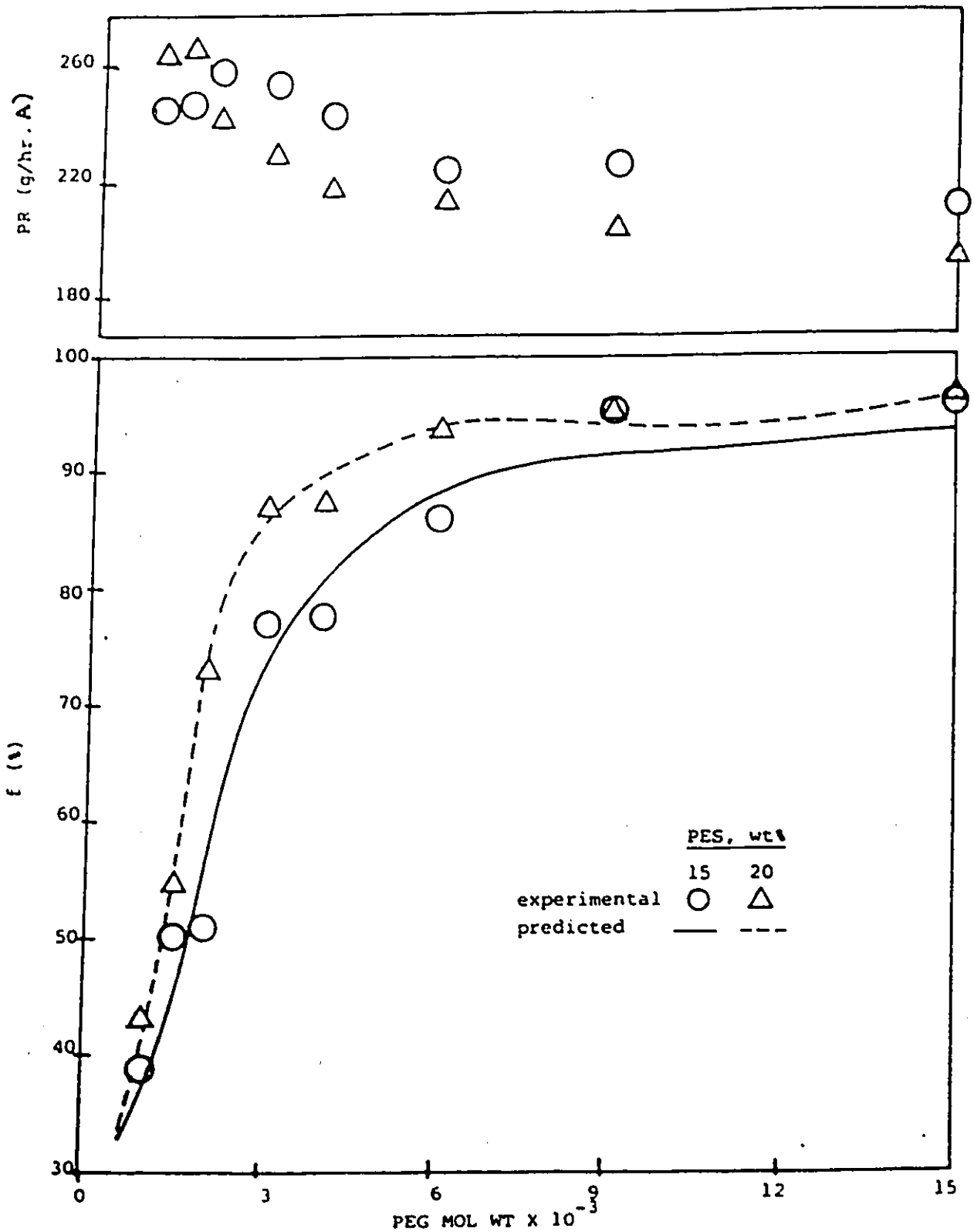
PR (g/hr.A)
260
220
180
100
90
80
70
60
50
40
30
ε (%)
0
3
6
9
12
15
PEG MOL WT X 10^-3
PES, wt%
15
20
experimental
predicted

FIGURE 13

DEPENDENCE OF INTRINSIC VISCOSITY ON THE WEIGHT RATIO PVP/PES IN THE CASTING SOLUTION; AT 25°C

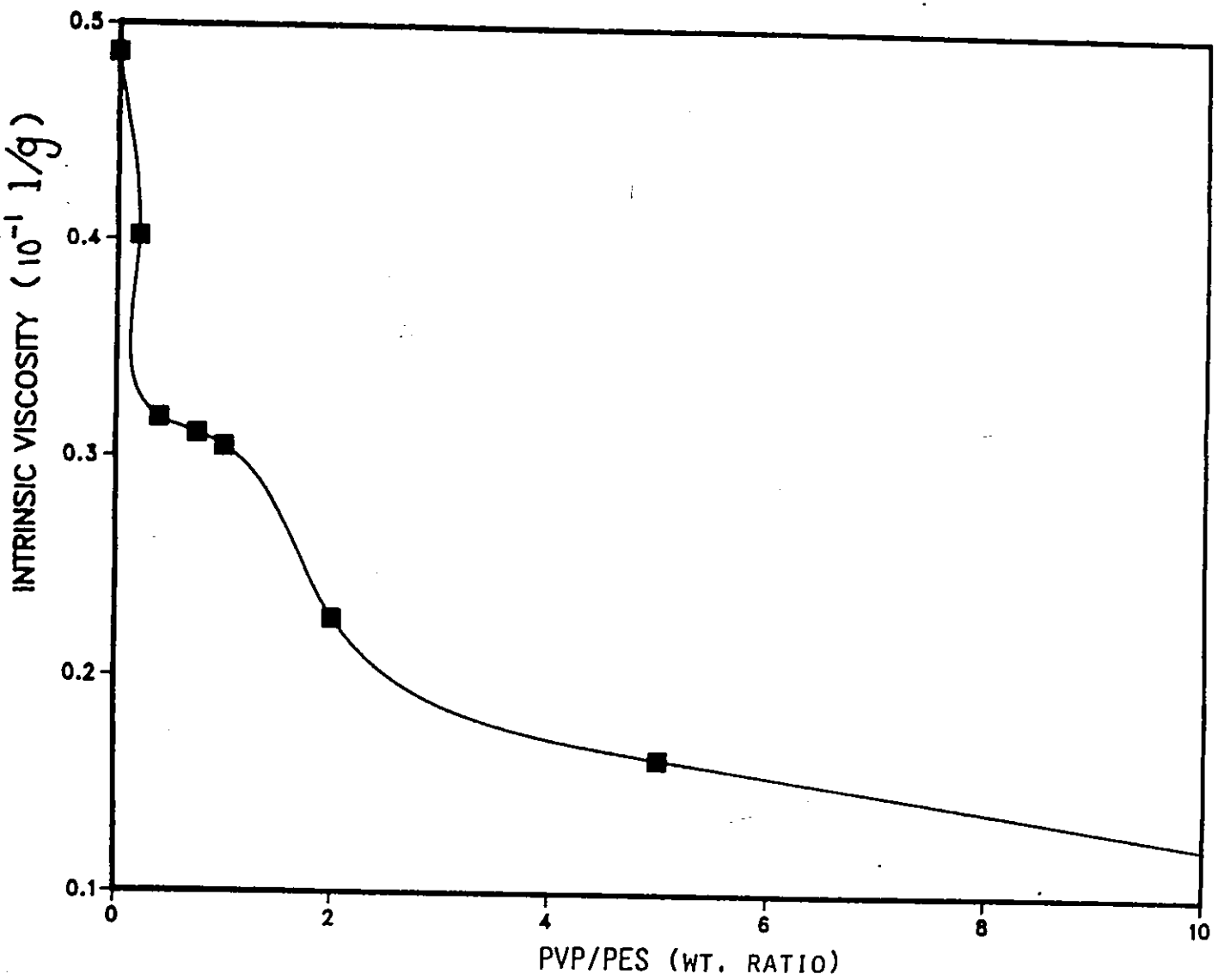
INTRINSIC VISCOSITY (10^{-1} 1/g)
0.5
0.4
0.3
0.2
0.1
0
2
4
6
8
10
PVP/PES (WT. RATIO)

FIGURE 14

DEPENDENCE OF INTRINSIC VISCOSITY ON THE WEIGHT FRACTION PES OF TOTAL POLYMER (PES + PVP) IN THE CASTING SOLUTION; AT 25°C

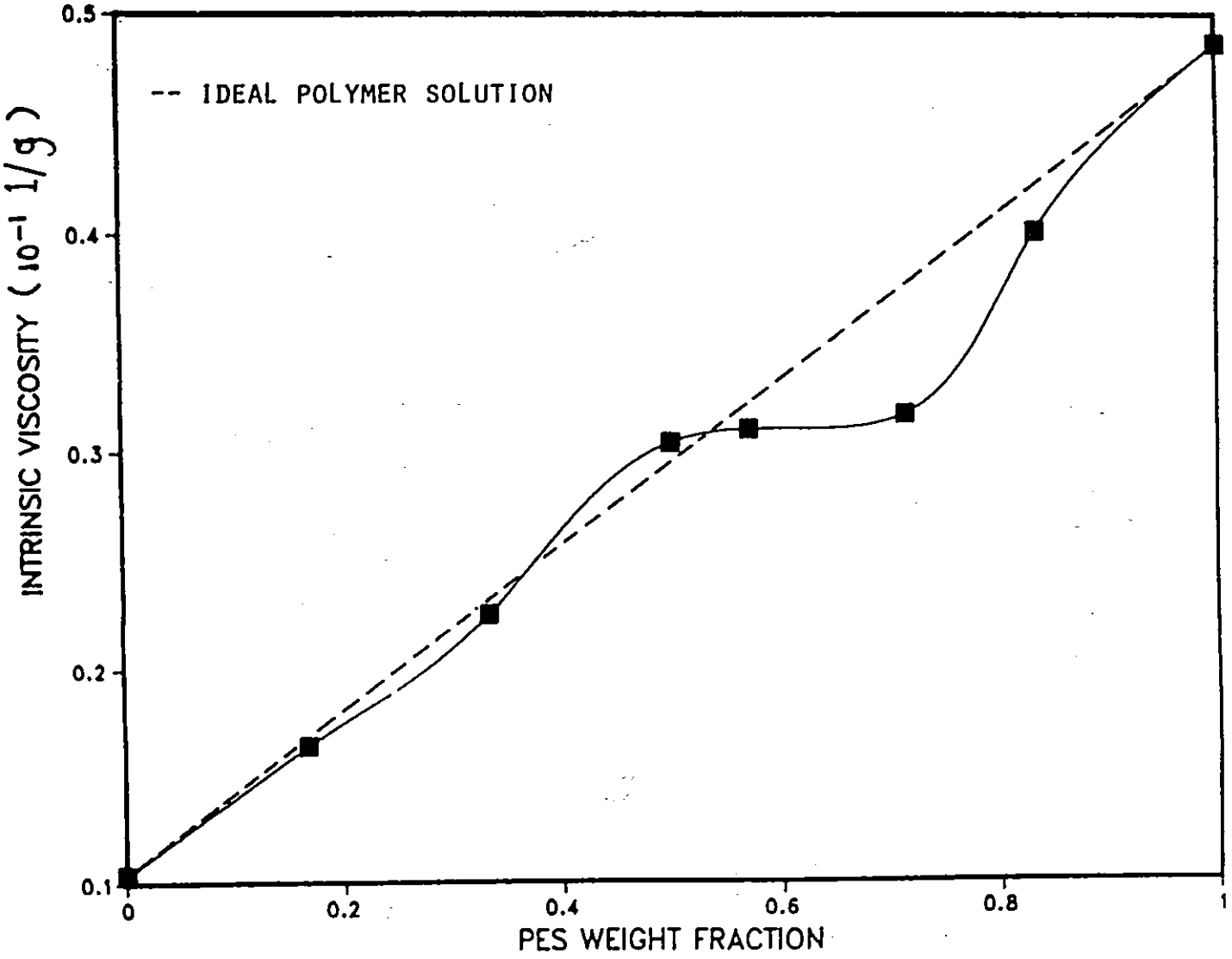
-- IDEAL POLYMER SOLUTION
INTRINSIC VISCOSITY (10^{-1} 1/g)
0.5
0.4
0.3
0.2
0.1
0
0.2
0.4
0.6
0.8
1
PES WEIGHT FRACTION

A comprehensive view of the plots revealed a transition region in the range of PVP/PES = 0.4 - 1.0 (w/w) and PES weight fraction = 0.5 - 0.7. In Figure 14, the response curve for an ideal polymer mixture (with no polymer-polymer interaction) is shown for comparison. The intrinsic viscosity of an ideal polymer mixture is equal to the linear combination of the intrinsic viscosities of the pure polymers, where the weight fractions are the proportionality constants. An analysis of the plots in Figure 14 demonstrates the non-ideality of the polymer mixture PVP/PES, imparted by PVP-PES interactions.

5. DISCUSSION

In this study the effect of the casting solution composition and of the resulting solution structure on the average pore size and pore size distribution at the surface of polyethersulfone membranes was investigated. The pore size distribution was determined from the analysis of the membrane performance data obtained by RO/UF experiments. The solution structure was predicted on the basis of the intrinsic viscosity data for the casting solution.

The experimental strategy was to first establish a standard fabrication technique for the polyethersulfone membranes. The objective was to minimize variability while producing membranes with good performance. The preliminary studies which pursued this objective are discussed in Section 5.1. The main study on the effect of casting solution composition on membrane performance and pore size distribution is discussed in Section 5.2. The viscoelastic approach to pore formation is discussed in Section 5.3. Lastly, the commercial potential of the polyethersulfone membranes developed -which impact on the practical significance of this work- is discussed in Section 5.4.

5.1 MEMBRANE FABRICATION TECHNIQUES

The properties of asymmetric membranes which determine their performance can be changed to some extent by variations in the membrane preparation procedure. Properties of the asymmetric membranes which can be controlled are the thickness of the active layer which affect the hydraulic resistance, the porous structure of the substrate which affect the mechanical strenght, and the pore stucture at the surface (size and number of pores) which affect the overall performance of the membrane in RO/UF experiments. In addition, the membranes can be subjected to post-treatments, such as annealing, to adjust the porous structure to given specifications.

In the preliminary studies various membrane fabrication techniques were investigated for their effects on membrane performance and also on the reproducibility. In particular, the effects of solvent purity in the casting solution, membrane post-treatments (e.g. annealing), the immersion mode in the gelation step, and casting on a backing material were investigated. The results were subsequently used in establishing a standard procedure for the fabrication of the polyethersulfone membranes for use in the main study.

5.1.1 EFFECT OF SOLVENT PURITY

To assist in the selection of NMP solvent, membranes from each of two casting solutions differing by the grade of NMP solvent, practical versus purified, were prepared. Further, to assess membrane reproducibility several membranes of each type were prepared and several samples of these evaluated.

The results exhibited an important standard deviation in product rate in the range of 50% and 100% respectively for membranes from practical (Table 5) and purified (Table 6) NMP solvent. Significance tests conducted based on these results, however, indicated that membranes from a common casting solution were not significantly different and could belong to the same population.

The experimental results in Tables 5 and 6 could not be compared directly because the test conditions were different. Despite this, a significance test to determine whether the membranes made from practical NMP (Table 5) and those made from purified NMP (Table 6) could belong to the same population was conducted. The results, summarized below, show that on the basis of solute separation, as opposed to product rate, the two sets of membranes are significantly different. The results are justified by the different molecular weight PEG solutes (PEG-6000 versus PEG-4000) used to test the two sets of membranes which affects solute separation but not product rate. Hence, there are no reasons to conclude that the solvent purity in the casting solution had a significant effect on membrane performance. To ensure consistency of the solvent supply it was decided to prepare all future casting solutions using purified grade NMP.

Test of Significance: Practical versus Purifed NMP in casting solution

Test Ratio		F (1, 25, α = 0.05)
PR	f	
0.57	40.39	4.24

5.1.2 EFFECT OF MEMBRANE POST-TREATMENT

Polyethersulfone membranes have inherently large pore size at their surface which limits their use to ultrafiltration applications. The possibility of reducing the pore size using annealing post- treatments was investigated.

Initially, annealing treatments using three different medium were attempted (as described in Table 3A). Their effect was evaluated qualitatively by comparing the membrane performance data in Table 6 (untreated) against those in Table 7 (annealed) for membranes made from the casting solution with purified NMP. Neither of the two annealing treatments, in water and in a sulfuric acid aqueous solution respectively, showed improvements. Annealing in ethylene glycol (treatment III) produced the best results with improvements in both solute separation and product rate. A test of significance (Table 8) confirmed that only annealing in ethylene glycol had a significant effect on membrane performance; more specifically on the product rate.

5.1.3 EFFECT OF ANNEALING IN ETHYLENE GLYCOL

Further studies on the annealing treatment in ethylene glycol focused on the effects of temperature and duration of the treatment (detailed in Table 3B). The performance data for membranes subjected to each annealing treatment was compared with untreated membranes. The membranes in this study and subsequent ones which were made using the fast by comparison with the slow immersion technique (discussed in section 5.1.4) for previous membranes, in particular those in Table 7, could not be compared, however.

The results suggested both the temperature and duration of the annealing treatment had significant effects on the performance of resulting membranes. Compared with untreated membranes those subjected to the fifteen minutes annealing had a lower solute separation and increased product rate. This effect was accentuated with the increase in temperature. At 150°C the product rate dropped to a low level and solute separation reached only 5 %. Five minutes annealing was undesirable as it produced membranes with both reduced solute separation and product rate compared to untreated membranes. In this case, the effect of increasing temperature was to reduce solute separation with very little change in product rate.

The effects observed with annealing in ethylene glycol could also be interpreted with respect to physical changes of the membrane. The usual effect expected from an annealing treatment is shrinkage of the membrane porous structure which is reflected by an increase in solute separation and a corresponding decrease in product rate. In this case, however, the decrease in solute separation observed suggests the membrane structure must have collapsed to yield larger pores at the membrane surface. Prolonging the treatment to fifteen minutes resulted in an increased porosity. Annealing at 150°C and 170°C caused the membranes to shrink by 21 % and 34 % respectively, further the membranes appeared as if they had melted.

A possible explanation for the detrimental effect of annealing on the performance of polyethersulfone membranes could be that some unextracted solvent redissolved the membrane at the high annealing temperature. An alternative explanation would be the degradation of the polymer under these conditions. In particular, the temperatures 150°C and 170°C could be above the melting point of the polymer in ethylene glycol.

5.1.4 EFFECT OF THE IMMERSION MODE*

Disturbances occuring at the immersion of the membrane in the gelation bath, such as waves, were suggested as a possible source of variability in the performance of resulting membranes. To verify this postula, an investigation to determine the effect of the immersion mode was undertaken. The immersion mode is concerned with the speed and orientation of the membrane, or film of casting solution, upon contact with the gelation medium (water).

* The fast immersion mode is a process that has been developed at the National Research Council and is the subject of a patent application in the name of Thomas A. Tweddle, Oleh Kutowy, Andre Tremblay.

Membranes were prepared using two different immersion modes, referred as slow and fast respectively. With the slow immersion mode the membrane was immersed horizontally in a shallow gelation bath which produced disturbances (e.g. waves) at the surface. With the fast immersion mode the membrane was dropped vertically in a deep gelation bath (e.g. a pail). In this case, the membrane had more momentum upon entering the gelation medium (water). Also, the fast immersion was more easily controlled than the slow immersion.

As shown in Figure 8, membranes produced by slow immersion resulted in a significantly lower product rate but approximately equal solute separation as membranes produced by fast immersion. Thus it appears that the two immersion modes (fast and slow) produced membranes with approximately equal pore structure at the surface. However, the fast immersion mode produced membranes with either a larger number of such pores and/or a thinner active surface layer to account for the improved productivity.

Typically, the thin active surface layer of the membrane is ,in most part, formed in the evaporation period preceeding the immersion. It is known (7), however, that for the casting system PES/NMP/PVP the evaporation time does not significantly affect the performance of PES membranes. This is possibly due to the relatively non-volatile nature of the solvent NMP.

This result further suggests that the role of the immersion mode in the membrane formation process could be concerned with the formation of the thin surface layer. The faster the immersion the more pores are formed at the membrane surface and/or the thinner the active thin layer. This theory could generally apply to membranes from other polymer solution systems with non-volatile solvents. If this theory is plausible then for some polymer solution systems there exists an intermediate step in the membrane formation process, between evaporation and gelation, which is called immersion, or "quench".

5.1.5 EFFECT OF CASTING SURFACE

For purpose of industrial applications supported membranes, cast on a support material, are often prefered to unsupported membranes, cast on a glass plate (from which it is detached), due to their improved mechanical strength. The support material (also called backing) can be a woven or nonwoven cloth, must not dissolve in the casting solvent, and preferably its temperature resistance must compare with that of the polymer material for the membrane. Because of their superior mechanical strenght the polysulfone membranes are often themselves used as backing material to other polymeric membranes; this combination is called composite membrane.

Two types of support materials were tried for making supported polyethersulfone membranes. Their performance was compared with that of unsupported membranes, cast on a glass plate surface. Generally, the supported membranes had a lower solute separation than unsupported membranes. Moreover, the different support materials produced membranes with different performances.

5.1.6 THE STANDARD MEMBRANE MAKING PROCEDURE

A standard membrane making procedure had to be established in view of the main study on the effect of casting solution composition on membrane performance. To allow the effect of only one parameter in membrane formation to be examined, it was necessary to choose a membrane fabrication procedure with the least potential for variations.

On the basis of the results obtained in the preliminary study the following standard membrane making procedure was defined. The purified NMP solvent was selected to ensure consistency of supply, even though there were no indication of disadvantages from using the practical grade solvent. The membranes were to be cast on a smooth glass plate and immersed at high speed (vertical mode) in the gelation bath. Finally, the membranes were not to be subjected to a post-treatment since none were found beneficial for the membranes, and they could only have introduced more sources for variations.

5.2 EFFECT OF CASTING SOLUTION COMPOSITION ON MEMBRANE CHARACTERISTICS

The effect of the casting solution composition on membrane performance and also on the average pore size and pore size distribution at the membrane surface will be discussed in this section. For the study, membranes were prepared from several of different casting solution compositions. Each membrane was characterized by subjecting it to a sequence of RO/UF experiments using aqueous solutions of PEG-solutes of different molecular weight. These results were subsequently used for the analysis of pore size distribution.

The approach used to select the casting solution compositions and plan the RO/UF experiments have already been described in sections 3.3.2 and 4.2. In brief, the compositions for the casting solutions were selected systematically from the corresponding ternary solubility diagram. An experimental program was implemented to test the large number of membranes effectively. The purpose was to minimize the overall number of RO/UF experiments while maximizing the useful information from the results.

5.2.1 EFFECT ON MEMBRANE PERFORMANCE

For the investigation, membranes from each of the 36 casting solutions were evaluated in RO/UF experiments following the two level test program. Two RO/UF experiments at the first level were used to select the best membrane samples for each casting solution composition. These samples were subsequently used at the second level where they were subjected to a longer series of RO/UF experiments;called the characterization experiments.

The effect of casting solution composition on membrane performance will be discussed with respect to RO/UF results at both test levels. Since the test solute PEG-6000 was used at both levels, the corresponding RO/UF results were chosen for the comparison.

i) EFFECT OF NONSOLVENT TO POLYMER RATIO (PVP/PES, w/w)

The effect of the nonsolvent to polymer weight ratio (PVP/PES) in the casting solution was judged from the plot of membrane performance as a function of the weight ratio PVP/PES. Plots for polymer concentrations 15, 20, and 25 wt.% PES were given in Figures 9 and 10, for first and second level tests respectively.

The difference between the corresponding curves from Figures 9 and 10 indicated a change in membrane performance with time on stream; more specifically from the first to the second-level tests. A decrease in product rate and a corresponding increase in solute separation were observed in all cases. The lower polymer concentration, 15 wt.% PES, resulted in the greatest change in membrane performance. Also, at the second level tests (Figure 10) the performance curves were smoother which was evidence that the membranes had reached maturity or steady-state. The change in membrane physical state responsible for the change in performance could have been the effect of compaction of the membrane substructure and/or fouling at the membrane surface (deposition of macromolecules which can block pores, particularly larger pores).

In Figure 9 the effect of the ratio PVP/PES on membrane product rate was generally the same for the three polymer concentrations. Each product rate curve featured one local minima, and two maxima; one of which was the global maxima. Conversely, the effect of PVP/PES on solute separation could not be generalized over the polymer concentration range. The solute separation curve for 25 wt.% PES was almost constant at 96.% ; for 20 wt.% PES, it fluctuated between 80. and 95.% ; and for 15 wt.% PES, it increased from 25. to 95.%.

In Figure 10 compared to Figure 9 there was only one inflexion in the product curve. Generally, for all polymer concentrations the product rate curve had a maxima in the vicinity of PVP/PES equals 1.0. This coincides with the position of the local maxima obtained with respect to the first level tests in Figure 9. Such behavior suggest that the casting solutions with PVP/PES in the vicinity of 1.0 produced membranes with enhanced mechanical strength, less susceptible to the aging effects. Further, the fact

that the maxima in product rate was higher for 20 wt.% PES than for 15 wt.% PES in Figure 10, and not in Figure 9, also suggest that the effects of membrane aging increased with decreasing polymer content. As opposed to product rate, the effect of PVP/PES on solute separation in Figure 10 was relatively small.

ii. EFFECT OF POLYMER CONCENTRATION

The effect of the polymer concentration in the casting solution was judged from the plot of membrane performance as a function of PES wt.%. Plots for various PVP/PES weight ratios were given in Figure 11A for PVP/PES equal to 0.2, 0.5, and 1.0, and in Figure 11B for PVP/PES equal to 1.0, 1.5, and 2.0. The data from the second level tests only are represented. Generally, the plots showed an increase in polymer concentration and a corresponding decrease in product rate. In addition, these results confirm that with increasing PVP/PES the product rate reaches a maximum at a PVP/PES value in the vicinity of 1.0.

The membrane performance data in Figures 9, 10 and 11 were the average of several membrane samples; with a few exceptions. The standard deviations in the product rate and solute separation data cross-referenced with Figure 9 are given in Table 11, and in Table 12 for Figures 10 and 11. The experimental error associated with the membrane performance data obtained from the experimental RO/UF results was also calculated (see Appendix 12). It was approximately +/- 7. for solute separation, f (%), and +/- 5 percent of the value for product rate, PR (g/hr.A). Although significant in some cases, neither of the standard deviation or the experimental error would significantly affect the general trends of the performance curves in Figures 9, 10 and 11.

5.2.2 EFFECT ON PORE SIZE DISTRIBUTION

The casting solution composition is a key variable in the membrane formation process. In turn, the surface pore structure of the resulting membrane, which is determined by the variables in membrane formation, is a major factor governing membrane performance in RO/UF experiments.

TABLE 11

SAMPLE STANDARD DEVIATION ASSOCIATED WITH THE AVERAGE MEMBRANE PERFORMANCE DATA IN FIGURE 9

15 wt% PES			20 wt% PES			25 wt% PES		
PVP/PES (w/w)	σ_{PR}	σ_f	PVP/PES (w/w)	σ_{PR}	σ_f	PVP/PES (w/w)	σ_{PR}	σ_f
0.0	53.	9.7	0.0	58.	7.2	0.08	35.	7.4
0.2	85.	2.7	0.2	55.	7.8	0.2	56.	3.7
0.5	47.	7.0	0.5	115.	10.0	0.6	68.	2.8
0.75	27.	6.8	0.75	17.	4.4	0.75	22.	1.2
1.0	61.	12.2	1.0	19.	7.0	1.0	33.	2.4
2.0	35.	6.9	1.5	42.	11.0	1.4	9.	1.5
2.7	10.	9.4	2.0	11.	4.2			

Units: σ_{PR} (=) g/hr. A, A = 14.5 cm^2
σ_f (=) %

TABLE 12

SAMPLE STANDARD DEVIATION ASSOCIATED WITH THE AVERAGE MEMBRANE PERFORMANCE DATA IN FIGURES 10 AND 11

15 wt% PES			20 wt% PES			25 wt% PES			30 wt% PES		
PVP/PES	σ_{PR}	σ_f	PVP/PES	σ_{PR}	σ_f	PVP/PES	σ_{PR}	σ_f	PVP/PES	σ_{PR}	σ_f
0.0	42.	21.2	0.0	4.	0.5	0.2	19.	1.5	0.2	-	-
0.2	-	-	0.2	-	-	0.6	28.	2.7	0.5	8.	12.4
0.5	50.	7.4	0.5 1.0	4. 47.	1.1 5.6	1.0	1.	1.8	1.0	3.	0.5
1.0	21.	23.3	1.5	9.	2.6	1.4	1.	1.1			
2.0	6.	0.0	2.0	1.	3.8						
2.7	4.	8.8									

Units: σ_{PR} (=) g/hr. A, A = 14.5 cm^2
σ_f (=) %

The effect of the casting solution composition on the pore size distribution of polyethersulfone membranes was investigated using RO/UF results from the characterization experiments (second level tests). The procedure was to apply the transport model to the solute separation and product rate data with respect to the eight PEG solutes of different molecular weight to estimate the five parameters in the bi-normal pore size distribution: $\bar{R}_1$, σ_1, $\bar{R}_2$, σ_2 and h_2. In turn, these parameters were used to predict solute separation. Then, by fitting the predicted solute separation data on the basis of the transport model to the experimental data (for the eight PEG probe solutes) the optimum pore size distribution of the membrane, occuring at the minimum sum of squares of residuals, was determined. Table 12 gives the pore size distribution of some PES membranes from the casting solutions of concentrations 15, 20 and 25 wt.% PES. Figure 12 is a comparison of the predicted solute separation at the optimum pore size distribution and the experimental data for two membranes; the raw data is in Appendix 13.

A computer program incorporating a nonlinear regression routine was used for the operation. Because of the complexity of the transport model (ie. the integration), and the large number of parameters and experimental data involved, the minimum sum of squares of residuals was not necessarily the absolute one. A more complex convergence routine or a larger number of iterations would be required to further optimize.

Generally, the network pore size $\bar{R}_1$ ranged from 5 to 17 Å and had a wide standard deviation; while the aggregate pore size $\bar{R}_2$ ranged from 30 to 47 Å and had a relatively narrower standard deviation. As expected h_2 was small since the network pores are more abundant. Of interest, the polysulfone membrane's pore size data obtained by SEM by Zeman et al (26), and by means of pure water permeability measurements and BET-surface area determination by Bodzek (23) are of the same order of magnitude as the aggregate pore size $\bar{R}_2$ in this work. This coincidence suggests that these analytical methods can only resolve the larger pores, in the order of $\bar{R}_2$, but not the smaller pores, in the order of $\bar{R}_1$.

An analysis of the data in Table 12 demonstrated no evidence of a consistent trend between either of the parameters R_1 and σ_1 for the network pores and casting solution composition. However, on the basis of the data for 15 and 20 wt.% PES only there was an apparent decrease in R_1 with increase in polymer concentration. There was also an apparent decrease in both the parameters R_2 and σ_2 for the aggregate pores with increase in polymer concentration. These apparent trends would explain the decrease in product rate and corresponding increase in solute separation observed with increase in polymer concentration.

Concurrent with the pore size decrease, there was an apparent increase in the parameter h_2 with increase in polymer concentration. The increase in the relative number of aggregate pores to network pores is contradictory to the decrease in product rate and increase in solute separation observed. Thus, the change in the size of pores compared to the change in the relative number of pores must have had an overriding effect on membrane performance. This is in accord with Hagen-Poiseuille's theory which says that the rate of material transport through the membrane pores is proportional to the pore radius at the fourth power.

Generally, the PVP/PES weight ratio in the casting solution had no consistent effect on any of the parameters R_1, σ_1, and R_2. However, on the basis of the data for 15 wt.% PES only there was an apparent decrease in R_2 with increase in the PVP/PES weight ratio. Of interest, increasing PVP/PES resulted in a minimum in the parameter h_2 at PVP/PES in the vicinity of 1.0 (w/w).

The effect of the PVP/PES weight ratio on σ_2/R_2, the coefficient of variation, is shown in Figure 15 for the three polymer concentrations 15, 20 and 25 wt.% PES. The curve of $\ln(\sigma_2/R_2)$ as a function of PVP/PES has a maxima in the vicinity of 1.0. This coincides with the maxima in the product rate curve, shown in Figure 10, and with the minimum in the parameter h_2. At the 15 wt.% PES level the concurrence of inflexions is occuring despite the observed apparent decrease in the aggregate pore size R_2 whose effect would be to decrease product rate.

FIGURE 16

DEPENDENCE OF AGGREGATE (SECOND) PORE SIZE DISTRIBUTION, EXPRESSED AS $\ln \sigma_2/R_2$, ON THE CASTING SOLUTION COMPOSITION

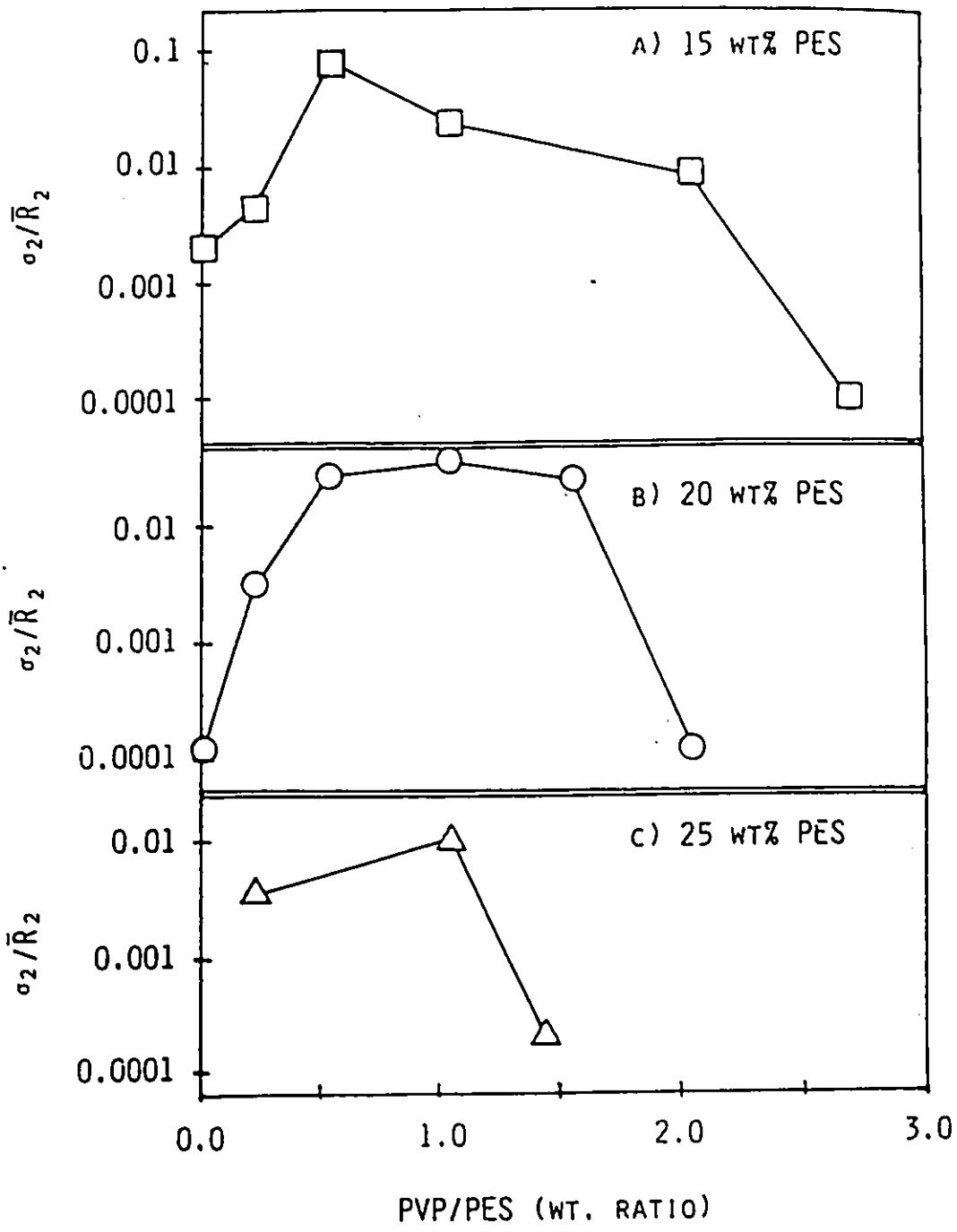
A) 15 WT% PES
B) 20 WT% PES
C) 25 WT% PES
0.1
0.01
0.001
0.0001
$\sigma_2/\bar{R}_2$
0.0
1.0
2.0
3.0
PVP/PES (WT. RATIO)

A test of model inadequacy was carried out (see Appendix 14) for the transport model used in the analysis of pore size distribution. Because the experimental data used in the analysis contained no replicates the test of model inadequacy described by Draper and Smith (42) was used which employs an 'external' estimate of pure error variance. The purpose of the significance tests were to determine whether the residual component due to an inadequacy in the form of the model fitted was appreciably larger than the pure error involved in the evaluation of solute separation. The experimental error (defined in Appendix 12) was used as an 'external' estimate of the pure error variance in the tests although this could possibly be larger than experimental error. The ensuing test ratio, T, for each membrane involved in the pore size distribution analysis is given in Table 13, along with the corresponding estimate of pure error variance, σ_E^2 , and the sum of squares of residuals or $\sum e_u^2$.

The significance of any inadequacy in the fitted model is tested by comparing the value of T with the value of F ((n-p), γ_E , α) at the desired probability level. For this test the value of (n-p) was 3 since there were n = 8 data points, for the eight probe solutes, and p = 5 parameters estimated. The degree of freedom associated with the estimate was γ_E = 8 since the 8 experimental data points had one degree of freedom each. The resulting F test value at the 95% probability level was F (3, 8, 0.05) = 4.07.

Comparison of T values with the F test resulted in only 3 'lack of fit' out of 15 membranes characterized. Considering that the estimate of pure error variance based on the experimental error alone could have been less than the actual pure error variance, the model used for the pore size analysis generally provided a good fit.

5.3 VISCOELASTIC APPROACH TO PORE FORMATION

This section is concerned with the study of the viscoelastic behavior of the polymer casting solution to gain insight into the membrane pore formation process. It had been suggested earlier in the theory that the polymer structure of the casting solution might control the surface pore structure, and

TABLE 13

TEST OF MODEL INADEQUACY IN PORE SIZE DISTRIBUTION ANALYSIS

Membrane		Statistical Data		
PES (wt. %)	PVP/PES (w/w)	Σe_u^2	$\hat{\sigma}_E^2$	T
15	0.0	251.	40.53	2.07
	0.2	92.	46.32	0.66
	0.5	200.	43.98	1.52
	1.0	426.	45.58	3.12
	2.0	169.	40.65	1.39
	2.7	474.	43.02	3.67
20	0.0	308.	41.31	2.88
	0.2	18.	48.83	0.12
	0.5	662.	45.63	4.84
	1.0	155.	46.25	1.12
	1.5	318.	38.73	2.74
	2.0	1058.	39.09	9.02
25	0.2	348.	45.49	2.55
	1.0	462.	45.30	3.40
	1.4	899.	42.23	7.10

$$T = \frac{[\Sigma e_u^2/(n-P)]}{\hat{\sigma}_E^2}; \quad n = 8, \; P = 5$$

average residual, $\bar{e}_u = [\Sigma e_u^2/n\,]^{1/2}$; given in Table 12.

average error, $\hat{\sigma}_{E_{AV.}} = (\hat{\sigma}_E^2)^{1/2}$ = 6. to 7. (%)

hence the performance of membranes. Further, the polymer casting solution structure could be studied on the basis of the viscosity measurements for dilute solutions.

5.3.1 VISCOELASTIC BEHAVIOR OF POLYMER CASTING SOLUTION

The viscoelastic behavior of the polymer casting solution can be studied on the basis of the intrinsic viscosity data for polymers PVP , PES, and mixtures thereof in NMP. Intrinsic viscosity was plotted as a function of the composition in the polymer mixture. In Figure 13, the composition was expressed as the weight ratio PVP/PES. Alternatively, in Figure 14, it was expressed as the weight fraction of PES in the polymer mixture. The standard deviation was calculated with respect to each intrinsic viscosity measurement and in all cases it was less than 1%; this has negligible effect on the plots in Figure 13 and 14. The viscosity data from which the intrinsic viscosity was determined by linear regression is in Appendix 15.

A comprehensive view of the plots revealed a transition region in the range of PVP/PES = 0.4 - 1.0 (w/w) and PES weight fraction = 0.5 - 0.7. In Figure 14, the response curve for an ideal polymer mixture (with no polymer-polymer interaction) is shown for comparison. The intrinsic viscosity of an ideal polymer mixture is equal to the linear combination of the intrinsic viscosities of the pure polymers, where the weight fractions are the proportionality constants. An analysis of the plots in Figure 14 demonstrates the non-ideality of the polymer mixture PVP/PES, imparted by PVP-PES interactions.

The formation of a complex between PVP and PES could have been explained on the basis of the properties of PVP. It is reported (43) that PVP is a water-soluble synthetic polymer notable for the ease with which it forms complexes in the solid state with a diversity of small-molecule substances. The high solvent power of PVP is presumably similar to that of its monomer unit analog NMP, the solvent for PES in the casting solution, and related to the amphiphilic character of the monomer unit.

The interaction between polymer segments of PVP and PES, designated as species A and B, appears to be of the noncovalent type and thus is represented by A-B. When the species A and B are brought together in the condensed phase of the medium C, NMP in this case, there is an exchange as follows:

Reaction Scheme:

$$A\text{-}C + B\text{-}C \rightleftharpoons A\text{-}B + C\text{-}C$$

On the basis of the reaction scheme, the equation for the intrinsic viscosity response curve in Figure 14 may be written as follows:

$$[\eta]_{\text{polymer mixture}} = W_A [\eta]_A + W_B [\eta]_B + W_{A\text{-}B} [\eta]_{A\text{-}B} \quad (15)$$

where W_i is the weight fraction of component i. Therefore, the continuity equation is:

$$W_A + W_B + W_{A\text{-}B} = 1.0 \quad (16)$$

By comparison, the equation for the case of an ideal polymer mixture is:

$$[\eta]^*_{\text{mixture}} = W^*_A [\eta]_A + W^*_B [\eta]_B \quad (17)$$

Substracting Equation 17 from Equation 15 yields a mathematical expression for the deviation from ideality in the intrinsic viscosity response curve:

$$([\eta]-[\eta]^*)_{\text{mixture}} = (W_A - W^*_A)[\eta]_A + (W_B - W^*_B)[\eta]_B + W_{A\text{-}B}[\eta]_{A\text{-}B} \quad (18)$$

There are four unknown variables (W_A, W_B, $W_{A\text{-}B}$, $[\eta]_{A\text{-}B}$) and only two equations (Equations 16 and 18), whereby the system is clearly underspecified. The system would become completely

specified if the stoichiometric parameters and the reaction constant were known. The evaluation of these parameters would require an extensive amount of experimental data, and hence has not been attempted. For the same reason the calculation of aggregate size and aggregate pore size have not been attempted.

Theoretically, the above mechanism of PVP-PES complex formation should lead to higher $[n]$ than $[n]^*$ in the entire range of PES weight fraction since $[n]_{A-B}$ must be substantially higher than $[n]_A$ and $[n]_B$. The experimental results indicate, however, an opposite trend in the range of high PES weight fractions. This suggests the need for considering the PES-PES complex in the pure PES solution which is broken down to form new PVP-PES complexes when PVP is added. No clear evidence for the presence of such complexes (PES-PES) can be presented at this stage.

A conjecture for the reaction mechanism can be obtained simply from the ratio of monomer units in the polymer mixture at compositions in the transition region identified earlier and particularly at the critical concentration PVP/PES = 1.0. The monomer ratio (PVP/PES) was calculated for the compositions in the transition region. The results are given below:

PVP/PES (weight)	PES (wt. fr.)	PVP/PES (monomer units)
0.43	0.7	0.89
0.75	0.57	1.56
0.90	0.53	1.87
1.00	0.5	2.07

Therefore, a PVP/PES monomer ratio ranging approximately from 0.9 to 2.1 exists in the transition region. This implies that the interaction between PVP and PES polymers is the strongest when from one to two $O{=}C{-}N{<}$ functional groups in the PVP polymer interacts with each of $O{=}S{=}O$ group which is apparently the most active polar functional group in the PES polymer. The interaction might as well be of the donor/ acceptor nature between $O{=}C{-}N{<}$ and an aromatic ring.

One possible representation of the complex A-B formed between PVP and PES is proposed below. NMP acting as a base takes a proton from PVP, thus creating a reaction site for the electrophilic groups.

Complex A-B (PVP-PES):

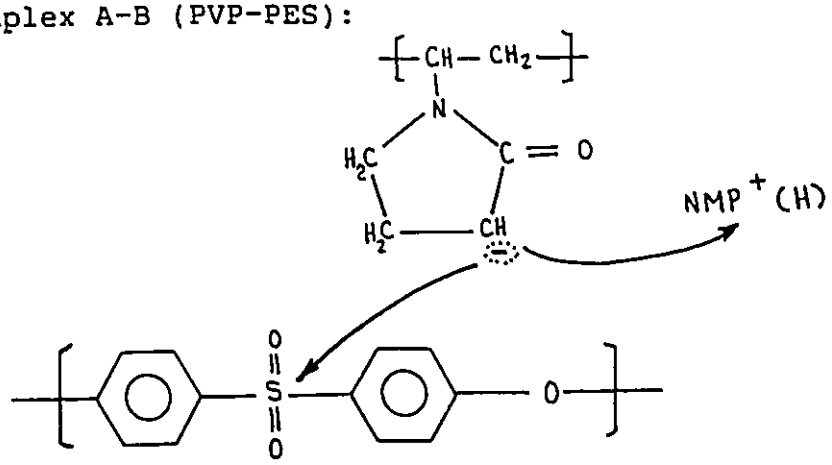

5.3.2 POLYMER SOLUTION STRUCTURE - MEMBRANE CHARACTERISTICS INTERRELATION

The pore characteristics of the membrane (pore size distribution, overall porosity) are among the principal factors governing its performance in RO/UF experiments. In turn, these pore characteristics are influenced by the physico-chemical properties of the polymer, the polymer structure in the casting solution and the method of preparation of the membrane.

The viscoelastic behavior of the concentrated polymer casting solution which is directly related to its polymer structure can be predicted on the basis of the intrinsic viscosity response curve (Figures 13 and 14) for dilute polymer solutions. Two significant features of this curve are its non-ideal character and the transition region in the composition range PVP/PES = 0.4 - 1.0. The non-ideal character is an indication of the existence of a copolymer aggregate (PVP - PES) in the casting solution. Consequently, three types of polymer aggregates could exist in the casting solution: pure polymer aggregates of PVP and PES respectively, as well as the PVP - PES copolymer aggregate. Moreover, different copolymer aggregates may exist with different polymer ratios.

The viscosity of the casting solution is determined by contributions from each polymer aggregate. The exact distribution of polymer aggregates in the casting solution, called solution structure, depends on the casting solution composition and more particularly on the ratio PVP/PES. Thus, the

effect of casting solution composition on the viscosity can be interpreted from the solution structure. Likewise, the transition region in the intrinsic viscosity response curve possibly corresponds to a transition in the polymer solution structure in that composition range. The distribution of polymer aggregates on the opposite sides of the transition region must therefore differ significantly. Also, the different types of polymer aggregates must have distinct viscometric properties. Further, within the transition region an intermediate solution structure must exist characterized by a higher concentration of the PVP - PES copolymer aggregates. Earlier in the discussion it was demonstrated that in the transition region the monomer ratio (PVP/PES) ranged approximately from 1 to 2. At the critical weight ratio (PVP/PES) of 1.0 the monomer ratio was approximately 2 which corresponded with the number of reaction sites on the PES monomer unit.

The plots of product rate and of the coefficient of variation, $\sigma_2/\bar{R}_2$, as a function of casting solution composition (Figures 10 and 15) both exhibited a shift, in this case a maxima, at PVP/PES in the vicinity of 1.0. This coincided with the transition region in the intrinsic viscosity curve, further related to solution structure. These results clearly indicated that the PVP-PES copolymer aggregate arising from interactions in the casting solution had an effect on the pore structure of the resulting PES membranes and consequently on membrane performance.

In the limit the PVP-PES interactions could have been strong enough as to inhibit the extraction of PVP by the gelation medium in the membrane fabrication process. In this event, PVP would become an integral part of the polymeric unit structure of the membrane instead of a simple additive in the casting solution.

Supporting evidence to the strongest interaction between PVP and PES polymers at PVP/PES weight ratio of unity was observed while preparing the PES membranes in the laboratory. Usually in the gelation process the water in the bath turns white because of the release of some low molecular weight PES from the film surface (Wumans and Smolders (46)). However, the degree of coloration was variable and depended on the composition of the casting solution used. The coloration of the water decreased with increasing PVP/PES ratio in the casting solution until,

at some critical value, practically clear water was obtained. For membranes prepared from the series of casting solutions with 15 wt.% PES the reversal occured at PVP/PES = 2.0. For membranes from the series of casting solutions with 20 wt.% PES the reversal occured at PVP/PES = 1.0. Also, the coloration of the water was more intense when used for the gelation of films made from casting solutions with 15 wt.% PES as opposed to 20 wt% PES. The above observations indicate that both the PVP/PES ratio and the PES concentration had an effect on the extent of PES released from the film of casting solution and ,hence, on the degree of polymer - polymer interactions.

Furthermore, PVP polymer which is entrapped in the PES polymer network and forms an integral part of the polymeric structure provides the polymer surface with a more hydrophilic nature than the surface of PES polymer only and causes a higher water flux through the membrane. The maximum in the product rate observed precisely at the point of the polymer structure transition, where the PVP-PES complex formation is most enhanced, seems therefore, to be reasonable.

Contrary to the above theories, the chemical analysis of membranes (referred to Appendix 16) from the transition region revealed that PVP/PES in the actual membrane material is less than 0.04 which is much different from 0.4 - 1.0 in the casting solutions. This implies that PVP in the PVP/PES copolymer aggregate does not become an integral part of the membrane and, therefore, must desorb over time when stored in water or when subjected to the pure water pressure. Because only a small fraction of PVP does remain as part of the membrane polymeric structure, the increase in hydrophilicity is not very significant although it may still contribute to the increase in product rate. It follows that the primary effect of PVP in the casting solution is in controlling the surface pore structure of the membrane, rather than its chemical nature. Accordingly, the trend in product rate is primarily the effect of the surface pore structure of the membrane which is controlled by the polymer structure in the casting solution.

5.4 POTENTIAL FOR COMMERCIALIZATION

Polysulfone membranes are often valued for their good thermal and chemical resistivity, and for their mechanical strength. Polysulfone membranes currently available commercially are mostly made from the polymers polysulfone and poly-phenylsulfone, supplied by Union Carbide Corp. under the tradenames Udel and Radel. Yet, membranes made from polyethersulfone, Victrex, supplied by ICI would be more promising due to its higher thermal stability (7). It would also be more suitable for water permeation due to its higher hydrophilicity.

In Table 14 the performance data of commercial polysulfone membranes (44) are compared to PES membranes from this work. The membranes were evaluated in the laboratory under the same test conditions. The commercial membranes were on a backing material while the laboratory PES membranes were unsupported. The results indicate that for the same level of solute separation, the PES membranes have a much superior product rate.

A comparison of the performance of PES membranes produced in this work with those produced by Tweddle et al (6) using an "acid gelation" technique (said to produce superior membranes) is made in Table 15. The membranes produced from this work have a superior product rate for an equivalent level of solute separation. Kai et al (7) do not report adequate membrane performance data for comparison. The maximum product rate they report is equivalent to 54 g/hr.A (A = 14.5 cm.sq. surface area) in this work.

Clearly the results obtained in this work have shown the PES membranes developed to be superior. Further, these PES membranes could have some commercial potential for which there exists a substantial market.

TABLE 14

PERFORMANCE COMPARISON WITH COMMERCIAL POLYSULFONE MEMBRANES

MEMBRANE			PERFORMANCE	
No.	Source	Casting Surface	PR (g/hr. A)	f (%)
1	DDS GR82 (see note 1)	Backing Material	41.	94.
2	Osmonics OK	Backing Material	207.	30.
3	Amicon PM-10	Backing Material	642.	10.
4	This work	Glass	374.±17.	93.5±4.4
5	" "	"	425.±56. (at maturity)	90.2±2.0 (at maturity)
6	" "	"	638.±47. (262.±50.)	25.1±7.0 (83.4±7.4)
7	" "	"	660.	8.8

Test Conditions: 200 ppm PEG-6000 aqueous feed

2.2 L/min. feed rate

50 psig feed pressure

25°C

A = 14.5 cm^2

NOTES: (1) De Danske Sukkerfarikker Co. Denmark

TABLE 15

PERFORMANCE COMPARISON WITH POLYETHERSULFONE MEMBRANES REPORTED IN THE LITERATURE

MEMBRANE			PERFORMANCE	
No.	Source	Casting Surface	PR (g/hr. A)	f (%)
1	Kai et al.(7) (see note 1)	Glass	54. (maximum)	-
2	Tweddle et al. (6) (see note 2)	Glass, Acid Gel.	253.	91.
3	" "	Glass, Acid Gel.	173.	98.
4	This work	Glass	425.±56.	90.2±2.0
5	" "	"	374.±17. (at maturity)	93.5±4.4 (at maturity)
6	" "	"	146.±33. (117.±1.)	98.3±2.4 (97.9±1.8)
7	" "	"	221.	98.6

Test Conditions: 200 ppm PEG-6000 aqueous feed

2.2 L/min. feed rate

50 psig

25°C

A = 14.5 cm^2

NOTES: (1) National Research Council of Canada, Chem. Eng. Dept.
(2) Daicel Chemical Industries, Ltd., Japan

CONCLUSION

A major thrust of this work has been the demonstration of an interrelationship between the structure of the casting solution in presence of the polymeric nonsolvent swelling agent, polyvinyl pyrrolidone (PVP), and the performance of the resulting polyethersulfone (PES) membrane and the pore size distribution at the membrane surface. Concurrently, highly productive polyethersulfone membranes with potential for commercialization have been developed. The specific conclusions are:

1. The relationship existing between casting solution composition and performance of the polyethersulfone membrane is now known:

   i) The effect of increasing polymer concentration is to increase solute separation and decrease product rate.

   ii) The effect of increasing the weight ratio of nonsolvent to polymer (PVP/PES) is to increase product rate until a maximum is reached in the vicinity of PVP/PES = 1.0; while solute separation is relatively constant.

2. The apparent relationship existing between casting solution composition and pore size distribution at the surface of the polyethersulfone membrane is as follows:

   i) The effect of increasing polymer concentration is to decrease the average and standard deviation of aggregate pore size, R_2 and σ_2 respectively; this explains the increase in solute separation and corresponding decrease in product rate observed.

   ii) The effect of increasing the nonsolvent to polymer weight ratio (PVP/PES) is a maximum in the coefficient of variation of aggregate pore size, σ_2/R_2, and a minimum in the number ratio of aggregate to network pores, h_2, both in the vicinity of PVP/PES = 1.0 (w/w); this is coincident with the maximum observed in product rate.

3. The viscoelastic behaviour of the casting solution for the polyethersulfone membrane is now known:

   i) The non-ideal character of the intrinsic viscosity response curve suggest the existence of PVP-PES interactions in the casting solution leading to the formation of PVP-PES copolymer aggregates. In particular, the inflexion observed in the vicinity of PVP/PES = 1.0 (w/w) indicates stronger interactions in that composition range.

   ii) As expected, the overall effect of increasing the nonsolvent to polymer weight ratio (PVP/PES) is to increase the intrinsic viscosity and, hence, the average polymer aggregate size.

4. A concurrence of inflexions in solution structure, pore size distribution and product rate at the PVP/PES weight ratio in the vicinity of 1.0 for the casting solution was observed with the polyethersulfone membrane. Further, at PVP/PES = 1.0 (w/w) the monomer ratio equal to 2 coincides with the number of reaction sites on the PES monomer.

5. The mode of immersion used in the fabrication of the membrane significantly impacts on its performance. The fast immersion compared to the slow immersion yields membranes with superior productivity (an increase of almost 900% in product rate) at the same level of solute separation, as well as with much superior reproducibility.

6. The role of the immersion mode in membrane formation is now known: it controls the formation of the thin active layer at the membrane surface, and in particular the thickness of the active layer which contributes to the hydrodynamic resistance.

7. The sample standard deviation in membrane performance (a measure of membrane reproducibility) compared with experimental error was not significantly different in terms of solute separation (+/-6 versus +/-7) but was significantly larger in terms of product rate (+/-19 versus +/-5 percent).

8. For the majority of membranes characterized, it has been demonstrated that any inadequacy in the transport model used in the analysis of pore size distribution was not significantly larger than experimental error.

9. Membrane performance changes with time on stream. An increase in solute separation and corresponding decrease in product rate was noticed by comparing first-level to second-level tests results. The smoothing of the performance curves noticed by a similar comparison of the results is due to stabilization of the membrane porous structure arising from the compaction of the porous substratum.

10. Annealing the polyethersulfone membrane in ethylene glycol at temperatures up to 120°C results in an increase in product rate and decrease in solute separation. At temperatures 150°C and above the membrane shrinks and deteriorates.

11. The polyethersulfone membranes developed in this work surpass existing commercial polysulfone membranes with respect to productivity at a given level of solute separation.

RECOMMENDATIONS FOR FUTURE WORK

The viscoelastic approach proposed to control the pore size distribution at the membrane surface, and simultaneously the performance in RO/UF applications, by the control of the polymer structure in the casting solution was studied using the polyethersulfone membrane. It is recommended that the effect of other nonsolvent swelling agents than polyvinyl pyrrolidone and other solvents than N-methyl-pyrrolidone in the formation of this membrane should also be studied using the viscoelastic approach. Similarly, the formation of other polymeric membranes should be studied by this approach and the information consolidated.

The fundamental and practical significance of the disclosures made in this work with respect to the polyethersulfone membrane could extend to other polymeric membranes. Use of polymeric additives interacting with the membrane polymer material in the casting solution to optimize membrane productivity should be exploited. Also, the technique to improve membrane productivity and also the reproducibility which is concerned with the mode of immersion should be exploited.

ACKNOWLEDGEMENT

I would like to acknowledge my thesis directors Dr. T. Matsuura, National Research Council of Canada (NRCC), Dr. S. Sourirajan, Industrial Membrane Research Institute, University of Ottawa, and Dr. F.D.F. Talbot, Chemical Engineering Department, University of Ottawa, for their sustained encouragement and support throughout my graduate studies. I am also endebted to T.A. Tweddle, NRCC, for technical assistance and to A.Y. Tremblay, NRCC, and Dr. T.D. Nguyen, formerly from NRCC, for enlightening discussions on the subject. For the determination of the molecular weight of polyethersulfone polymer, I would like to thank Dr. S. Coulombe, Canmet, Energy Mines and Resources Canada. I also acknowledge Mrs. D. McCallum, Esso Petroleum Research Canada, for her assistance in typing parts of this manuscript. I wish to thank all the others who I may have forgotten or omitted by fear of discrimination.

For financial support of this project, I acknowledge the National Research Council of Canada, and also the Natural Sciences and Engineering Research Council and the School of Graduate Studies of the University of Ottawa for the award of scholarships.

NOMENCLATURE

A	membrane surface area	m^2
A	constant characterizing electrostatic repulsion force	m
∂	activity	
B	constant characterizing vander Waals attraction force	m^3
b	frictional function	
C_{A1}	bulk feed solute concentration defined by Figure 1	$gmol/m^3$
C_{A2}	interfacial feed solute concentration defined by Figure 1	$gmol/m^3$
C_{A3}	product solute concentration defined by Figure 1	$gmol/m^3$
C_{feed}	Total Organic Carbon (TOC) in feed	ppm wt.
C_{PR}	TOC in product	ppm wt.
C_{pwp}	TOC in permeated water	ppm wt.
C_{dw}	TOC in distilled water	ppm wt.
C^*_{feed}	corrected feed TOC	ppm wt.
C^*_{PR}	corrected product TOC	ppm wt.
c	polymer solution concentration	g/l
D	constant characterizing steric repulsion at interface	m
D_{ab}	diffusivity of solute in water	m^2/s
E	conversion criterion	
eu	residual	
f	solute separation	%
f'	interfacial solute separation	%
f*	predicted solute separation	%
F	transport function in equation x	
F	significance test	
IPWP	initial pure water permeation	g/hr. A
h_2	number ratio of aggregate pores to network pores	
K	Mark-Houwink constant defined by equation	
K	correction factor defined by equation	
k	viscometer constant defined by equation	
Mn	molecular weight of polymer aggregate	g
Mn*	molecular weight of polymer aggregate in presence of nonsolvent	g
n	no. of polymer molecules in polymer aggregate as defined by equation	
n	number of probe solutes	
[n]	intrinsic viscosity	l/g
[n]*	intrinsic viscosity of an ideal polymer solution	l/g
n_{sp}	specific viscosity	
$n_{rel.}$	relative viscosity	
P	applied pressure	psig
ΔP	transmembrane pressure difference	psig
P	flow function as defined by equation	
PR	product rate	g/hr. A
PWP	pure water permeation	g/hr. A
P	polymer concentration in casting solution	wt%
R	single pore radius	Å
R	average pore radius in single normal distribution	Å
R_i	average pore radius of the ith distribution in a multi normal distribution	Å
R	gas constant	
R	PVP/PES weight ratio in casting solution	wt./wt.
SSR	sum of residuals	

<S>	radius of a spherical polymer aggregate	m
T	temperature	°C
T	absolute temperature	K
t	annealing time	minutes
t_s	sampling time	minutes
t_o	efflux time of pure solvent	s
t_s	efflux time of solution	s
T	significance test for model adequacy	
v	volume of unsolvated polymer molecule	m^3
W_s	sample weight	g
W	weight fraction PBS in polymer mixture	
W*	weight fraction PBS in ideal polymer mixture	
Y	normal distribution function defined in equation	

Greek Letters

α	Mark-Houwink constant defined in equation	
α	significance level	
$\alpha(\delta)$	dimensionless solution velocity profile in a cylindrical pore	
B_1	dimensionless solution viscosity	
B_2	dimensionless operating pressure	
Γ	surface exces of solute	$gmol/m^2$
γ	interfacial tension at the air-solution interface	N/m
Ξ	effective volume factor	
ν	degrees of freedom in significance test	
δ	dimensionless radial distance	
σ	standard deviation of the normal pore size distribution	Å
σ_i	standard deviation of the ith normal pore size distribution	Å
σ_f	standard deviation in solute separation	%
σ_{PR}	standard deviation in permeation rate	g/hr. A
σ_E^2	estimate of pure error variance in solute separation	$(\%)^2$
$\Delta\pi$	transmembrane osmotic pressure difference	psig

REFERENCES

1. Matsuura, T. and Sourirajan, S., (1985) in "Reverse Osmosis and Ultrafiltration", Sourirajan, S. and Matsuura, T., Eds., ACS Symposium Series 281, 1985, pp. 1-19.

2. Nguyen, T.D.; Chan, K.; Matsuura, T. and Sourirajan, S., (1985) Ind. Eng. Chem. Prod. Res. Dev., 1985, 24, 655.

3. Nguyen, T.D.; Matsuura, T. and Sourirajan, S.; Chem. Eng. Comm. in press 1987a.

4. Nguyen, T.D.; Matsuura, T. and Sourirajan, S.; Chem. Eng. Comm. in press 1987b.

5. Nguyen, T.D.; Matsuura, T. in Proceedings of International Membrane Conference, September 24-26, 1986, Ottawa, Malaiyandi, M., Talbot, F.D.F. and Kutowy, O., Eds., National Research Council of Canada, pp. 99-114.

6. Tweddle, T.A.; Kutowy, O.; Thayer, W.L.; Sourirajan, S., Ind. Eng. Chem. Prod. Res. Dev., 1983, 22, 320.

7. Kai, M.; Ishii, K.; Isugaya, H.; Miyano, T., in "Reverse Osmosis and Ultrafiltration", Sourirajan S. and Matsuura, T., Eds., ACS Symposium Series 281, 1985, pp. 21-33.

8. Loeb, S.; Sourirajan, S.; Adv. Chem. Ser. 38 (1962) 117.

9. Reid, C.E.; Breton, E.J.; J. Appl. Polym. Sci. 1 (1959) 133.

10. Riley, R.L.; Gardner, J.O.; Merten, U.; Science 143 (1964) 801.

11. Schultz, R.; Asunmaa, S.; Recent Progr. Surface Sci., 1970, 3, 801.

12. Pusch, W.; Walch, A.; Angew. Chem. Int. Ed. Engl. 21 (1982) 660-685.

13. Kesting, R.E.; Synthetic Polymeric Membranes, McGraw Hill, New York, N.Y., 1971.

14. Strathmann, H.; Kock, K.; Amar, P.; Desalination, 16 (1975) 179-203.

15. Koenhen, D.M.; Mulder, M.H.V. and Smolders, C.A., J. Appl. Polym. Sci., 21 (1977) 199.

16. Wijmans, J.G.; Baaij, J.P.B. and Smolders, C.A., Journal of Membrane Science, 14 (1983) 263-274.

17. Baaij, J.P.B., patent applied for by Wafilin B.V., Hardenberg, The Netherlands (1981).

18. Kesting, R.E., "Membranes", Cellulose and Cellulose Derivatives, V.N.M. Bikales and L. Segal, eds., Wiley-Interscience, New York, 1233 (1971).

19. Neogi, P., AIChE Journal, Vol. 29, No. 3, 1983.

20. Sourirajan, S., "Lectures on Reverse Osmosis", Divison of Chemistry, National Research Council Canada, Ottawa, 1983.

21. Sourirajan, S.; Matsuura, T.; "Reverse Osmosis and Ultrafiltration" in Encyclopedia of Fluid Mechanics, N.P. Cheremisinoff, ed., 1985.

22. Smolders, C.A.; Vugteveen, E.; in "Materials Science of Synthetic Membranes", Lloyd, D.R., Ed., ACS Symposium Series 269, 1985, pp. 327-338.

23. Bodzek, M.; Polish Journal of Chemistry, 57 1983, 919-930, (Eng.).

24. Rudie, B., in Proceedings of Internationsl Membrane Conference, September 24-26, 1986, Ottawa, Malaiyandi, M.; Talbot, F.D.F., and Kutowy, O., Eds., National Research Council of Canada, pp.

25. Tremblay, A.Y., in Proceedings of International Membrane Conference, September 24-26, 1986, Ottawa, Malaiyandi, M.; Talbot, F.D.F.; and Kutowy, O., Eds., National Research Council of Canada, pp.

26. Zeman, L.; Tkacik, G.; in "Materials Science of Synthetic Membranes", Lloyd, D.R., Ed., ACS Symposioum Series 269, 1985, pp. 339-350.

27. Matsuura, T.; Taketani, Y.; Sourirajan, S.; in ACS Symp. Ser. 154, "Synthetic Membranes, Vol. II", A.F. Turbak, ed., pp. 315-338, American Chemical Society, Washington, D.C., 1981.

28. Matsuura, T. and Sourirajan, S. (1981): Reverse Osmosis Transport through Capillary Pores under the Influence of Surface Forces, Ind. Eng. Chem. Process Des. Dev., 20: 273-282.

29. Chan, K.; Matsuura, T. and Sourirajan, S., Ind. Eng. Chem. Prod. Res. Dev., 21, 605 (1982).

30. Sourirajan, S., Ind. Eng. Chem. Fundam., 2, 51, (1963).

31. Sourirajan, S. and Matsuura, T. (1985): Reverse Osmosis/ Ultrafiltration Process Principles, Chapter 4, National Research Council of Canada, Ottawa.

32. Lonsdale, H.K.; Merten, U.; Riley, R.L.; J. Appl. Polym. Sci., 9, 1341 (1965).

33. Riley, R.L.; Lonsdale, H.K.; Lyons, C.R.; Merten, U.; J. Appl. Polym. Sci., 11, 2143 (1967).

34. Mazid, M.A.; Separation Science and Technology, 19 (687), pp. 357-373, 1984.

35. Cabasso, I.; Klein, E.; Smith, J.K.; J. Appl. Polym. Sci., 20 (1976) 2377.

36. Aptel, P.; Ivaldi, F.; Lafaille, J.P.; "Development of Polysulfone Hollow Fibres: Spinning Process and Transport Properties in Ultrafiltration".

37. Dreger, D.R.; Mach. Des., 1978, 50 (1), 114.

38. "Victrex" Polyethersulphone Technical Service Information Notes VX 102 and VX AD 17.78, Imperial Chemical Industries (ICI), Plastics Division.

39. Taketani, Y.; Matsuura, T.; and Sourirajan, S.; Separation Science and Technology, 17 (6), pp. 821-838, 1982.

40. Rudin, A.; Johnston, H.K.; J. Paint Technol. 1971, 43, 39.

41. Johnston, H.K.; Sourirajan, S.; J. Appl. Polym. Sci., 1973, 17, 3717.

42. Draper, N.R.; and Smith, H.; "Applied Regression Analysis", John Wiley, New York, 1966.

43. Molineux, P.; "The Physical Chemistry and Parmaceutical Applications of Polyvinylpyrrolidone".

44. Tweddle, T.A.; not published.

45. Matsuura, T. and Sourirajan, S. (1985): Fundamentals of Reverse Osmosis, National Research Council Ottawa, Canada, a) p. 102, b) p. 82.

46. Wumans, J.G.; Smolders, C.A.; Eur. Polym. J., 1983, 19, 1143.

APPENDIX 1

Properties of Victrex Polyethersulfone (38)

TABLE I

Typical Physical Properties of Various Victrex Grades

Many of the values assigned to properties of thermoplastics are dependent upon processing conditions and so the test results given below are typical values only. These results were obtained using standard test conditions and, with the exception of specific gravity, should not be used as a basis for design.

Property	Test Method	Units	Values for 'Victrex' grades 200P and 300P	420P*	430P*
General					
Form	–	–	Granules or Powder	Granules	Granules
Appearance (natural)	–	–	Amber/Transparent	Brown/Opaque	Brown/Opaque
Relative density	ASTM D 792	–	1.37	1.51	1.60
Refractive index	–	–	1.65	–	–
Shrinkage of moulding	–	%	0.6	0.3	0.2
Glass content	–	%	0	20	30
Mechanical					
Tensile strength at 20°C	ASTM D 638	MN/m^2	84	124	140
at 180°C	(DIN 53455)		41	60	100
Elongation at break	ASTM D 638	%	40–80	3	3
Flexural strength	ASTM D 790	MN/m^2	129	172	190
Flexural modulus at 20°C	ASTM D 790	GN/m^2	2.6	5.9	8.4
at 180°C			2.3	5.6	8.0
Izod impact strength	ASTM D 256	J/m			
6.4 mm specimen notched			84	75	80
6.4 mm specimen unnotched			No Break	430	540
Rockwell hardness	ASTM D 785		M88	M98	M98
Taber abrasion	ASTM D 1044	mg/1000			
	(1 kg–CS17)	rev	6	8	–
Thermal					
Heat distortion temperature at 1.82 MN/m^2	ASTM D 648 (ISO R75)	°C	203	210	216
Vicat softening point 1 kg	ASTM D 1525	°C	226	>226	>226
5 kg	(ISO R306)	°C	222	>222	>222
Coefficient of linear thermal expansion	ASTM D 696	per deg C	5.5×10^{-5}	2.6×10^{-5}	2.3×10^{-5}
Underwriters' Laboratories temperature index	UL 746	°C	180	–	–
Electrical					
Volume resistivity	ASTM D 257	Ohm cm	10^{17}–10^{18}	$>10^{16}$	$>10^{16}$
Permittivity 60 Hz	ASTM D 150	–	3.5	–	–
10^6 Hz			3.5	–	–
Loss tangent 60 Hz	ASTM D 150	–	0.001	–	–
10^6 Hz			0.0035	–	–
Dielectric strength	ASTM D 149	kV/mm	16	–	16
Corrosion liability factor	IEC 426	–	5	–	8
Tracking resistance	DIN 53480 VDE 0303	Volts	150	150	140
Arc resistance (tungsten carbide electrodes)	ASTM D 495	–	20–120	–	–
High voltage arc ignition	UL 746	Seconds	300	–	–
High amp arc ignition	UL 746	Arcs	200	–	–
Flammability and Burning Behaviour					
Flammability rating Underwriters' Laboratories	ASTM D 635	AEB/ATB	4.1/- (Immediate extinction)		
flammability rating 1.6 mm	UL 94	–	V–0	V–0	V–0
0.5 mm			V–0	–	–
0.3 mm			V–1	–	–
Limiting Oxygen Index 0.5 mm	ASTM D 286	–	34	–	–
1.6 mm			38	–	–
Hot wire ignition	UL 746	Seconds	80	–	–
Smoke emission (flaming condition, 1.6 mm)	NBS smoke chamber	Specific optical density (DM)	50	–	–

TABLE II

Chemical Resistance of Victrex at Room Temperature

Chemical resistance

The compatibility of 'Victrex' with many chemicals has been investigated in the laboratory and the results are given in Table 2.

The results have been categorised as follows:

A = No attack. Little or no absorption at 20°C

B = Slight attack. Some absorption causes swelling at 20°C. Satisfactory use of 'Victrex' will depend on the application.

C = Bad attack. 'Victrex' should not be used for any application where these environmental conditions are present.

The use of a small letter indicates that 'Victrex' has not been tested specifically with that chemical but that the result can be predicted from tests with similar chemicals.

The results are derived from tests in which unstressed specimens were completely immersed in a wide range of chemical environments at room temperature. These results may differ considerably from those found in service, especially in the effects of stresses and strains set up during fabrication, or in use at elevated temperatures. These conditions, particularly those of stress and strain, are difficult to reproduce in the laboratory. The table, therefore, should be used as a guide, and the user should satisfy himself beforehand of the suitability of polyethersulphone for the in-service environment.

A summary of the resistances of 'Victrex' to water and organic and inorganic chemicals is given below:

a) Water

Polyethersulphone is not attacked chemically by water – the physical effects of water upon the material at various temperatures have been discussed earlier in the Note.

b) Inorganic chemicals

Polyethersulphone is unaffected by most inorganic reagents. Aqueous solutions do not generally attack polyethersulphone although the physical properties may be affected by the slight plasticisation action of the absorbed water. Polyethersulphone is attacked by concentrated oxidising mineral acids at room temperature but is not affected by more dilute acids. Resistance to alkalis is good.

c) Organic chemicals

Aliphatic hydrocarbons, alcohols, benzene, petroleum spirit, organic acids, oils and fats do not usually attack polyethersulphone. In some cases slight absorption occurs, but this does not usually cause degradation or permanent chemical change. Polyethersulphone is soluble in highly polar organic solvents such as dimethysulphoxide, aromatic amines and nitrobenzene, as well as certain chlorinated hydrocarbons such as dichloromethane and chloroform.

Table 2. The resistance of 'Victrex' to chemical attack

Chemical	Result
Acetaldehyde	C
Acetic acid – glacial	A
Acetic acid – 10% §	A
Acetone	C
Aluminium salts	a
Ammonia – 880	A
Ammonium hydroxide – 10%	A
Ammonium chloride – 10%	A
Amyl acetate	B
Aniline	C
'Arcton' propellants	a
Aviation hydraulic fluid	B
Aviation spirit	A
Barium salts	a
Benzaldehyde	C
Benzene	A
Benzoic acid	A
Benzene sulphonic acid	a
Bleach	A
Boric acid	a
Brake fluid	B
Brine	A
Butane	A
Butanol	A
Butyl acetate	b
Calcium nitrate	A
Calcium hypochlorite	A
Carbon disulphide	b
Carbon tetrachloride	A
Chlorobenzene	C
Chloroform	C
Chlorosulphonic acid	c
Chromic acid	A
Citric acid §	A
Copper sulphate	A
Creosote	A
Cresols	C
Cyclohexane	A

Chemical	Result
Cyclohexanol	A
Cyclohexanone	C
Detergent solutions	A
Dibutyl phthalate	A
Dichloroethane	C
Dichloroethylene	B
Dichlorobenzene	C
Diesel oil	A
Diethylamine	A
Diethyl ether	A
Dimethyl formamide	C
Dioctyl phthalate	A
Dioxane	b
Edible fats and oils §	A
Ethyl acetate	C
Ethyl alcohol §	A
Ethylene glycol	A
Ferric chloride	A
Formaldehyde	A
Formic acid	A
Glycerol §	A
Heptane	A
Hexane	A
Hydrochloric acid – 10%	A
Hydrochloric acid – conc	A
Hydrogen peroxide	A
Hydrogen sulphide	a
Iodine in potassium iodide	B
Isopropanol	A
Iso-octane	A
Kerosene	A
Lactic acid §	a
Lead acetate	a
Linseed oil	A
Magnesium sulphate	A
Mercuric chloride	a
Mercurous chloride	a
Mercury	a
Methanol	A
Methyl ethyl ketone	C
Methylene chloride	C
Milk §	A
Motor oil	A
Nickel salts	a
Nitric acid – 10%	A
Nitric acid – conc	C
Nitrobenzene	C
Oils – vegetable §	A
Oleic acid	a
Oleum	C
Oxalic acid	A
Perchloroethylene	C
Petrol	A
Petroleum ether	A
Phenol	C
Potassium hydroxide – 10%	A
Potassium hydroxide – 50%	A
Propane	a
Pyridine	C
Silicone fluids	A
Silver nitrate	A
Soap solution	A
Sodium chloride	A
Sodium hydroxide – 10%	A
Sodium hydroxide – 50%	A
Sodium hypochlorite	a
Sulphuric acid – 10%	A
Sulphuric acid – conc	C
Sulphurous acid	c
Tar	a
Tartaric acid §	a
Tetrahydrofuran	C
Toluene	C
Transformer oil	A
Trichloroethylene	B
Turpentine	A
Vaseline	a
Varnish	A
Water §	A
Wax	a
White spirit	A
Wines and spirits §	a
Xylene	B
Zinc salts	a

§'Victrex' polyethersulphone has been approved by the National Water Council (UK) for contact with potable water.

'Victrex' polyethersulphone complies with FDA (US) regulation 21CFR 177.2440, 'Polyether sulfone resins for contact with foodstuffs'.

TABLE III

Solvents and Solvent Systems for Victrex

Solvents

The following list gives some of the more common solvents for 'Victrex' polyethersulphone together with the boiling points and threshold limiting values (TLV).

Solvent	TLV		Boiling Point °C	Comments
	Parts per million	mg/m^3		
Dichloromethane	100	360	40	
Chloroform	25	120	61	Solution unstable
1,2,dichloroethane	50	200		Solution unstable
1,1,2,2,tetrachloroethane	5	35	146	Solution unstable
Dimethylformamide (DMF)	10	30	153	
Dimethylsulphoxide (DMSO)	Not established		189	Solution unstable
N,methyl-2-pyrrolidone (NMP)	100	-	202	
Nitrobenzene	1	5	211	
Pyridine	5	19		Solution unstable
Aniline	5	19		Solution unstable
Dimethylphthalate	-	5	284	soluble on heating
Butyrolactone	Not established		204	
Cyclopentanone	-	-	130	
Conc. sulphuric acid			-	Reacts at high temperatures
Cyclohexanone	50	200	156	soluble on heating
1,1,2 trichloroethane	10	45	114	

Solution Stabilisers

The use of a single solvent will, in some cases, produce a cheese like solid (crystalline complex) with polyethersulphone. For this reason a combination of solvents is used to produce stable solution. The list gives the boiling points and TLV values for some of the diluents and solution stabilisers that can be used in conjunction with one or more of the solvents described.

Diluent	TLV		Boiling Point °C
	Parts per million	mg/m^3	
Toluene	200	750	111
Xylene	100	435	144-138
Methyl ethyl ketone	200	590	80
Acetone	1000	2400	56
Methanol	200	260	65

It must be noted that some of the diluents suggested above will be incompatible with one or two of the solvents either totally or at certain concentrations.

TABLE IV

Some Solution Properties of Victrex

Solvent	PES - 100P			PES - 200P			PES - 300P		
	Stability	Viscosity cps	Solution Clarity	Stability	Viscosity cps	Solution Clarity	Stability	Viscosity cps	Solution Clarity
Dimethylformamide Flash pt.(TOC) 153°F Boiling pt. 307°F									
10% PES	>1 month	25	clear	> 1 month	15	clear	> 1 month	20	clear
20% PES	3 weeks	350	clear	> 1 month	185	clear	> 1 month	347	clear
30% PES	1 week	4,500	clear	1 week	2,000	clear	> 1 month	9,620	clear
40% PES	36 hours	70,900	clear	36 hours	19,800	clear	24 hours	> 100,000	clear
N-Methyl Pyrrolidone Flash Pt.(TOC) 204°F Boiling pt. 395°F									
10% PES	>1 month	60	clear	>1 month	43	clear	> 1 month	60	clear
20% PES	>1 month	1,000	clear	>1 month	500	clear	> 1 month	1,000	clear
30% PES	>1 month	15,500	clear	>1 month	7,610	clear	> 1 month	14,240	clear
48% Methylene Chloride** 48% 1,1,2 Trichloro-ethane 4% Methanol Flash pt. 60°F Boiling pt. 125°F									
10% PES	>1 month	33	clear	>1 month	29	clear	3 weeks	32	clear
20% PES	1 week	600	clear	2 weeks	290	clear	1 week	600	clear
30% PES	1 week	9,260	cloudy*	1 week	2,600	cloudy*	48 hours	10,000	cloudy*

*Solutions are clear below 25% solids

**For concentrations below 15% solids, chloroform may be substituted for 1,1,2 trichloroethane with a slight ratio change to 53/43/4

All viscosities run at 23°C

All percentages are weight percent

For best results, polymers should be dried at 150°C for 3-4 hours before adding solvent, and solvents should contain a minimum amount of water.

APPENDIX 2

PROGRAM FLOWCHART FOR PORE SIZE DISTRIBUTION ANALYSIS

A nonlinear regression routine was used for the evaluation of the bi-normal pore size distribution parameters for the membrane. The computer program Nonlin from the Watfiv library at University of Ottawa was used, it called three subprograms: Resid, Deriv and Sepa. The subprogram SEPA was to calculate the separation for each probe solute (fi) on the basis of the transport model and using the pore size distribution parameter values assigned by DERIV or RESID from which SEPA was called. RESID was to compute the residual sum of squares (SSN) for a given set of parameter values. While DERIV was to determine the numerical partial derivatives for solute separation with respect to each parameter $(\delta f/\delta\theta(I))_i$. The five parameters $\bar{R}_1$, σ_1, $\bar{R}_2$, σ_2, h_2 were expressed as $\theta(I)$, I=1, ..., 5, in Nonlin. A block diagram describing the computing sequence is shown below. Flowcharts of the main program Nonlin and the subprogram SEPA follow; along with a dedicated nomenclature.

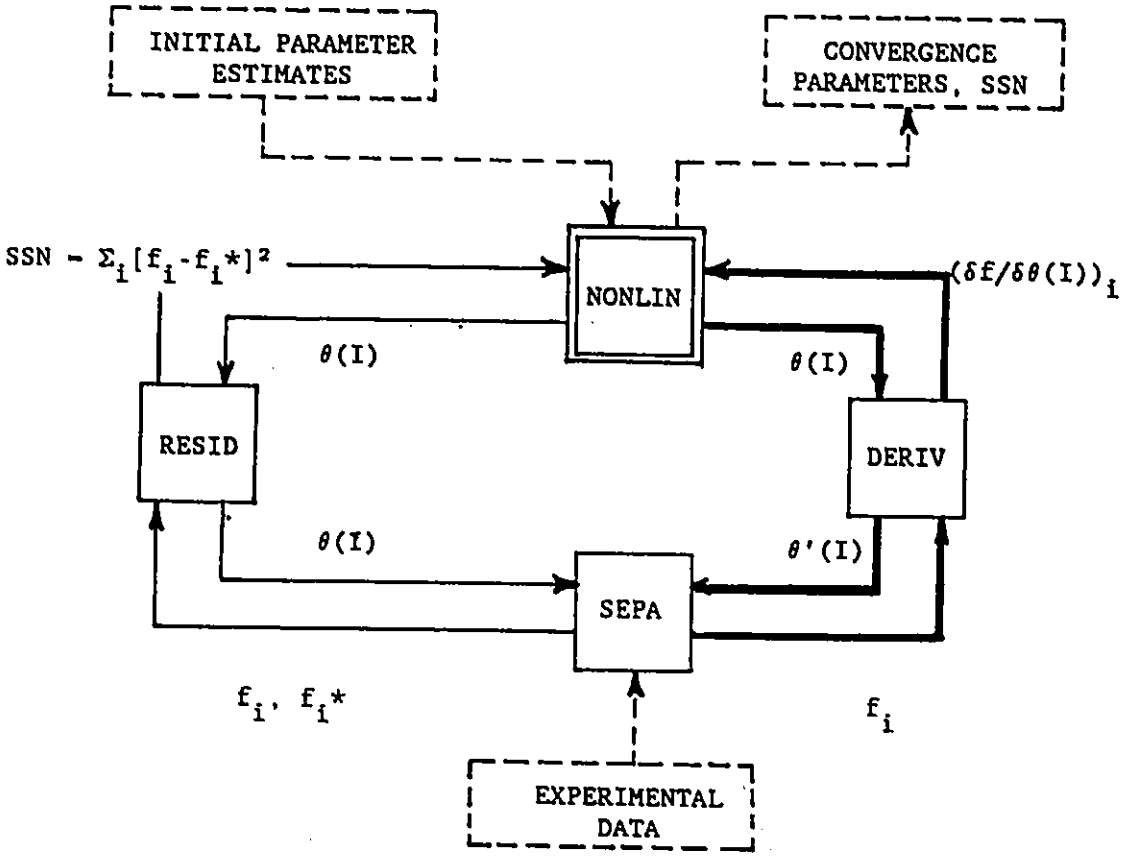

FLOWCHART: PROGRAM NONLIN

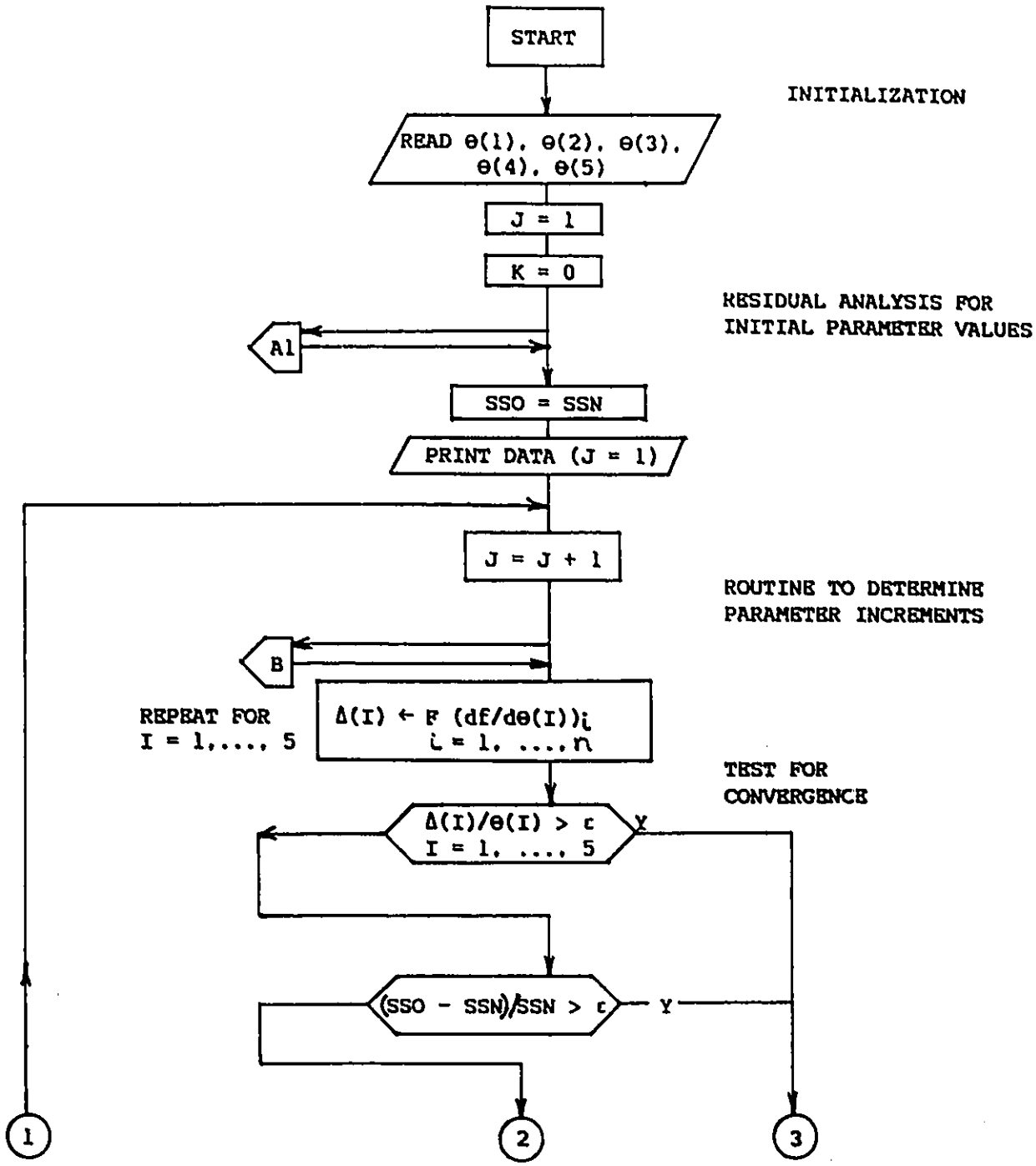

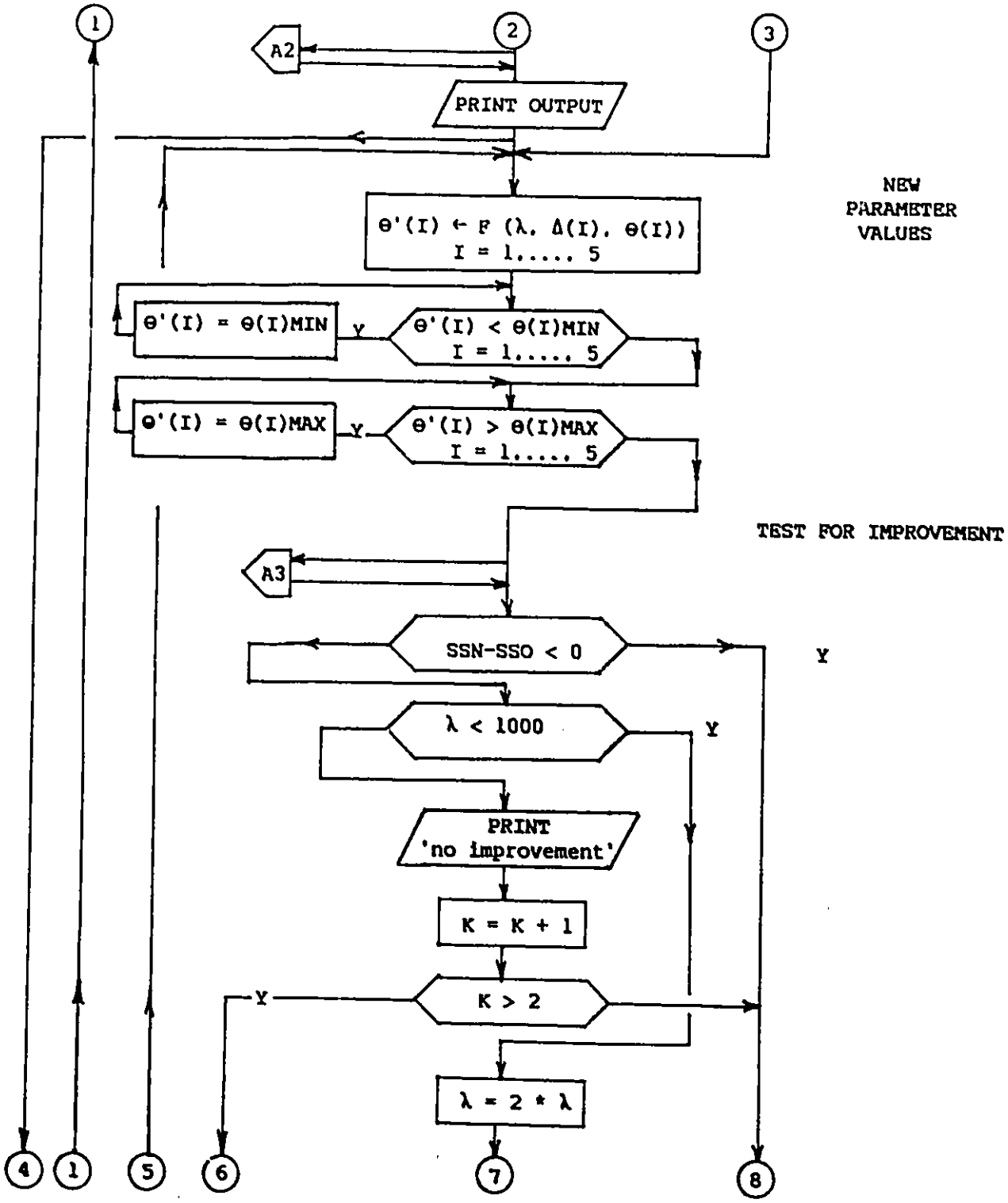
1
2
3
A2
PRINT OUTPUT
NEW PARAMETER VALUES
θ'(I) ← F (λ, Δ(I), θ(I))
I = 1,..... 5
θ'(I) = θ(I)MIN
Y
θ'(I) < θ(I)MIN
I = 1,..... 5
θ'(I) = θ(I)MAX
Y
θ'(I) > θ(I)MAX
I = 1,..... 5
TEST FOR IMPROVEMENT
A3
SSN-SSO < 0
Y
λ < 1000
Y
PRINT
'no improvement'
K = K + 1
K > 2
Y
λ = 2 * λ
4
1
5
6
7
8

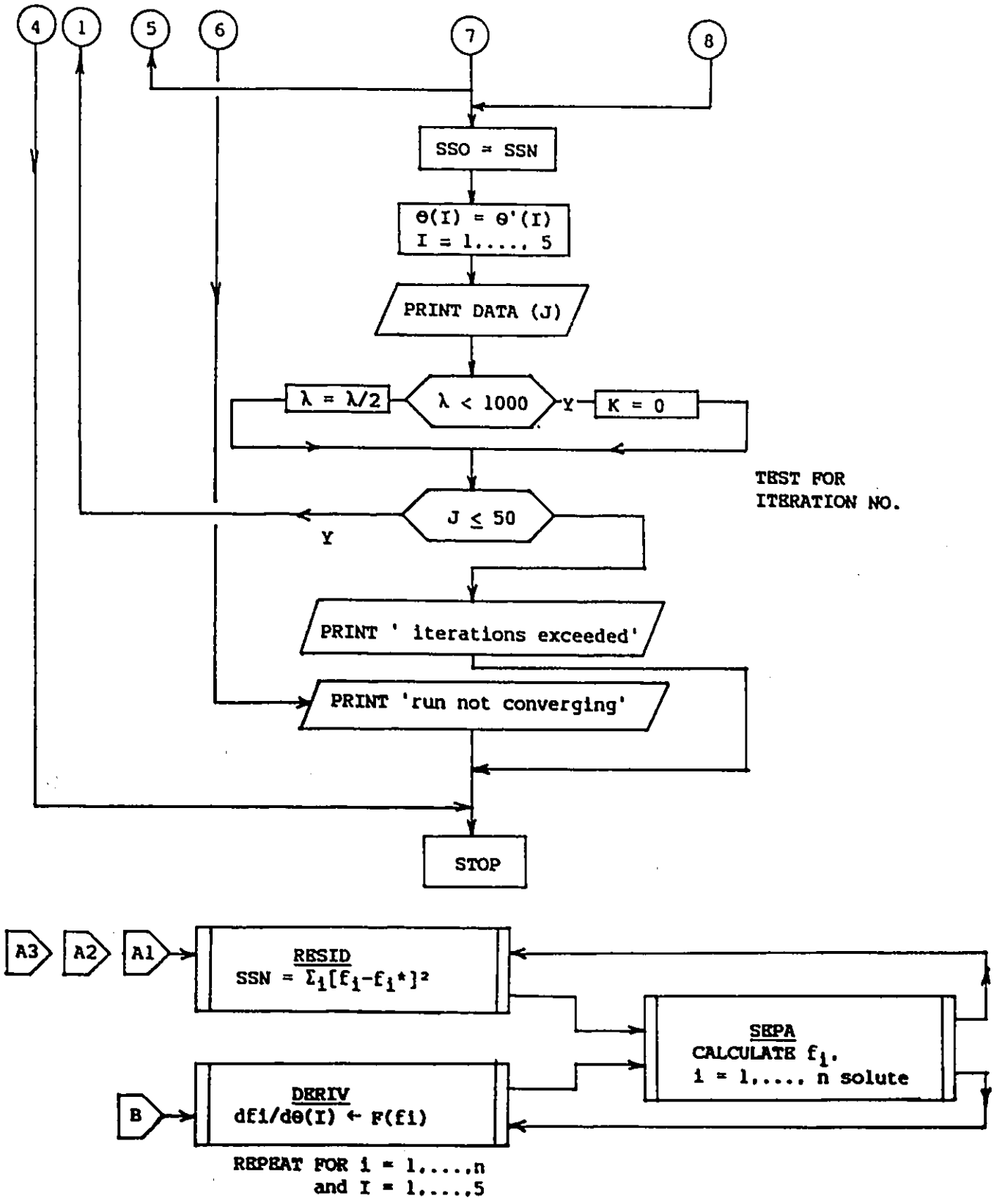
4
1
5
6
7
8
SSO = SSN
Θ(I) = Θ'(I)
I = 1,...., 5
PRINT DATA (J)
λ = λ/2
λ < 1000
Y
K = 0
TEST FOR
ITERATION NO.
J ≤ 50
Y
PRINT ' iterations exceeded'
PRINT 'run not converging'
STOP
A3
A2
A1
RESID
SSN = Σi[fi-fi*]²
SEPA
CALCULATE fi.
i = 1,.... n solute
B
DERIV
dfi/dθ(I) ← F(fi)
REPEAT FOR i = 1,....,n
and I = 1,....,5

FLOWCHART: SUBROUTINE SEPA

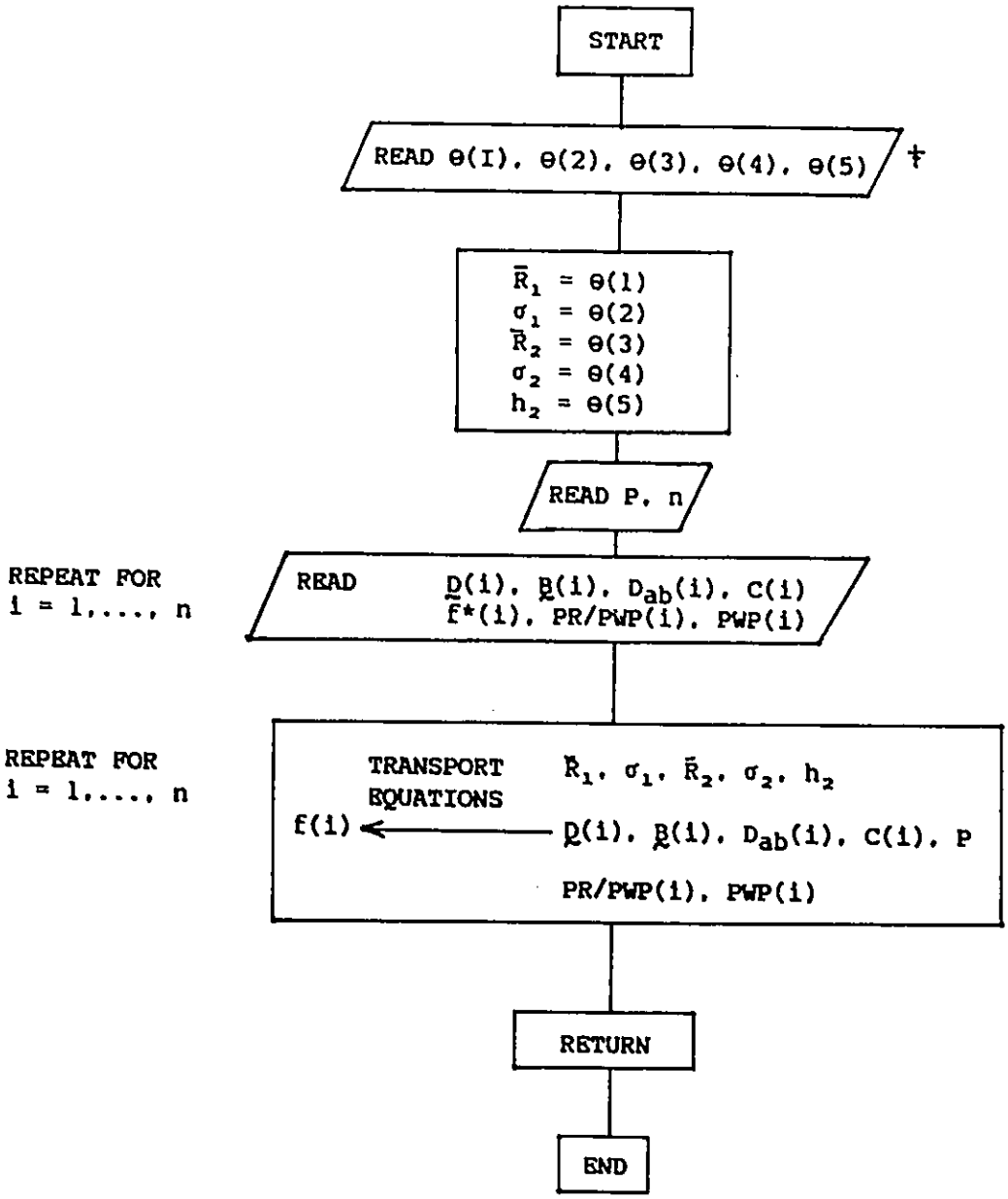

† transfered from DERIV or RESID

NOMENCLATURE:

$\theta(I)$ I = 1,..., 5	Five parameters describing the pore size distribution
J	Iteration no.; less than 51
K	Flag
$\Delta(I)$ I = 1,..., 5	Parameter increment
f_i	Predicted Solute Separation (the nonlinear function in the routine)
f_i^*	Experimental Solute Separation
i = 1, ...n	Probe solute number (usually n = 8)
SSN	Residual Sum of Squares for iteration J
SSO	Residual Sum of Squares for iteration (J-1)
ϵ	Flag - determines convergence
$\theta'(I)$ I = 1,..., 5	New parameter value
$\theta(I)$min I = 1,..., 5	Minimum parameter value limit
$\theta(I)$max I = 1,..., 5	Maximum parameter value limit
λ	Flag - determines increment size

NOTE: Other symbols defined in general Nomenclature for thesis.

APPENDIX 3

PARAMETERS USED IN PORE SIZE DISTRIBUTION ANALYSIS - INTERFACIAL PARAMETERS (β, ρ), SOLUTE DIFFUSIVITY (Dab) AND SOLUTE CONCENTRATION (C); FOR THE SYSTEM POLYETHERSULFONE-POLYETHYLENE GLYCOL - WATER

PEG M.W.	β, A^3	ρ, Å	Dab, m^2/s	C, $gmol/m^3$
300	-42.551	4.72	4.87	6.667×10^{-1}
600	551.495	6.27	3.67	3.333×10^{-1}
1000	2331.117	7.89	2.91	2.000×10^{-1}
1500	5062.441	9.95	2.31	1.333×10^{-1}
2000	7854.216	11.43	2.01	1.000×10^{-1}
3000	14919.99	14.06	1.63	6.667×10^{-2}
4000	19801.84	15.34	1.50	5.000×10^{-2}
6000	80912.23	25.00	0.919	3.333×10^{-2}
9000	118052.4	28.24	0.814	2.222×10^{-2}
15000	197237.9	33.65	0.683	1.333×10^{-2}

THEORY

The interfacial equilibrium distribution coefficient K_A' is related to the potential function ϕ ($\underset{\sim}{d}$), and therefore to the parameters $\underset{\sim}{B}$ and $\underset{\sim}{D}$ through equation 1, as follows:

$$K_A' = \frac{\int_{\underset{\sim}{D}_w}^{\infty} [\exp(-\phi(\underset{\sim}{d})) - 1]\, d(\underset{\sim}{d})}{t_i} + 1 \qquad \text{Eq. (1)}$$

$$\phi(\underset{\sim}{d}) = \begin{cases} \infty & \underset{\sim}{D}_w < \underset{\sim}{d} \leq \underset{\sim}{D} \\ \dfrac{-\underset{\sim}{B}}{\underset{\sim}{d}^3} & \underset{\sim}{d} > \underset{\sim}{D} \end{cases}$$

where $\underset{\sim}{D}_w = 0.87 \times 10^{-10}$m, w refers to water

$t_i = 8.3 \times 10^{-10}$m is the interfacial water layer thickness for polyethersulfone (Victrex)

DETERMINATION OF THE INTERFACIAL PARAMETERS

i) $\underset{\sim}{D}$

$\underset{\sim}{D}$ values for PEG solutes of molecular weight 600 to 6000 which were approximated by the stokes radius had been reported (45a). $\underset{\sim}{D}$ values for the other PEG-solutes of molecular weight 300, 9000 and 15,000 were determined simply by extrapolation.

ii) $\underset{\sim}{B}$

The procedure to determine $\underset{\sim}{B}$ values was more complex. K_A' values for PEG-600, 1500, 4000 and 6000 had been reported (45b) for Victrex-polyethersulfone. $\Delta\Delta G$ for these PEG solutes was then calculated using

$$\Delta\Delta G = -RT \ln K_A'$$

and plotted as a function of the molecular weight. $\Delta\Delta G$ values for the other PEG solutes were then determined by extrapolation, and the corresponding K_A' values calculated.

On the basis of $\underset{\sim}{D}$ and K_A' the $\underset{\sim}{B}$ values for each PEG solute were calculated using equation 1. A computer program available at NRCC was used for the computation.

DETERMINATION OF SOLUTE DIFFUSIVITY Dab

Dab was calculated using the Stokes radius equation which follows:

$$r_A = \frac{k\ T}{6\pi\ n\ Dab}$$

where r_A, m
Dab, m^2/s
k = Boltsmanns constant
T = temperature, k
n = viscosity, Pa.s

Substituting values for water at 25°C,

$$r_A = \frac{22.98 \times 10^{-20}}{Dab},\ m$$

Given D values, which were equalled with the Stokes radius r_A, Dab values for each solute could be calculated.

APPENDIX 4

Sample Calibration Curve for Total Organic Carbon Analyzer

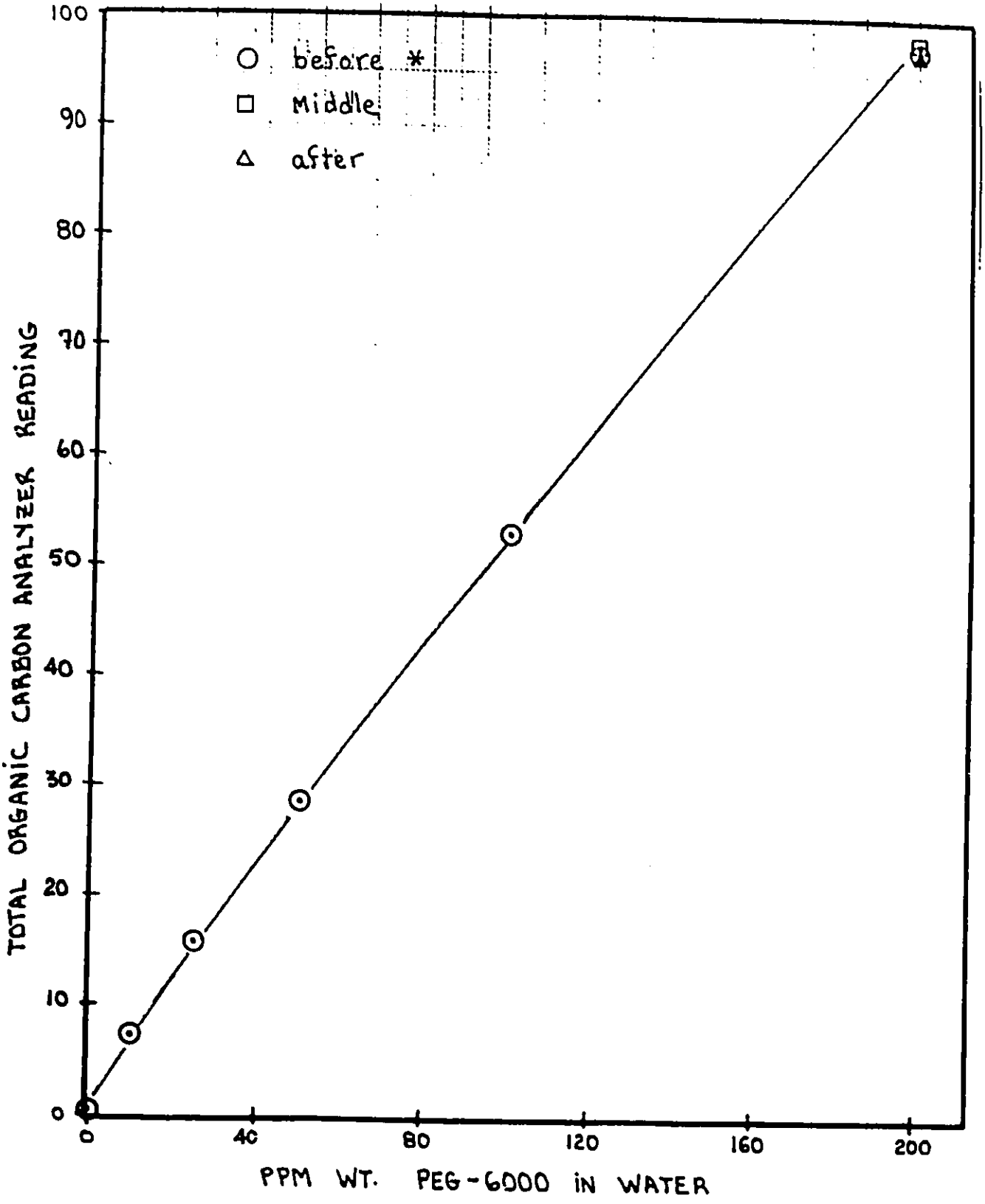

* Time relating to actual use for sample analysis.

APPENDIX 5

EXPERIMENTAL DATA - CROSS-REFERENCED WITH TABLE 5 -

ULTRAFILTRATION RESULTS FOR PES MEMBRANES PREPARED USING BAKER PRACTICAL NMP

Membrane Fabrication: Reference Casting Solution Composition
Standard Conditions
Slow Immersion

Test Conditions: 200 ppm PEG-6000 aqueous feed
(distilled water feed for IPWP and PWP)
1.0 L/min feed rate
65 psig, 25°C
A = 14.5 cm^2

Membrane No.	Sample No.	IPWP g/hr. A	PWP g/hr. A	PR g/hr. A	f %
B1	1	13.2	9.33	8.7	96.9
	2	52.7	36.6	37.8	89.2
	3	40.3	26.1	25.9	92.3
	4	38.6	18.3	17.6	95.1
B2	1	41.3	33.2	29.7	91.7
	2	23.2	18.5	17.0	78.7
	3	64.7	47.3	44.1	96.7
	4	70.2	54.7	50.1	91.8
B3	1	16.3	10.5	10.1	94.8
	2	41.0	29.9	28.6	90.7
	3	14.8	10.8	9.8	88.6
B4	1	43.1	31.1	30.1	90.3
	2	31.1	23.2	21.8	81.4
	3	76.1	51.8	49.4	89.5
	4	68.7	47.7	44.4	91.1

APPENDIX 6

EXPERIMENTAL DATA - CROSS-REFERENCED WITH TABLE 6 -

ULTRAFILTRATION RESULTS FOR PES MEMBRANES PREPARED USING FISHER PURIFIED NMP

Membrane Fabrication: Reference Casting Solution Composition
Standard Conditions
Slow Immersion

Test Conditions: 200 ppm PEG-4000 aqueous feed
(distilled water feed for IPWP and PWP)
2.0 L/min feed rate
65 psig, 25°C
A = 14.5 cm^2

Membrane No.	Sample No.	IPWP g/hr. A	PWP g/hr. A	PR g/hr. A	f %
F1	1	23.25	10.08	8.4	86.7
	2	16.96	7.93	6.95	71.2
F2	1	105.31	46.24	41.32	74.1
	2	32.29	14.25	12.75	61.0
	3	151.81	49.01	42.17	72.8
F3	1	146.3	85.56	83.10	83.0
	2	25.0	14.68	13.40	77.5
F4	1	30.0	15.29	14.37	62.0
	2	16.9	11.40	10.79	42.6
F5	1	113.85	33.05	28.20	72.3
	2	14.77	4.82	4.12	67.4
	3	32.07	10.87	9.31	60.1

APPENDIX 7

EXPERIMENTAL DATA - CROSS-REFERENCED WITH TABLE 7

ULTRAFILTRATION RESULTS FOR ANNEALED PES MEMBRANES PREPARED FROM FISHER PURIFIED NMP

Membrane Fabrication: Reference Casting Solution Composition
Standard Conditions
Slow Immersion

Test Conditions: 200 ppm PEG-4000 aqueous feed
(distilled water feed for IPWP and PWP)
2.0 L/min feed rate
65 psig, 25°C
A = 14.5 cm^2

Treatment	Membrane No.	Sample No.	IPWP g/hr. A	PWP g/hr. A	PR g/hr. A	f %
I	F2	4	76.05	27.04	24.23	82.8
	F3	3	75.74	37.23	36.26	91.7
		4	146.6	68.78	68.27	77.5
	F4	3	13.6	7.93	7.62	65.40
		4	49.3	23.68	22.50	77.2
II	F2	5	1.18	0.83	0.7	96.5
	F5	4	34.20	11.0	9.58	65.4
III	F3	5	221.6	105.5	107.3	91.3
		6	109.5	53.03	52.57	78.5
	F4	5	145.5	58.20	57.23	59.3
		6	119.0	45.72	44.54	84.5

APPENDIX 8

EXPERIMENTAL DATA - CROSS REFERENCED WITH FIGURE 6

Membrane Fabrication
* reference casting solution S(20-0.2)
* standard conditions
* fast immersion

A) MEMBRANE IDENTIFICATION - Annealing Post-Treatment Conditions

Annealing Period = 15 minutes

Sample no.	Membrane no.	Annealing Temperature, C (a)
1	1	100
2	2	100
3	3	100
4	4	100
5	1	120
6	2	120
7	3	120
8	4	120
9	3	150 (b)
10	1	untreated
11	2	"
12	3	"
13	3	"
14	4	"
15	4	"
16	5	"
17	5	"
18	6	"
19	6	"

Notes:
(a) Membrane samples which were annealed at 170 C are not shown. These had shrunk and partially melted and hence were not suitable for use in the RO/UF experiments.

(b) Of the four membrane samples annealed at 150 C only one could be used in RO/UF experiments; the others were affected too severely.

Annealing Period = 5 minutes

Sample no.	Membrane no.	Annealing Temperature, C
20	7	50
21	7	50
22	7	100
23	7	100
24	8	120
25	8	120
26	9	150 (c)
27	9	150
28	9	150
29	10	untreated
30	10	"
31	10	"

Notes:

(c) Membrane samples annealed at 150 C were practically not permeable and, therefore, the corresponding RO/UF results will not be included in the following tables.

B) MEMBRANE PERFORMANCE RESULTS

Test conditions :

PEG aqueous feed solution
100 ppm for samples nos 1 - 19
200 ppm for samples nos 20 - 31
(distilled water feed for PWP)

2.2 l/min feed rate
50 psig, 25 C
A = 14.5 cm. sq.

Solute		PEG-600		PEG-1000		PEG-1500	
Sample no.	PWP	PR	f	PR	f	PR	f
1	146.5	150.9	30.8	121.5	33.5	124.8	48.6
2	6.5			2.6	38.1	2.4	51.3
3	24.5	24.5	6.8	22.2	3.6	22.0	9.3
4	349.2			277.8	14.5	222.5	67.9
5	240.9	242.6	24.9	188.9	23.8	193.1	34.4
6	383.1			282.2	19.8	247.8	55.7
7	195.8	199.0	32.9	175.4	10.5	173.3	20.6
8	94.2			78.1	9.9	73.4	56.1
9	14.3	12.1	16.7	9.8	0.3	10.9	
10	163.5	165.7	45.8	134.7	58.7	136.1	74.4
11	9.8			7.9	36.6	7.7	89.0
12	216.6	217.8	35.2	197.2	41.4	195.6	59.7
13	203.4	205.7	41.9	165.0	53.8	166.7	67.7
14	238.6			200.9	37.5	166.2	92.8
15	35.9			29.1	34.5	25.6	85.8
16	21.9	21.5	19.4	19.9	30.8	20.0	25.9
17	40.5	34.3	33.5	38.2	43.9	40.3	49.2
18	350.9			225.0	43.5	204.1	93.7
19	123.5			79.8	39.2	72.6	90.7
20	47.9	50.8	6.3	49.9	9.8	47.4	29.1
21	184.8	209.8	9.8	198.9	21.0		39.2
22	101.0	106.3	23.3	99.4	44.8		72.6
23	52.4	52.9	11.8	52.7	28.5	47.1	58.8
24	92.0	98.3		95.1	11.8	88.8	23.7
25	22.6	23.6	2.3	23.4	2.3	23.2	8.1
29	189.0	202.1	37.7	195.6	57.3	180.6	82.3
30	76.4	77.7	24.1	75.4	38.3	65.5	71.4
31	134.3	136.6	41.6	128.5	60.5	121.9	79.4

MEMBRANE PERFORMANCE - continued

Solute	PEG-2000		PEG-3000		PEG-4000	
Sample no.	PR	f	PR	f	PR	f
1	138.7	52.1	137.1	59.6	143.6	62.2
2	2.4	52.0	2.6	27.9	3.5	45.1
3	23.0	21.6	22.5	26.2	22.8	8.5*
4	273.9	33.8	322.8	27.2	313.2	45.8
5	229.6	32.1	226.1	38.8	232.5	39.9
6	297.0	34.2	351.8	28.7	338.5	42.2
7	182.6	24.0	180.4	28.5	195.1	31.9
8	86.0	21.3	92.7	22.8	89.1	36.8
9			3.2		6.7	
10	154.5	84.8	153.5	91.6	154.0	91.1
11	8.5	67.1	9.5	74.0	9.3	86.0
12	219.7	61.3	211.8	74.7	213.1	73.1
13	191.0	73.8	187.8	83.8	188.9	80.9
14	200.6	65.3	219.5	63.4	210.3	76.8
15	28.9	66.5	29.5	73.8	30.9	76.8
16	20.5	53.7	20.3	57.8	20.8	37.9*
17	55.8	67.6	54.9	76.3	55.6	77.4
18	249.0	66.6	294.6	69.6	305.5	75.1
19	89.0	65.2	103.7	64.0	110.8	76.9
20	47.4	29.1			45.9	41.3
21		39.2			184.4	52.5
22		72.6			82.2	80.5
23	47.1	58.8			44.7	70.8
24	88.8	23.7			87.0	25.5
25	23.2	8.1			22.3	15.3
29	180.6	82.3			169.1	91.3
30	65.5	71.4			62.8	81.3
31	121.9	79.4			112.7	89.0

* uncertain number

MEMBRANE PERFORMANCE - continued

Solute	PEG-6000		PEG-15000		
Sample no.	PR	f	PR	f	PWP
1	138.7	78.9			153.5
2	4.4	72.7	2.4	51.3	2.4
3	22.8	40.6	222.5	67.9	22.7
4	297.5	63.6			312.8
5	230.7	41.2			252.1
6	343.8	53.0	247.8	55.7	306.1
7	209.0	35.8			204.0
8	89.4	60.8	73.4	56.1	82.7
9	30.3	4.8			13.1
10	155.6	90.2			153.4
11	9.5	98.8	7.7	89.0	8.1
12	186.0	90.4			216.3
13	174.0	89.2			189.3
14	205.8	94.6	166.2	92.8	222.0
15	31.1	88.1	25.6	85.8	31.8
16	19.3	37.7			20.3
17	52.8	81.1			54.3
18	302.2	95.0	204.1	93.7	241.0
19	108.6	93.1	72.6	90.7	85.3
20	44.3	56.8	43.3	69.6	47.5
21	173.6	60.1	165.8	75.6	187.3
22	78.5	94.1	78.3	95.7	73.5
23	41.2	83.8	41.5	90.5	43.9
24	86.7	44.9	86.2	55.4	90.2
25	22.0	40.7	22.0	48.0	23.0
29	165.5	96.2	165.3	98.0	170.3
30	59.9	93.4	59.6	94.4	62.5
31	107.9	93.4	107.3	96.4	114.3

C) STATISTICAL ANALYSIS

The average membrane performance with respect to probe solute PEG-6000 was determined for each annealing treatment and the results shown in Figure 6. In a few cases, membrane samples which deviated significantly from the average were excluded. The average and standard deviation for each set of membrane samples are given below.

Annealing T, C	PR		f		excluded sample nos
	x	s	x	s	
* 15 minutes annealing					
100	153.0	137.9	61.0	19.3	2
120	261.2	72.4	43.3	8.8	8
150	30.3		4.8		
UT	152.0	87.4	90.2	4.5	11, 16
* 5 minutes annealing					
50 (a)	109.0	91.4	58.5	2.3	
100	59.9	26.4	89.0	7.3	
120	54.4	45.8	42.8	3.0	
UT	111.1	52.9	94.3	1.6	

Note (a) Data for 50 C do not appear on Figure 6 because they were questionable.

A significance test for the effect of annealing temperature on membrane performance was carried out for each annealing time. The results are summarized below.

	F - value		F - test
	PR	f	
15 minutes (a)	1.51	28.79	F(2,11,0.05) = 3.98
5 minutes (b)	1.20	104.9	F(2,4,0.05) = 6.94

Because F - value for f is larger than the F - test then the annealing temperature had a significant effect on solute separation; conversely, it did not have a significant effect on the product rate.

Notes

(a) Because there was only one result at 150 C it was not incorporated.

(b) Data for 50 C were excluded and do not appear on Figure 6. That is because the set of data was questionable.

APPENDIX 9

MEMBRANE PERFORMANCE DATA FROM FIRST-LEVEL TESTS

Tests Conditions

200 ppm solute aqueous feed
2.2 L/min feed rate
50 psig, 25 C

Units

PWP, PR (=) g/hr.A, A = 14.5 cm. sq.
f (=) %

Notes

i. Membranes were identified by their casting solution composition expressed as S(P - R) where

P is PES wt.%
R is PVP/PES wt. ratio

ii. Sample averages and standard deviations were given with respect to each measurement (i.e. PWP, PR, f).

iii. Membrane samples selected for use in the second-level tests were circled.

Membrane S(15 - 0.0)

Sample no.		PEG - 6000		DEXTRAN - 71.5K	
	PWP	PR	f	PR	f
1	343.	320.	31.3	191.	91.3
(2)	450.	406.	26.2	231.	91.3
3	525.	440.	15.5	276.	80.1
(4)	399.	358.	38.5	219.	90.3
$\bar{x}$	429.	381.	27.9	229.	88.3
s_x	77.	53.	9.7	35.	5.5

Membrane S(15 - 0.2)

Sample no.		PEG - 6000		DEXTRAN - 71.5K	
	PWP	PR	f	PR	f
1	444.	392.	36.2	244.	88.2
2	410.	360.	31.8	208.	88.8
3	621.	468.	32.0	288.	88.7
(4)	644.	550.	36.9	349.	90.1
$\bar{x}$	530.	443.	34.2	272.	89.0
s_x	120.	85.	2.7	61.	0.8

Membrane S(15 - 0.5)

Sample no.		PEG - 6000		DEXTRAN - 71.5K	
	PWP	PR	f	PR	f
(1)	791.	634.	28.5	383.	87.6
2	767.	600.	22.5	313.	84.0
3	806.	614.	16.7	337.	83.3
(4)	895.	705.	32.7	420.	80.5
$\bar{x}$	815.	638.	25.1	363.	83.9
s_x	56.	47.	7.0	48.	2.9

Membrane S(15 - 1.0)

Sample no.		PEG - 6000		DEXTRAN - 71.5K	
	PWP	PR	f	PR	f
1	538.	435.	36.4	318.	79.1
2	641.	545.	56.1	384.	79.7
③	660.	575.	53.6	412.	77.4
4	525.	447.	49.1	344.	80.6
⑤	536.	481.	70.2	386.	85.1
$\bar{x}$	580.	497.	53.1	369.	80.4
s_x	65.	61.	12.2	37.	2.9

Membrane S(15 - 2.0)

Sample no.		PEG - 6000		DEXTRAN - 71.5K	
	PWP	PR	f	PR	f
①	202.	187.	88.1	185.	93.4
②	193.	138.	97.9	181.	96.5
$\bar{x}$	198.	163.	93.0	183.	95.0
s_x	6.	35.	6.9	3.	2.2

Membrane S(15 - 2.7)

Sample no.		PEG - 6000		DEXTRAN - 71.5K	
	PWP	PR	f	PR	f
1	69.	85.?	75.5	67.	94.3
②	62.	62.	97.4	62.	97.2
3	64.	66.	86.2	67.	83.4
④	71.	71.	91.8	70.	92.7
$\bar{x}$	67.	71.	87.7	67.	91.9
s_x	4.	10.	9.4	3.	6.0

Membrane S(20 - 0.0)

Sample no.		PEG - 1000		PEG - 6000	
	PWP	PR	f	PR	f
①	321.	284.	38.7	266.	97.0
2	567.	380.	31.4	313.	81.0
3	195.	181.	24.5	174.	95.4
④	304.	274.	26.7	252.	91.8
$\bar{x}$	347.	280.	30.3	251.	91.3
s_x	157.	81.	6.3	58.	7.2

Membrane S(20 - 0.2)

Sample no.		PEG - 1000		PEG - 6000	
	PWP	PR	f	PR	f
1	752.	643.	14.4	464.	75.1
2	447.	392.	23.6	330.	88.5
3	640.	558.	14.1	405.	76.9
④	522.	461.	32.0	395.	90.2
$\bar{x}$	590.	514.	21.0	399.	82.7
s_x	134.	110.	8.5	55.	7.8

Membrane S(20 - 0.5)

Sample no.		PEG - 1000		PEG - 6000	
	PWP	PR	f	PR	f
1	595.	523.	12.2	412.	72.6
②	778.	664.	17.0	506.	81.5
3	383.	342.	13.0	267.	80.8
④	426.	382.	30.2	352.	96.4
5	233.	229.	21.9	217.	94.1
$\bar{x}$	483.	428.	18.9	351.	85.0
s_x	209.	169.	7.4	115.	10.0

Membrane S(20 - 1.0)

Sample no.		PEG - 1000		PEG - 6000	
	PWP	PR	f	PR	f
1	539.	499.	15.9	>398.	75.6
②	532.	497.	22.4	>405.	85.7
3	434.	403.	16.5	355.	80.9
④	423.	387.	29.0	374.	94.4
5	424.	419.	23.4	374.	87.1
$\bar{x}$	470.	441.	21.4	381.	84.7
s_x	60.	53.	5.4	19.	7.0

Membrane S(20 - 1.5)

Sample no.		PEG - 1000		PEG - 6000	
	PWP	PR	f	PR	f
1	337.	345.	16.7	313.	74.7
②	278.	233.	33.4	234.	96.6
3	341.	339.	22.4	315.	82.3
④	273.	261.	33.2	322.	97.1
$\bar{x}$	30.7	295.	26.4	296.	87.7
s_x	37.	56.	8.3	42.	11.0

Membrane S(20 - 2.0)

Sample no.		PEG - 1000		PEG - 6000	
	PWP	PR	f	PR	f
①	79.	81.	48.2	80.	98.1
②	97.	99.	35.3	96.	91.6
3	97.	98.	28.7	95.	91.9
4	73.	73.	37.3	73.	99.7
$\bar{x}$	87.	88.	37.4	86.	95.3
s_x	12.	13.	8.1	11.	4.2

Membrane S(25 - 0.0)

	Sample no.	PWP	PEG - 1000 PR	PEG - 1000 f	PEG - 6000 PR	PEG - 6000 f
rejected	1	0.	0.4		0.4	
rejected	2	3.2	3.8		3.1	
	3	8.8	8.9	31.2	8.8	39.8
	$\bar{x}$					
	s_x					

Membrane S(25 - 0.2)

	Sample no.	PWP	PEG - 1000 PR	PEG - 1000 f	PEG - 6000 PR	PEG - 6000 f
	1	125.	76.	59.0	111.	91.5
	2	224.	199.	44.8	187.	96.6
	(3)	246.	132.	65.2	221.	98.6
rejected	(4)	5.6	5.5	80.2	6.0	86.2
	$\bar{x}$	198.	136.	56.3	173.	95.6
	s_x	64.	62.	10.5	56.	3.7

Membrane S(25 - 0.6)

Sample no.	PWP	PEG - 1000 PR	PEG - 1000 f	PEG - 6000 PR	PEG - 6000 f
(1)	258.	232.	51.9	216.	92.4
2	92.	90.	54.8	87.	96.7
(3)	100.	95.	56.3	95.	98.4
(4)	226.	213.	58.4	205.	96.7
5	73.	78.	64.5	79.	99.8
$\bar{x}$	150.	142.	57.2	136.	96.8
s_x	85.	74.	4.7	68.	2.8

Membrane S(25 - 1.0)

Sample no.	PWP	PEG - 1000 PR	PEG - 1000 f	PEG - 6000 PR	PEG - 6000 f
1	144.	145.	46.1	138.	99.8
2	207.	208.	39.8	194.	94.7
(3)	130.	130.	50.5	125.	99.2
(4)	128.	128.	59.7	126.	99.6
$\bar{x}$	152.	153.	49.0	146.	98.3
s_x	37.	38.	8.4	33.	2.4

Membrane S(25 - 1.4)

Sample no.	PWP	PEG - 1000 PR	PEG - 1000 f	PEG - 6000 PR	PEG - 6000 f
(1)	53.	54.	52.2	53.	98.4
2	56.	57.	46.2	55.	96.0
3	38.	38.	53.0	38.	98.7
(4)	38.	39.	54.5	39.	99.6
$\bar{x}$	46.	47.	51.5	46.	98.2
s_x	10.	10.	3.6	9.	1.5

Membrane S(30 - 0.0)

Sample no.	PWP	PEG - 1000 PR	PEG - 1000 f	PEG - 6000 PR	PEG - 6000 f
1	0.1	0.7		0.4	
2	0.0	0.2		0.4	
3	0.2	0.4		0.3	
4	22.9	0.3		0.2	
$\bar{x}$					
s_x					

Membrane S(30 - 0.2)

Sample no.		PEG - 1000		PEG - 6000	
	PWP	PR	f	PR	f
1	0.2	0.3		0.2	
2	0.6	0.4		0.5	
3	0.2	0.3		0.2	
④	13.8	10.9	77.8	11.1	94.6
$\bar{x}$					
s_x					

Membrane S(30 - 0.5)

Sample no.		PEG - 1000		PEG - 6000	
	PWP	PR	f	PR	f
1	36.	37.	61.3	35.	92.8
2	31.	32.	50.3	31.	92.3
③	57.	57.	61.8	55.	92.8
④	43.	44.	56.9	43.	95.9
$\bar{x}$	42.	43.	57.6	41.	93.5
s_x	11.	11.	5.3	11.	1.7

Membrane S(30 - 1.0)

Sample no.		PEG - 1000		PEG - 6000	
	PWP	PR	f	PR	f
①	50.	50.	67.8	50.	100.
②	41.	41.	67.7	41.	99.1
3	33.	34.	69.5	34.	97.9
4	37.	37.	64.4	36.	98.8
$\bar{x}$	40.	41.	67.4	40.	99.0
s_x	7.	7.	2.1	7.	0.9

Membrane S(32 - 1.0)

Membranes from this casting solution composition could not be prepared because the polymer was not soluble in this system.

Membrane S(35 - 0.0)

Membranes from this casting solution were not permeable.

Membrane S(35 - 0.2)

Sample no.		PEG - 1000		PEG - 6000	
	PWP	PR	f	PR	f
1	0.2	0.1		0.1	
2	0.5	0.3		0.6	
3	0.0	0.0		0.0	
4	0.1	0.1		0.1	
$\bar{x}$					
s_x					

Membrane S(35 - 0.5)

Sample no.		PEG - 1000		PEG - 6000	
	PWP	PR	f	PR	f
1	1.8	2.0		1.6	
2	1.5	1.8		1.7	
3	445.	68.	0.5	136.	0.0
4	2.0	2.1		1.9	
$\bar{x}$					
s_x					

APPENDIX 10

MEMBRANE PERFORMANCE DATA FROM SECOND - LEVEL TESTS

Test Conditions

200 ppm PEG solute aqueous feed
2.2 L/min feed rate
50 psig, 25 C

Units

PWP, PR (=) g/hr.A , A = 14.5 cm. sq.
f (=) %

Ultrafiltration results with respect to eight PEG solutes of different molecular weight are given for each membrane sample. PWP measurements at three times during the test run are given which are defined as follows:

PWPa or IPWP	before pressurization
PWPb	at the start of the test run
PWPc	at the end of the test run

Membrane samples which have been used in the analysis of pore size distribution were circled.

Membrane S(15 - 0.0)

Sample no.	②		4	
PEG - M. W.	PR	f	PR	f
- 1000	269.	24.9	163.	39.8
- 1500	267.	35.0	163.	53.7
- 2000	259.	31.3	169.	60.6
- 3000	251.	52.5	166.	76.1
- 4000	237.	58.9	162.	77.2
- 6000	213.	61.4	153.	91.4
- 9000	205.	77.2	149.	82.7
- 15000	191.	89.1	143.	92.3
PWPa	321.		223.	
PWPb	267.		172.	
PWPc	206.		150.	

Membrane S(15 - 0.2)

Sample no.	④		-	
PEG - M. W.	PR	f	PR	f
- 1000	245.	38.8		
- 1500	247.	50.2		
- 2000	258.	50.8		
- 3000	254.	77.0		
- 4000	243.	77.5		
- 6000	224.	86.1		
- 9000	226.	95.1		
- 15000	212.	96.1		
PWPa	286.			
PWPb	260.			
PWPc	222.			

Membrane S(15 - 0.5)

Sample no.	1		④	
PEG - M. W.	PR	f	PR	f
- 1000	261.	22.0	350.	26.6
- 1500	261.	30.0	350.	35.6
- 2000	271.	31.8	359.	43.8
- 3000	259.	51.0	344.	62.0
- 4000	255.	51.3	329.	70.6
- 6000	226.	78.1	297.	88.6
- 9000	214.	86.2	288.	88.8
- 15000	201.	92.9	273.	96.8
PWPa	327.		454.	
PWPb	273.		381.	
PWPc	230.		289.	

Membrane S(15 - 1.0)

Sample no.	3		⑤	
PEG - M. W.	PR	f	PR	f
- 1000	347.	11.5	295.	30.3
- 1500	345.	14.9	299.	41.5
- 2000	356.	16.1	313.	47.0
- 3000	337.	25.5	300.	69.7
- 4000	326.	27.1	286.	74.5
- 6000	287.	62.3	257.	95.3
- 9000	259.	79.1	248.	94.0
- 15000	242.	87.5	239.	98.8
PWPa	386.		330.	
PWPb	351.		319.	
PWPc	284.		252.	

Membrane S(15 - 2.0)

Sample no.	①		2	
PEG - M. W.	PR	f	PR	f
- 300	198.	13.2	210.	11.6
- 600	213.	21.9	220.	18.6
- 1000	207.	37.6	215.	37.1
- 1500	201.	50.3	204.	46.9
- 2000	204.	62.7	205.	62.2
- 3000	202.	71.2	203.	70.4
- 4000	202.	78.9	210.	78.9
- 6000	187.	93.5	196.	93.5
PWPa				
PWPb	218.		235.	
PWPc	195.		200.	

Membrane S(15 - 2.7)

Sample no.	②		4	
PEG - M. W.	PR	f	PR	f
- 300	70.	13.5	175.?	5.3
- 600	69.	30.3	97.	20.3
- 1000	69.	61.2	101.	37.7
- 1500	70.	59.5	94.	40.8
- 2000	70.	73.8	82.	60.6
- 3000	69.	68.1	98.	58.0
- 4000	70.	90.4	82.	61.4
- 6000	68.	92.0	74.	79.6
PWPa	74.		?	
PWPb	70.		?	
PWPc	70.		80.	

Membrane S(20 - 0.0)

Sample no.	1		④	
PEG - M. W.	PR	f	PR	f
- 300	132.?	11.4	121.?	13.6
- 600	185.	18.0	185.	15.4
- 1000	160.	35.5	158.	38.2
- 1500	159.	49.5	155.	49.7
- 2000	159.	60.4	155.	63.5
- 3000	156.	69.0	152.	73.7
- 4000	128.	89.3	116.	91.6
- 6000	123.	97.8	117.	97.1
PWPa				
PWPb	208.		213.	
PWPc	134.		122.	

Membrane S(20 - 0.2)

Sample no.	④		-	
PEG - M. W.	PR	f	PR	f
- 1000	264.	43.1		
- 1500	266.	54.8		
- 2000	242.	73.0		
- 3000	230.	86.9		
- 4000	218.	87.4		
- 6000	214.	93.9		
- 9000	204.	95.3		
- 15000	194.	96.7		
PWPa	291.			
PWPb	272.			
PWPc	209.			

Membrane S(20 - 0.5)

Sample no.	②		4	
PEG - M. W.	PR	f	PR	f
- 1000	299.	38.4	293.	22.7
- 1500	311.	47.1	295.	27.4
- 2000	283.	65.6	297.	39.8
- 3000	272.	77.3	281.	60.0
- 4000	249.	71.0	275.	63.8
- 6000	242.	79.7	248.	81.3
- 9000	227.	87.9	230.	82.7
- 15000	215.	90.1	215.	90.5
PWPa	319.		335.	
PWPb	308.		295.	
PWPc	233.		257.	

Membrane S(20 - 1.0)

Sample no.	②		4	
PEG - M. W.	PR	f	PR	f
- 1000	294.	38.4	394.	22.1
- 1500	310.	42.9	393.	27.7
- 2000	296.	64.3	402.	34.8
- 3000	304.	74.5	377.	55.2
- 4000	274.	76.0	368.	58.0
- 6000	264.	90.7	330.	82.8
- 9000	253.	90.1	309.	89.2
- 15000	241.	93.4	291.	94.2
PWPa	303.		420.	
PWPb	302.		386.	
PWPc	249.		345.	

Membrane S(20 - 1.5)

Sample no.	2		④	
PEG - M. W.	PR	f	PR	f
- 300	264.?	9.7	262.?	8.2
- 600	276.	12.2	292.	12.7
- 1000	273.	26.6	286.	30.4
- 1500	272.	36.7	286.	39.6
- 2000	275.	45.2	289.	51.9
- 3000	275.	61.2	287.	69.3
- 4000	268.	67.7	271.	74.7
- 6000	232.	88.2	245.	91.9
PWPa				
PWPb	286.		313.	
PWPc	258.		262.	

Membrane S(20 - 2.0)

Sample no.	1		②	
PEG - M. W.	PR	f	PR	f
- 300	108.	5.5	106.	6.6
- 600	108.	13.9	105.	14.4
- 1000	110.	27.9	107.	32.6
- 1500	110.	31.7	107.	36.5
- 2000	111.	46.7	108.	54.5
- 3000	110.	67.3	107.	78.0
- 4000	109.	70.3	107.	74.7
- 6000	108.	84.7	106.	90.0
PWPa	106.		104.	
PWPb	109.		107.	
PWPc	110.		108.	

Membrane S(25 - 0.2)

Sample no.	3		④	
PEG - M. W.	PR	f	PR	f
- 300	78.?	19.2	106.?	16.9
- 600	129.	28.7	140.	37.2
- 1000	92.	61.8	115.	65.5
- 1500	94.	72.7	118.	73.2
- 2000	96.	83.4	121.	83.4
- 3000	97.	79.5	123.	79.8
- 4000	73.	98.9	102.	94.1
- 6000	75.	101.1	102.	97.9
PWPa				
PWPb	135.		156.	
PWPc	78.		106.	

Membrane S(25 - 0.6)

Sample no.	1		3		④	
PEG - M. W.	PR	f	PR	f	PR	f
- 300	134.	17.3	70.	16.5	113.	20.5
- 600	146.	32.4	70.	41.5	142.	38.8
- 1000	133.	53.9	72.	77.5	116.	68.7
- 1500	132.	70.1	72.	77.2	120.	74.8
- 2000	135.	77.8	72.	90.6	124.	83.2
- 3000	137.	70.1	73.	95.8	126.	85.4
- 4000	131.	91.3	71.	99.8	110.	89.7
- 6000	127.	94.8	71.	101.2	105.	96.5
PWPa						
PWPb	142.		72.		136.	
PWPc	134.		73.		112.	

Membrane S(25 - 1.0)

Sample no.	3		④	
PEG - M. W.	PR	f	PR	f
- 300	130.	14.8	113.	15.9
- 600	124.	25.5	118.	33.2
- 1000	122.	47.1	116.	57.6
- 1500	121.	62.9	115.	72.0
- 2000	123.	75.4	117.	84.0
- 3000	125.	80.6	119.	87.3
- 4000	123.	89.4	116.	92.9
- 6000	117.	96.6	221.?	99.2
PWPa				
PWPb	123.		115.	
PWPc	124.		116.	

Membrane S(25 - 1.4)

Sample no.	①		4	
PEG - M. W.	PR	f	PR	f
- 300	55.	4.7	53.	7.1
- 600	54.	20.9	52.	22.7
- 1000	55.	47.1	53.	47.6
- 1500	55.	50.8	53.	53.2
- 2000	56.	65.6	54.	68.3
- 3000	54.	91.3	53.	66.3
- 4000	55.	85.8	53.	90.5
- 6000	55.	97.9	53.	96.3
PWPa	52.		50.	
PWPb	54.		53.	
PWPc	55.		53.	

Membrane S(30 - 0.2)

Sample no.	4		-	
PEG - M. W.	PR	f	PR	f
- 300	7.	24.0		
- 600	7.	32.1		
- 1000	7.	73.5		
- 1500	7.	62.2		
- 2000	6.	65.1		
- 3000	6.	71.8		
- 4000	6.	48.0		
- 6000	6.	76.3		
PWPa	6.			
PWPb	7.			
PWPc	6.			

Membrane S(30 - 0.5)

Sample no.	3		4	
PEG - M. W.	PR	f	PR	f
- 300	44.	16.5	36.	16.9
- 600	44.	44.1	36.	42.1
- 1000	45.	81.4	34.	80.8
- 1500	45.	64.1	34.	79.7
- 2000	45.	81.2	32.	89.7
- 3000	44.	63.0	32.	98.5
- 4000	44.	91.1	32.	97.4
- 6000	42.	100.2	31.	82.5
PWPa	43.		36.	
PWPb	45.		37.	
PWPc	45.		32.	

Membrane S(30 - 1.0)

Sample no.	1		2	
PEG - M. W.	PR	f	PR	f
- 300	40.	10.6	36.	11.1
- 600	39.	30.0	36.	28.7
- 1000	41.	66.1	36.	69.3
- 1500	40.	66.1	36.	70.9
- 2000	41.	75.5	37.	84.0
- 3000	40.	84.8	37.	96.9
- 4000	41.	88.7	37.	92.2
- 6000	40.	95.0	36.	95.7
PWPa	38.		34.	
PWPb	40.		36.	
PWPc	41.		37.	

APPENDIX 11

ADDITIONAL MEMBRANE PERFORMANCE DATA

Test Conditions

200 ppm PEG solute aqueous feed
2.2 L/min feed rate
50 psig, 25 C

Units

PWP, PR (=) g/hr.A , A = 14.5 cm. sq.
f (=) %

Ultrafiltration results with respect to eight PEG solutes of different molecular weight are given for each membrane sample. PWP measurements at three times during the test run are given which are defined as follows:

PWPa or IPWP	before pressurization
PWPb	at the start of the test run
PWPc	at the end of the test run

Membrane S(15 - 0.75)

Sample no.	1		2	
PEG - M. W.	PR	f	PR	f
- 300	601.	0.0	667.	0.8
- 600	661.	7.5	706.	9.1
- 1000	594.	6.7	621.	8.4
- 1500	585.	13.5	623.	12.7
- 2000	599.	11.8	630.	16.5
- 3000	559.	21.9	599.	28.9
- 4000	551.	20.1	548.	29.8
- 6000	447.	52.6	485.	62.2
PWPa				
PWPb	596.		652.	
PWPc	562.		587.	

Membrane S(25 - 0.75)

Sample no.	1		2		3	
PEG - M.W.	PR	f	PR	f	PR	f
- 300	213.	10.1	207.	7.1	175.	10.3
- 600	178.	34.6	198.	24.9	149.	34.3
- 1000	165.	59.	187.	44.5	143.	57.4
- 1500	153.	75.1	188.	58.2	132.	73.2
- 2000	151.	87.2	183.	68.3	131.	88.9
- 3000	149.	97.0	183.	87.8	131.	97.5
- 4000	144.	95.9	176.	80.6	130.	89.9
- 6000	144.	96.3	172.	97.1	129.	98.7
PWPa						
PWPb	217.		209.		175.	
PWPc	150.		181.		131.	

Membrane S(25 - 0.08)

Sample no.	1		2	
PEG - M. W.	PR	f	PR	f
- 300	229.	17.9	90.	19.
- 600	160.	42.6	83.	35.5
- 1000	137.	66.6	77.	62.8
- 1500	132.	78.2	74.	77.2
- 2000	132.	85.0	70.	87.7
- 3000	128.	89.9	68.	91.8
- 4000	117.	91.3	63.	89.4
- 6000	116.	84.8	67.	95.3
PWPa				
PWPb	234.		91.	
PWPc	132.		69.	

Membrane S(20 - 0.0)

Sample no.	1		2		3	
PEG - M.W.	PR	f	PR	f	PR	f
- 300	387.	5.7				
- 600	377.	22.3				
- 1000	348.	35.3				
- 1500	344.	51.5				
- 2000	349.	59.9				
- 3000	331.	80.5				
- 4000	321.	81.0				
- 6000	300.	91.0	179.	87.0	221.	90.5
PWPa						
PWPb	393.		200.		240.	
PWPc	344.					

Membranes tested with only probe solute PEG-6000:

Sample no.	1		2		3		4	
Membrane	PR	f	PR	f	PR	f	PR	f
S(18-0.75)	442.	92.3	363.	89.9	470.	88.4		
S(20-0.75)	363.	89.5	358.	97.1	395.	89.9	378.	97.5
S(21-0.75)	238.	95.5	343.	92.8	295.	94.6		
PWPa:								
S(18-0.75)	530.		441.		512.			
S(20-0.75)	415.		372.		473.		389.	
S(21-0.75)	256.		376.		324.			

APPENDIX 12

CALCULATION OF EXPERIMENTAL ERROR ASSOCIATED WITH THE MEMBRANE PERFORMANCE DATA

A. PERMEATION RATES: PWP, PR

Given that PR, and similarly PWP, is determined by the following method:

$$PR = \frac{W_s}{t_s} \times k \times 60, \quad W_s = W_f - W_e$$

where W_s = sample weight, g

W_f = weight of full sample bottle, g

W_e = weight of empty sample bottle, g

t_s = sampling time, minutes

k = correction factor for water at 25°C

Then, the experimental error for PR is obtained using the following equation

$$\%\Delta PR = \left(\frac{\Delta W_s}{W_s} + \frac{\Delta t_s}{t_s} + \frac{\Delta K}{K} \right) \times 100\%$$

and $\Delta W_s = \Delta W_f + \Delta W_e$

$\Delta k = k_T - k_{T+\Delta T}$

The error associated with each measurement is given below:

Measurement	error (Δ)
W_f	0.01 g
W_e	0.01 g
t_s	0.07 min.
T	0.5°C

Also, $\Delta k = 0.01$ (from slope of k vs T)

Hence, $\Delta W_s = 0.02$ g

and $$\%\Delta PR = \left(\frac{0.02}{W_s} + \frac{0.07}{t_s} + \frac{0.01}{k} \right) \times 100\%$$

Given W_S, t_S and k values%ΔPR was calculated for a set of membranes and for an RO/UF experiment using PEG-6000 solute:

%ΔPR - for PEG-6000 permeation results at the 1st and 2nd level tests

Membrane S(P-R)	15-0.2	15-0.5	15-1.0	20-0.2	20-0.5	20-1.0
Level 1:						
W_S	12.84	18.49	22.71	17.20	15.13	22.68
t_S	2.	2.	3.07	3.	3.	4.
k	1.15	1.15	1.12	1.16	1.16	1.12
%ΔPR	4.53	4.48	3.26	3.31	3.33	2.73
Level 2:						
W_S	14.60	17.08	17.73	13.95	15.97	16.94
t_S	4.	4.	4.	4.	4.	3.5
k	1.0228	1.0228	1.0228	1.0228	1.0228	1.0228
%ΔPR	2.86	2.84	2.84	2.87	2.85	3.10

Overall the error %ΔPR ranges from 2.7 to 4.5% for this set of data. We can assume that this set of data is representative of the complete set (data in Figures 9, 10 and 11). Hence, a conservative %ΔPR of 5.0% will be assumed for the complete set.

B. SOLUTE SEPARATION: f

Given that f is determined by the following method:

$$f = \frac{C^*feed - C^*PR}{C^*feed} \times 100\%$$

where $C^*feed = C\ feed - C\ dw$

$C^*PR = C\ PR - C\ PWP$

Then the experimental error on f is obtained by the following equation:

$$\Delta f = f \left(\frac{(\Delta C^*feed + \Delta C^*PR)}{(C^*feed - C^*PR)} + \frac{\Delta C^*feed}{C^*feed} \right)$$

Or, rearranging,

$$\Delta f = \frac{100}{C^*feed} \left[(2\Delta C^*feed + \Delta C^*PR) - \Delta C^*feed \left(1 - \frac{f}{100} \right) \right]$$

The experimental error associated with each solute concentration measurement determined using the average of peaks from the carbon analyzer (TOC) is approximately

$$\Delta C = 2.5 \text{ ppm}$$

Hence, the error ΔC^* is

$$\Delta C^* = 2\Delta C = 5 \text{ ppm}$$

Assuming that Cfeed and Cdw equal 200 ppm and 0 ppm is true (which is often the case) then C*feed = 200 ppm. Substituting this and the error values in the equation for Δf gives

$$\Delta f = 0.5 \left[15 - 5 \left(1 - \frac{f}{100} \right) \right]$$

Δf was calculated for a range of f values.

f, %	Δf	$\%\Delta f$
30.	5.75	19.17
50.	6.25	12.5
70.	6.75	9.64
90.	7.25	8.06
95.	7.38	7.76

Overall, the experimental error Δf is of the order of 7 and represents about 20 to 7% of f depending on the value of f.

APPENDIX 13

SOME PORE SIZE DISTRIBUTION REGRESSION ANALYSIS RESULTS - PREDICTED VERSUS EXPERIMENTAL SOLUTE SEPARATION FOR 3 MEMBRANES

	S (15 - 0.2)		S (20 - 0.2)		S(25 - 0.2)	
	f exp.	f pred.	f exp.	f pred.	f exp.	f pred.
PEG - M.W.						
-300					16.9	26.4
-600					37.2	43.2
-1000	38.8	36.3	43.1	40.0	65.5	56.0
-1500	50.2	47.1	54.8	55.9	73.2	70.2
-2000	50.8	53.9	73.0	73.1	83.4	76.9
-3000	77.0	74.5	86.9	88.1	79.8	88.2
-4000	77.5	81.0	87.4	89.1	94.1	93.3
-6000	86.1	89.3	93.9	93.7	97.9	99.9
-9000	95.1	89.8	95.3	93.6		
-15,000	96.1	93.5	96.7	96.1		
SSR	89.9		18.4		343.	
E_f	3.4		1.5		6.6	

CALCULATIONS

i. Sum of Squares of Residuals, SSR

$$SSR = \sum_{i=1}^{n} (f \text{ exp.} - f \text{ pred.})^2, \quad n = \text{no. solutes}$$

ii. Average Error on Predicted Separation, E_f

$$E_f = \sqrt{\frac{SSR}{n}}, \quad n = \text{no. solutes} = 8$$

By comparison, the standard deviation would be

$$\sigma = \sqrt{\frac{SSR}{n-p}}, \quad p = \text{no. of parameters} = 5$$

Note: The predicted solute separation data for the other membranes involved in the pore size distribution analysis are not available. A different computer output format which emphasized the statistical results but which did not display the separation data was used for these membranes. The SSR was one statistical results in the output and this was used to calculate E_f for each membrane in Table 7.

APPENDIX 14

SIGNIFICANCE TEST FOR TRANSPORT MODEL INADEQUACY

A test of model inadequacy will be carried out for the transport model used in the analysis of pore size distribution. The model involved five parameters, and the response was solute separation, f. Solute separation data for eight different solutes were in the response data set of each membrane. There were no replicates.

Significance tests will determine whether the residual component due to an inadequacy in the form of the transport model fitted is appreciably larger than the error in the experimental determination of solute separation.

For situations, as this one, in which the data used in the analysis contain no replicates, Draper and Smith (42) described a test for model inadequacy that uses an 'external' estimate of pure error variance. The test ratio is

$$T = \frac{\sum_{u=1}^{n} e_u^2/n-p}{\hat{\sigma}_E^2}$$

where $\hat{\sigma}_E^2$ is the external estimate of pure error variance having Υ_E degrees of freedom

e_u^2 sum of squares of residuals $= \sum_{u=1}^{n} (Y_u - Y_u)^2$

n number of data points = 8

P number of parameters = 5

Y_u measured response = f

$\hat{Y}_u$ predicted response = f*

Normally, the pure error variance σ^2 would be obtained from the difference in solute separation for a membrane subjected repeatedly to the same RO/UF experiment. The pure error variance so obtained would be the effect of the membrane performing differently and/or experimental error in the analysis of the permeate samples leading to the evaluation of solute separation. Since the membranes in the Level 2 tests were only subjected once to each solute, hence that there were no actual replicates, the pure error variance could not be calculated. However, an estimate of the pure error variance using the experimental error would be adequate.

The experimental error determined in Appendix 12 will be used to calculate the estimate $\hat{\sigma}_E^2$. It was shown that the experimental error Δf is a function of f, as follows:

$$\Delta f = 0.5 \left(15 - 5 \frac{f}{100}\right) \text{, based on } \Delta C = 2.5 \text{ ppm}$$

$\hat{\sigma}_E^2$ can be approximated by $(\Delta f)^2$ for one solute. Since Δf is the average deviation between two or more measurements then the smallest degree of freedom for $\hat{\sigma}_E^2$ is $\gamma_E = 1$. A pooled estimate, $\hat{\sigma}_E^2$ pooled, can be evaluated from the experimental error with respect to several solutes. In this case, the degree of freedom would equal the number of solutes.

The equation for $\hat{\sigma}_E^2$ pooled is

$$\hat{\sigma}_E^2 \text{ pooled} = \sum_{i=1}^{n} \gamma_{Ei} (\Delta f)_i^2 / \sum_{i=1}^{n} \gamma_{Ei}$$

The value of $\hat{\sigma}_E^2$ pooled for each membrane involved in the pore size distribution analysis can be calculated using the solute separation data given in Appendix 10. Subsequently, the value of T corresponding to each membrane can be calculated. T is then compared with F [(n-p), γ_E pooled, α] where

$n-p = 8-5 = 3$

γ_E pooled $= 8$

$\alpha = 0.05$

The resulting F test value is F (3, 8, 0.05) = 4.07

Values of $\hat{\sigma}_E^2$ pooled determined from Δf which is based on the solute concentration error $\Delta C = 2.5$ ppm are given in Table I attached. Corresponding T values, as well as Σe_u^2 used in their calculation, are given in Table I for each membrane involved in the pore size distribution analysis. Comparison of these T values with the test F = 4.07 revealed that, on the basis of $\Delta C = 2.5$ ppm, there was a significant lack of fit (at 95% significance level) in the model for only 3 of the 15 membranes characterized. Considering that the estimate of pure error variance based on the experimental error alone could have been less than the actual pure error variance, the model used for the pore size analysis generally provided a good fit.

Example: Membrane from S (25-0.2)

This membrane was characterized using 8 probe solutes. The data set for f is the one given in Appendix 10, reproduced below. The corresponding Δf values on the basis of $\Delta C = 2.5$ ppm are shown below.

PEG-MW	300	600	1000	1500	2000	3000	4000	6000
f	16.9	37.2	65.5	73.2	83.4	79.8	94.1	97.9
Δf	5.42	6.57	6.64	6.83	7.09	7.00	7.35	7.45

$\hat{\sigma}_E{}^2$ pooled can now be calculated as follows:

$$\hat{\sigma}_E{}^2 \text{ pooled} = \sum_1^8 (\Delta f)_i^2 \div 8$$

$\hat{\sigma}_E{}^2$ pooled = 45.49

We can now calculate the test ratio given that for this membrane sample

$$\sum_{u=1}^{n} e_u{}^2 = 348$$

$$T = \frac{\sum_{u=1}^{n} e_u{}^2/n-p}{\sigma_E{}^2}$$

$$T = \frac{348/(8-5)}{45.49}$$

$$T = 2.55$$

Comparison of the T value with the test F = 4.07 indicates there is no significant lack of fit of the model with this membrane.

TABLE I

Membrane	Σeu^2	$\hat{\sigma}_E^2$ pooled	T
15-0.0	251	40.53	2.07
0.2	92	46.32	0.66
0.5	200	43.98	1.52
1.0	426	45.58	3.12
2.0	169	40.65	1.39
2.7	474	43.02	3.67
20-0.0	308	41.31	2.88
0.2	18	48.83	0.12
0.5	662	45.63	4.84
1.0	155	46.25	1.12
1.5	318	38.73	2.74
2.0	1058	39.09	9.02
25-0.2	348	45.49	2.55
1.0	462	45.30	3.40
1.4	899	42.23	7.10

APPENDIX 15

INTRINSIC VISCOSITY DETERMINATION

The intrinsic viscosity data were determined based on the viscosity measurements for polyethersulfone (PES) - polyvinylpyrrolidone (PVP) polymer mixtures in solution with N-methyl-pyrrolidone (NMP). The experimental results leading to the viscosity measurements are given in Table I for each polymer mixture; the composition is expressed as the PVP/PES wt. ratio. The linear regression results leading to the intrinsic viscosity data are given in Table II, also for each polymer mixture.

Definitions:

$n_{rel.}$ = relative viscosity

n_{sp} = specific viscosity

$[n]$ = intrinsic viscosity, l/g

k = least square parameter i.e. slope

R^2 = regression coefficient

t = efflux time, seconds

c = polymer concentration, g/l

Calculations:

$n_{rel.}$ = t/to, to = t at C = 0

n_{sp} = $n_{rel.} - 1$

$[n]$ = $\lim_{C \to 0} n_{sp}/C$

TABLE I

VISCOSITY MEASUREMENTS IN NMP AT 25°C

PVP/PES (wt. ratio)	Viscometer No.	C (10 g/l)	t (seconds)	$n_{rel.}$	n_{sp}	n_{sp}/C (10^{-1} l/g)
0.0	100	0.0	106.5			
		0.258	120.05	1.127	0.127	0.493
		0.34	124.75	1.171	0.171	0.504
		0.515	134.2	1.260	0.260	0.505
		0.69	144.25	1.354	0.354	0.513
		0.85	154.0	1.446	0.446	0.525
		1.03	163.8	1.538	0.538	0.522
0.2	75	0.0	187.7			
		0.175	201.4	1.073	0.073	0.417
		0.515	230.9	1.230	0.230	0.447
		0.562	235.05	1.252	0.252	0.449
		0.634	242.05	1.290	0.290	0.457
		0.690	247.3	1.318	0.318	0.460
0.4	75	0.0	188.3			
		0.424	218.4	1.160	0.160	0.377
		0.601	233.68	1.241	0.241	0.401
		0.698	242.8	1.289	0.289	0.415
0.75	100	0.0	107.0			
		0.424	122.1	1.141	0.141	0.333
		0.601	129.0	1.206	0.206	0.342
		0.759	135.4	1.265	0.265	0.350
		0.832	138.5	1.295	0.295	0.354

TABLE I (CONTINUED)

VISCOSITY MEASUREMENTS IN NMP AT 25°C

PVP/PES (wt. ratio)	Viscometer No.	C (10 g/l)	t (seconds)	$n_{rel.}$	n_{sp}	n_{sp}/C (10^{-1} l/g)
1.0	75	0.0	185.4	1.164	0.164	
		0.515	215.9	1.164	0.164	0.319
		0.618	222.3	1.199	0.199	0.322
		0.736	229.7	1.239	0.239	0.325
		0.801	234.03	1.262	0.262	0.328
2.0	100	0.0	106.53			
		0.429	117.5	1.103	0.103	0.240
		1.060	134.9	1.266	0.266	0.251
		1.349	143.5	1.347	0.347	0.257
		1.687	154.25	1.448	0.448	0.266
		1.795	157.88	1.482	0.482	0.269
5.0	100	0.0	106.05			
		0.858	122.2	1.152	0.152	0.177
		1.288	131.3	1.238	0.238	0.185
		1.545	137.37	1.295	0.295	0.191
		1.839	143.85	1.356	0.356	0.194
		2.003	147.85	1.394	0.394	0.197
1/0	75	0.0	188.0			
		0.858	205.8	1.095	0.095	0.110
		1.545	221.3	1.177	0.177	0.115
		1.839	228.5	1.215	0.215	0.117
		2.06	234.3	1.246	0.246	0.120
		2.107	234.13	1.251	0.251	0.119

TABLE II

INTRINSIC VISCOSITY DATA

Polymer Mixture		Least sq. Parameters		Statistic	
PVP/PES (wt. ratio)	PES (wt. fr.)	[n] 10^{-1} l/g	k	R^2	σ^2
0.0	1.0	0.487	0.038	0.89	2.08 E-5
0.2	0.833	0.402	0.085	1.0	1.17 E-6
0.4	0.714	0.318	0.138	1.0	2.60 E-8
0.75	0.571	0.311	0.052	1.0	1.73 E-7
1.0	0.500	0.305	0.027	0.99	2.20 E-7
2.0	0 333	0.230	0.024	0.99	1.43 E-7
5.0	0.167	0.163	0.017	0.99	1.17 E-6
1/0	0.0	0.104	0.007	0.99	2.85 E-7

$$\sigma^2 = \frac{RSS}{n-p} = \frac{RSS}{n-2}$$

where RSS = $\Sigma[(nsp/C)\ calc. - (nsp/C)\ exp]^2$

n = no. of experimental points

p = no. of regression parameters,
p = 2 in this case

APPENDIX 16

CHEMICAL ANALYSIS OF POLYETHERSULFONE MEMBRANES

DETERMINATION OF PVP CONTENT

Since polyethersulfone (PES) does not contain the element N but polyvinylpyrrolidone (PVP) does then the PVP content of the membrane could be calculated on the basis of the N content of the membrane determined by chemical analysis. The approach used was to dissolve the membrane in a solvent which did not contain N; dimethylsulfoxide (DMSO) was selected. A chemical analysis for N in the solution was then performed, the results were given in mg N/l solution. The N content was related to the PVP content as follows:

Given the monomer unit of PVP

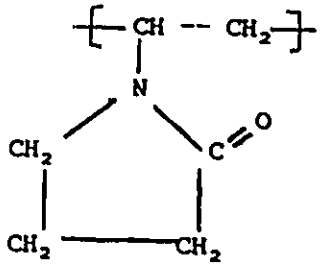

which has a molecular weight of 111.16. Hence, N represents 12.60 wt% of PVP. Or else, for each weight unit of N there is 7.93 weight units of PVP in the solution.

The results for four membranes analyzed will now be given.

Solution Composition

Membrane Type	Weight, g			Volume, ml	mg Membrane / l solution
	Membrane	DMSO	Solution		
S(20-0.0)	1.22	54.69	55.91	50.79	24.02×10^3
S(30-0.5)	1.57	54.64	56.21	51.00	30.78×10^3
S(15-2.7)	0.99	54.67	55.66	50.60	19.57×10^3
S(25-1.0)	1.51	54.60	56.11	50.92	29.65×10^3

ρ PBS = 1.37
ρ DMSO = 1.096

Assumptions:
- o ρ membrane = ρ PBS
- o V solution = V DMSO + V membrane

where V DMSO = W DMSO/ρ DMSO
V membrane = W membrane/ρ PBS

Solution Analysis

Membrane Type	Composition, mg/l			
	N	N*	PVP	PES
S(20-0.0)	11.9	0.0	0	24.02×10^3
S(30-0.5)	137.9	122.7	972.1	29.81×10^3
S(15-2.7)	107.9	98.2	779.1	18.79×10^3
S(25-1.0)	88.9	74.2	588.2	29.06×10^3

Notes:

i. N composition is for the membrane only since it was adjusted for N impurities from the solvent. This was achieved by analyzing a blank solvent sample for N, and substracting the value (2.1 mg/L) from the N content for the sample.

ii. Since N in the first membrane S(20-0.0) is supposed to be nul because it does not contain PVP, this N content was interpreted as impurities in the membrane.

iii. N* is the N associated with PVP. It was adjusted by substracting the N fraction as impurity (i.e. 11.9 mg/L).

Example: Let a, b refer to S(20-0.0) and S(30-0.5) respectively, then:

$$N^*_b = N_b - Na \frac{W_b}{W_a}$$

$$= 137.9 - (11.9) \frac{(1.57)}{(1.22)}$$

$$= 122 \text{ mg/L}$$

$$PVP_b = 7.93\ N^*_b$$
$$= 972.1 \text{ mg/L}$$

$$PES_b = 30.78 \times 10^3 - 972.1$$

$$= 29.81 \times 10^3 \text{ mg/L}$$

Membrane Composition Analysis

Membrane Type	Membrane Composition		Percent PVP in casting solution left in membrane (1)
	PVP wt%	PVP/PES wt. Ratio	
S(20-0.0)	0.0	0.0	-
S(30-0.5)	3.16	0.0326	6.52
S(15-2.7)	3.98	0.0415	1.54
S(25-1.0)	1.98	0.0202	2.02

(1) Example: S(30-0.5)

$$6.52\% = \frac{0.0326}{0.5} \times 100\%$$